PHYSICAL REVIEW D **83,** 036004 (2011)

Anatomy of new physics in B-$\bar{B}$ mixing

A. Lenz[1,2,*] and U. Nierste[3,†]

[1]*Institut für Physik, Technische Universität Dortmund, D-44221 Dortmund, Germany*
[2]*Institut für Theoretische Physik, Universität Regensburg, D-93949 Regensburg, Germany*
[3]*Institut für Theoretische Teilchenphysik, Universität Karlsruhe, Karlsruhe Institute of Technology, D-76128 Karlsruhe, Germany*

J. Charles,[4,‡] S. Descotes-Genon,[5,§] A. Jantsch,[6,‖] C. Kaufhold,[7,¶] H. Lacker,[8,**] S. Monteil,[9,††] V. Niess,[9,‡‡] and S. T'Jampens[7,§§]

(CKMfitter Group)

[4]*Centre de Physique Théorique, Campus de Luminy, Case 907, F-13288 Marseille Cedex 9, France (UMR 6207 du CNRS associée aux Universités d'Aix-Marseille I et II et Université du Sud Toulon-Var; laboratoire affilié à la FRUMAM-FR2291)*
[5]*Laboratoire de Physique Théorique d'Orsay, UMR8627, CNRS/Université Paris-Sud 11, 91405 Orsay Cedex, France*
[6]*Max-Planck-Institut für Physik (Werner-Heisenberg-Institut), Föhringer Ring 6, 80805 München, Germany*
[7]*Laboratoire d'Annecy-Le-Vieux de Physique des Particules, 9 Chemin de Bellevue, BP 110, F-74941 Annecy-le-Vieux Cedex, France (UMR 5814 du CNRS-IN2P3 associée à l'Université de Savoie)*
[8]*Humboldt-Universität zu Berlin, Institut für Physik, Newtonstr. 15, D-12489 Berlin, Germany*
[9]*Laboratoire de Physique Corpusculaire de Clermont-Ferrand, Université Blaise Pascal, 24 Avenue des Landais F-63177 Aubière Cedex, (UMR 6533 du CNRS-IN2P3 associée à l'Université Blaise Pascal)*

(Received 16 November 2010; published 14 February 2011)

We analyze three different new physics scenarios for $\Delta F = 2$ flavor-changing neutral currents in the quark sector in the light of recent data on neutral-meson mixing. We parametrize generic new physics contributions to B_q-$\bar{B}_q$ mixing, $q = d, s$, in terms of one complex quantity Δ_q, while three parameters Δ_K^{tt}, Δ_K^{ct}, and Δ_K^{cc} are needed to describe K-$\bar{K}$ mixing. In scenario I, we consider uncorrelated new physics contributions in the B_d, B_s, and K sectors. In this scenario, it is only possible to constrain the parameters Δ_d and Δ_s whereas there are no nontrivial constraints on the kaon parameters. In scenario II, we study the case of minimal flavor violation (MFV) and small bottom Yukawa coupling, where $\Delta \equiv \Delta_d = \Delta_s = \Delta_K^{tt}$. We show that Δ must then be real, so that no new CP phases can be accommodated, and express the remaining parameters Δ_K^{cc} and Δ_K^{ct} in terms of Δ in this scenario. Scenario III is the generic MFV case with large bottom Yukawa couplings. In this case, the kaon sector is uncorrelated to the B_d and B_s sectors. As in the second scenario one has $\Delta_d = \Delta_s \equiv \Delta$, however, now with a complex parameter Δ. Our quantitative analyses consist of global Cabibbo-Kobayashi-Maskawa (CKM) fits within the Rfit frequentist statistical approach, determining the standard model parameters and the new physics parameters of the studied scenarios simultaneously. We find that the recent measurements indicating discrepancies with the standard model are well accommodated in Scenarios I and III with new mixing phases, with a slight preference for Scenario I that permits different new CP phases in the B_d and B_s systems. Within our statistical framework, we find evidence of new physics in both B_d and B_s systems. The standard model hypothesis $\Delta_d = \Delta_s = 1$ is disfavored with p-values of 3.6σ and 3.3σ in Scenarios I and III, respectively. We also present an exhaustive list of numerical predictions in each scenario. In particular, we predict the CP phase in $B_s \to J/\psi\phi$ and the difference between the B_s and B_d semileptonic asymmetries, which will be both measured by the LHCb experiment.

DOI: 10.1103/PhysRevD.83.036004 PACS numbers: 11.30.Er, 12.15.Hh, 12.15.Mm, 12.60.−i

*Alexander.Lenz@physik.uni-regensburg.de
†nierste@particle.uni-karlsruhe.de
‡charles@cpt.univ-mrs.fr
§sebastien.descotes-genon@th.u-psud.fr
‖jantsch@mppmu.mpg.de
¶kaufhold@lapp.in2p3.fr
**lacker@physik.hu-berlin.de
††monteil@clermont.in2p3.fr
‡‡niess@clermont.in2p3.fr
§§tjampens@lapp.in2p3.fr

I. INTRODUCTION

Considerations of the stability of the electroweak scale lead to the general belief that there is new physics with particle masses below 1 TeV. While the high-p_T experiments at the LHC should produce these new particles directly, one can study their dynamics also indirectly, through their impact on precision measurements at lower energies. To this end flavor-changing neutral current (FCNC) processes are extremely useful. On one hand

 © 2011 American Physical Society

they are highly suppressed in the standard model and are therefore very sensitive to new physics. On the other hand FCNC processes of K, B_d, and B_s mesons are still large enough to be studied with high statistics in dedicated experiments. Here meson-antimeson mixing plays an outstanding role. First, meson-antimeson oscillations occur at time scales which are sufficiently close to the meson lifetimes to permit their experimental investigation. Second, the standard model contribution to meson-antimeson mixing is loop-suppressed and comes with two or more small elements of the Cabibbo-Kobayashi-Maskawa (CKM) matrix [1]. Third, the decays of oscillating mesons give access to many mixing-induced CP asymmetries through the time-dependent study of decays into CP eigenstates, which in some cases one can relate to the parameters of the underlying theory with negligible hadronic uncertainties.

The B-factories have revealed that the dominant $b \to d$ and $b \to u$ transitions fit into the pattern of the CKM mechanism and are in agreement with the information on $s \to d$ transitions gained in more than forty years of kaon physics. The success of the CKM picture is evident from the many different measurements combining into a consistent and precise determination of the apex $(\bar{\rho}, \bar{\eta})$ of the B-meson unitarity triangle (in terms of the Wolfenstein parametrization of the CKM matrix [2,3]). As a consequence, any contribution from the expected new TeV-scale physics to the measured flavor-changing processes must be suppressed compared to the established CKM mechanism.

Models with only CKM-like flavor violation are said to respect the principle of *minimal flavor violation (MFV)* [4,5]. This principle is often invoked in an *ad hoc* way to suppress excessive FCNC amplitudes for model-building purposes. In the minimal supersymmetric standard model (MSSM), new sources of flavor violation solely stem from the supersymmetry-breaking sector. A sufficient condition for MFV are supersymmetry-breaking terms which are flavor-blind at a given energy scale. This situation occurs in supergravity with a flat Kähler metric [6] or if supersymmetry breaking is mediated by gauge interactions [7]. The overall picture of experimental data does not require sizeable corrections to MFV. Still it is difficult to probe the CKM picture with a better accuracy than, say, 30%, because most quantities entering the global fit of the unitarity triangle suffer from sizeable hadronic uncertainties. It should also be stressed that the accuracy of the determination of the CKM parameters decreases notably when one assumes that one or several crucial input(s) could be affected by new physics contributions. Interestingly, several authors have detected possible hints of new physics in the data. For example it has been argued in the literature that one starts to see a discrepancy between the measurement of $\sin 2\beta$ and the region preferred by $|V_{ub}|$ from semileptonic decays on one hand, and $|\varepsilon_K|$ on the other hand [8,9]. Also the recently improved measurement of the $B \to \tau\nu$ branching ratio deviates from its indirect CKM fit prediction [10].

In addition there are anomalies in the data on $b \to s$ transitions. The latter processes do not involve $\bar{\rho}$ and $\bar{\eta}$ (to a good accuracy) and therefore directly probe the CKM mechanism. An ongoing debate addresses an extra contribution to $b \to s\bar{q}q$, $q = u, d, s$, decay amplitudes with a CP phase different from $\arg(V_{ts}^* V_{tb})$ that can alleviate the pattern of shifts between the measured CP asymmetries in these $b \to s$ penguin modes and the standard model predictions (see e.g. [11]).

However, the first place to look for new physics in $b \to s$ transitions is B_s-$\bar{B}_s$ mixing, where new physics can be parametrized in terms of just one complex parameter (or two real parameters) in a model-independent way, as we will discuss in great detail below. At the end of 2006 a combined analysis of several observables has pointed to the possibility of a new-physics contribution with a CP phase different from that of the standard model box diagram [12]. Models of supersymmetric grand unification can naturally accommodate new contributions to $b \to s$ transitions [13]: right-handed quarks reside in the same quintuplets of SU(5) as left-handed neutrinos, so that the large atmospheric neutrino mixing angle could well affect squark-gluino mediated $b \to s$ transitions. At the same time the grand unified theory (GUT) models of Refs. [13] do not induce too dangerous contributions to the well-measured rare decay $B \to X_s\gamma$. B_s-$\bar{B}_s$ mixing has been further investigated in other supersymmetric scenarios with [14] and without [15,16] GUT boundary conditions, in unparticle physics scenarios in Ref. [17], in multi-Higgs-doublet models [18], in models with extra gauge bosons Z' [19], warped extra dimensions [20], left-right symmetry [21], anomalous tWb-couplings [22], additional quark families [23] or an additional singlet quark [24], and in a little-Higgs model [25].

On the experimental side, the understanding of $b \to s$ transitions has made tremendous progress in the past years. The Tevatron experiments have discovered and precisely quantified B_s-$\bar{B}_s$ mixing oscillations [26,27] whose frequency is in good agreement with the standard model prediction, and presented first determinations of the associated CP-violating phase from tagged analyses of $B_s \to J/\psi\phi$ decays [28–32]. Recently, possible new physics in the CP phase of the B_s-$\bar{B}_s$ mixing amplitude has received new attention: The D0 Collaboration has reported a measurement of the dimuon charge asymmetry which disagrees with the standard model prediction by 3.2 standard deviations [33]. The CP asymmetry in semileptonic or, more generally, any flavor-specific decays, involves the B_s-$\bar{B}_s$ mixing phase just as $B_s \to J/\psi\phi$, so that both pieces of experimental information can be combined to constrain this phase. The new measurement of the dimuon charge asymmetry has already triggered considerable theoretical interest. Besides predictions for the CP phase of B_s-$\bar{B}_s$ mixing in specific models, as quoted above, also model-independent analyses of new physics effects have

appeared [34]. Because of the large size of the dimuon asymmetry it was also investigated whether sizeable new physics contributions to the decay of B_s mesons are possible. This alternative is however strongly constrained by the lifetime ratios of B-mesons (see e.g. [35]) as well as the semileptonic branching ratios and the the average number of charm quarks per b-decays (see e.g. [36]).

In the present article, we analyze generic scenarios of new physics which are compatible (at different levels) with the experimental picture sketched above. We set up our notation and define our theoretical framework in Sec. II, the relevant updated experimental and theoretical inputs to our global analysis are presented in Sec. III. In Sec. IV A we first present the current status of the standard model fit. In Sec. IV B we perform a fit in which we allow for new physics in the B_d-$\bar{B}_d$ mixing and the B_s-$\bar{B}_s$ mixing systems and we project the results onto the new physics parameters that describe the B_d-$\bar{B}_d$ mixing and the B_s-$\bar{B}_s$ mixing systems. Sections IV C and IV D are dedicated to two MFV scenarios with correlated effects in all meson-antimeson mixing amplitudes. Finally, we conclude and list a few perspectives for the near future.

II. SETTING THE SCENE

A. B-$\bar{B}$ mixing basics

B_q-$\bar{B}_q$ oscillations (with $q = d$ or $q = s$) are described by a Schrödinger equation:

$$\mathrm{i}\,\frac{d}{dt}\begin{pmatrix}|B_q(t)\rangle\\ |\bar{B}_q(t)\rangle\end{pmatrix} = \left(M^q - \frac{\mathrm{i}}{2}\Gamma^q\right)\begin{pmatrix}|B_q(t)\rangle\\ |\bar{B}_q(t)\rangle\end{pmatrix}, \tag{1}$$

with the mass matrix $M^q = M^{q\dagger}$ and the decay matrix $\Gamma^q = \Gamma^{q\dagger}$. The physical eigenstates $|B_H^q\rangle$ and $|B_L^q\rangle$ with masses M_H^q, M_L^q and decay rates Γ_H^q, Γ_L^q are obtained by diagonalizing $M^q - \mathrm{i}\Gamma^q/2$. The B_q-$\bar{B}_q$ oscillations in Eq. (1) involve the three physical quantities $|M_{12}^q|$, $|\Gamma_{12}^q|$, and the CP phase

$$\phi_q = \arg(-M_{12}^q/\Gamma_{12}^q). \tag{2}$$

We denote the average B_q mass and width by M_{B_q} and Γ_{B_q}, respectively. The mass and width differences between B_L^q and B_H^q are related to them as

$$\begin{aligned}\Delta M_q &= M_H^q - M_L^q = 2|M_{12}^q|,\\ \Delta\Gamma_q &= \Gamma_L^q - \Gamma_H^q = 2|\Gamma_{12}^q|\cos\phi_q,\end{aligned} \tag{3}$$

up to numerically irrelevant corrections of order m_b^2/M_W^2. ΔM_q simply equals the frequency of the B_q-$\bar{B}_q$ oscillations (for details see e.g. [37]). A third quantity probing mixing is

$$a_{\mathrm{fs}}^q = 2\left(1 - \left|\frac{q}{p}\right|\right) = \mathrm{Im}\frac{\Gamma_{12}^q}{M_{12}^q} = \frac{|\Gamma_{12}^q|}{|M_{12}^q|}\sin\phi_q = \frac{\Delta\Gamma_q}{\Delta M_q}\tan\phi_q. \tag{4}$$

a_{fs}^q is the CP asymmetry in *flavor-specific* $B_q \to f$ decays, i.e., the decays $\bar{B}_q \to f$ and $B_q \to \bar{f}$ are forbidden. The standard way to measure a_{fs}^q uses $B_q \to X\ell^+\nu_\ell$ decays, which explains the common name *semileptonic CP asymmetry* for a_{fs}^q, with the corresponding notation a_{SL}^q (for more details see e.g. [38]). In theoretical contexts, we use the notation a_{fs}^q in this paper, while we write a_{SL}^q when referring to the specific experimental observable inferred from semileptonic decays. Further

$$\frac{q}{p} = -\sqrt{\frac{2M_{12}^* - i\Gamma_{12}^*}{2M_{12} - i\Gamma_{12}}}. \tag{5}$$

Let us now discuss our theoretical understanding of the off-diagonal terms of the evolution matrix, which are responsible for B_q-$\bar{B}_q$ mixing. The dispersive term M_{12}^q is completely dominated by box diagrams involving virtual top quarks, and it is related to the effective $|\Delta B| = 2$ Hamiltonian $H_q^{|\Delta B|=2}$ as

$$M_{12}^q = \frac{\langle B_q|H_q^{|\Delta B|=2}|\bar{B}_q\rangle}{2M_{B_q}}. \tag{6}$$

The standard model expression for $H_q^{|\Delta B|=2}$ is [39]

$$H_q^{|\Delta B|=2} = (V_{tq}^* V_{tb})^2 CQ + \mathrm{H.c.} \tag{7}$$

with the four-quark operator

$$Q = \bar{q}_L\gamma_\mu b_L\bar{q}_L\gamma^\mu b_L, \tag{8}$$

$$q_L = \frac{1}{2}(1 - \gamma_5)q, \tag{9}$$

and the Wilson coefficient C, which depends on the heavy mass scales of the theory. In a wider class of models $H_q^{|\Delta B|=2}$ maintains the form of Eq. (7) (meaning that there is no operator other than Q involved), but with a value of C different from the value in the standard model:

$$C^{\mathrm{SM}} = \frac{G_{\mathrm{F}}^2}{4\pi^2}M_W^2\hat{\eta}_B S\left(\frac{\bar{m}_t^2}{M_W^2}\right). \tag{10}$$

Here $\bar{m}_t$ is the top quark mass defined in the $\overline{\mathrm{MS}}$ scheme, related to the pole mass m_t^{pole} determined at the Tevatron $\bar{m}_t(\bar{m}_t) = 0.957 m_t^{\mathrm{pole}}$ (at next-to-leading order of QCD). The Inami-Lim function S [40] is calculated from the box diagram with two internal top quarks and evaluates to $S(\bar{m}_t^2/M_W^2) = 2.35$ for the central value of $\bar{m}_t$ listed in Table VII. QCD corrections are comprised in [42,48]

$$\hat{\eta}_B = 0.8393 \pm 0.0034. \tag{11}$$

The hadronic matrix element involved is usually parametrized as

$$\langle B_q|Q(\mu_B)|\bar{B}_q\rangle = \frac{2}{3}M_{B_q}^2 f_{B_q}^2\mathcal{B}_{B_q}(\mu_B), \tag{12}$$

with the decay constant f_{B_q} and the "bag" factor $\mathcal{B}_{B_q}$. The product $\hat{\eta}_B\mathcal{B}_{B_q}$ is scale and scheme invariant. Our convention in Eq. (11) corresponds to a scale-dependent bag parameter with $\mathcal{B}_{B_q} = 1$ in vacuum insertion approximation. Typical values for the bag parameter obtained on the lattice are e.g. $\mathcal{B}_{B_s} \approx 0.84$; see Sec. III A. Sometimes a different normalization with a scale-independent bag

parameter $\hat{\mathcal{B}}_{B_q} = b_B(\mu_B)\mathcal{B}_{B_q}(\mu_B)$ is used. The corresponding quantities $\eta_B = \hat{\eta}_B(\mu_B)/b_B(\mu_B) = 0.551$ and $\hat{\mathcal{B}}_{B_s} \approx 1.28$ obviously satisfy $\eta_B \hat{\mathcal{B}}_{B_s} = \hat{\eta}_B \mathcal{B}_{B_s}$. The analytic formula for $b_B(\mu_B)$ can be found e.g. in Eq. (XIII.5) of [49].

The absorptive term Γ_{12}^q is dominated by on-shell charmed intermediate states, and it can be expressed as a two-point correlator of the $|\Delta B| = 1$ Hamiltonian $H_q^{|\Delta B|=1}$. By performing a $1/m_b$-expansion of this two-point correlator, one can express Γ_{12}^q in terms of Q and another four-quark operator

$$\tilde{Q}_S = \bar{q}_L^\alpha b_R^\beta \bar{q}_L^\beta b_R^\alpha, \tag{13}$$

where S stands for "scalar" and α, $\beta = 1, 2, 3$ are color indices; see [12]. The matrix element is expressed as

$$\begin{aligned}\langle B_q|\tilde{Q}_S|\bar{B}_q\rangle &= \frac{1}{12} M_{B_q}^2 f_{B_q}^2 \tilde{\mathcal{B}}_{S,B_q}\left(\frac{M_{B_q}}{\bar{m}_b + \bar{m}_q}\right)^2 \\ &=: \frac{1}{12} M_{B_q}^2 f_{B_q}^2 \tilde{\mathcal{B}}'_{S,B_q}.\end{aligned} \tag{14}$$

The prediction of Γ_{12}^q involves also operators which are subleading in the heavy quark expansion, the matrix elements of which are parametrized by the bag factors $\mathcal{B}_{R_{0,1,2,3}}$ and $\mathcal{B}_{\tilde{R}_{1,2,3}}$ [12], which satisfy two relations in the heavy quark limit [12,50]:

$$\mathcal{B}_{R_2} = \mathcal{B}_{\tilde{R}_2}, \qquad \mathcal{B}_{R_3} = \frac{5}{7}\mathcal{B}_{\tilde{R}_3} + \frac{2}{7}\mathcal{B}_{\tilde{R}_2}. \tag{15}$$

Even though we have not included the flavor of the light-quark in our notation, we consider these $1/m_b$-suppressed operators to have different values for B_d and B_s mesons.

Finally, we discuss the relative phase ϕ_q between the two off-diagonal terms. In contrast to M_{12}^q, Γ_{12}^q receives non-negligible contributions from subleading u and c CKM couplings, which implies that ϕ_q is not a pure CKM phase in the standard model. The standard model contribution to ϕ_q reads [12,51], with our updated inputs (see Table IX),

$$\begin{aligned}\phi_d^{\mathrm{SM}} &= (-10.1^{+3.7}_{-6.3}) \times 10^{-2}, \\ \phi_s^{\mathrm{SM}} &= (+7.4^{+0.8}_{-3.2}) \times 10^{-3},\end{aligned} \tag{16}$$

and thus in ϕ_s the standard model contribution is clearly subleading in the presence of generic new physics effects.

The previous quantities are expected to be affected by new physics in different ways. While M_{12}^q coming from box diagrams is very sensitive to new physics both for B_d and B_s, Γ_{12}^s stems from Cabibbo-favored tree-level decays and possible new physics effects are expected to be smaller than the hadronic uncertainties. In the case of Γ_{12}^d though, the contributing decays are Cabibbo-suppressed. In this paper, we only consider scenarios where new physics does not enter tree-level decays. More specifically, we assume that B decays proceeding through a four-flavor change (i.e., $b \to q_1\bar{q}_2 q_3$, $q_1 \neq q_2 \neq q_3$) obtain only standard model contributions (SM4FC) [52,53]. This assumption is better defined than just the neglect of new physics contributions to tree-mediated decays since on the non-perturbative level tree and penguin amplitudes cannot be well separated. Our class of four-flavor-change decays includes $b \to d$ decays in which the strong isospin changes by 3/2 units, i.e. we use strong isospin as the flavor quantum number of the first quark generation. Then the following inputs used in the fit are considered to be free from new physics contributions in their extraction from data: $|V_{ud}|$, $|V_{us}|$, $|V_{ub}|$, $|V_{cb}|$, and γ. Also the leptonic decays $B \to \tau\nu$ (or $D_s \to \tau\nu$ and $D_s \to \mu\nu$), which could be significantly affected by charged Higgs exchange contributions (see [54] and references within), are assumed to be standard-model-like. Using these inputs a reference unitarity triangle can be constructed (see the first two articles in Ref. [52]), as will be discussed further in Sec. III B (in Ref. [55], this triangle is compared with the universal unitarity triangle for models of constrained MFV introduced in Ref. [56]).

In addition, in order to take advantage of the measurement of the width differences $\Delta\Gamma_q$, and of the time-dependent CP-asymmetries in dominant $b \to c$ decays, we neglect possible nonstandard contributions to the $b \to c\bar{c}q$ ($q = d$, s) transitions, although they do not strictly enter the SM4FC family. Finally, we assume that the unitarity of the 3×3 CKM matrix still holds in the presence of new physics, which ensures that the standard model contribution to the neutral-meson mixing keeps its usual expression as a function of $(\bar{\rho}, \bar{\eta})$ and other parameters. Hence, our discussion would not hold in the case of an additional sequential fourth fermion family, which however is not excluded yet by experimental constraints (see Refs. [23] or [57] and references therein).

Thus, new physics can find its way into the quantities studied in this paper only by changing magnitude and/or phase of M_{12}^q. It is convenient to define the new physics complex parameters Δ_q and ϕ_q^Δ ($q = d$, s) through

$$M_{12}^q \equiv M_{12}^{\mathrm{SM},q} \cdot \Delta_q, \qquad \Delta_q \equiv |\Delta_q| e^{i\phi_q^\Delta} \tag{17}$$

(see e.g. [12]). With the definition in Eq. (17) the CP phase of Eq. (2) reads

$$\phi_q = \phi_q^{\mathrm{SM}} + \phi_q^\Delta. \tag{18}$$

As discussed in Sec. III, new physics in M_{12}^q will not only affect the neutral-meson mixing parameters, but also the time-dependent analyses of decays corresponding to an interference between mixing and decay.

The relation of Δ_q to the parameters used e.g. in [58–60] is $|\Delta_q| = r_q^2$, $\phi_q^\Delta = 2\theta_q$, and the standard model is of course located at $\Delta_q = 1$. It is more transparent to look at the Cartesian $\mathrm{Im}\Delta_q$ vs $\mathrm{Re}\Delta_q$ plot than the polar $2\theta_q$ vs r_q^2

one, because it visualizes the new physics contribution more clearly and it allows a simple geometrical interpretation of the shape of each individual constraint. For completeness, we note that some authors (e.g. [61–63]; see also [52]) prefer to split the standard model contribution from the pure new physics one in a polar parametrization. The two new physics parameters h_q and $2\sigma_q$ introduced in this way are defined by

$$\frac{M_{12}^q}{M_{12}^{\mathrm{SM},q}} = 1 + \frac{M_{12}^{\mathrm{NP},q}}{M_{12}^{\mathrm{SM},q}} = \Delta_q = 1 + h_q e^{i2\sigma_q}. \tag{19}$$

We will study the case of the neutral kaon system in the following section, defining analogous parameters Δ_K^{tt}, Δ_K^{ct}, and Δ_K^{cc}. But in this paper, we will not consider the neutral D meson system. Indeed, in the scenarios we consider here, D-$\bar{D}$ mixing is severely Glashow-Iliopoulos-Maiani (GIM)-suppressed and gives no useful constraint, as is already the case within the standard model; see e.g. [64].

B. K-$\bar{K}$ mixing basics

The effective $|\Delta S| = 2$ Hamiltonian describing K-$\bar{K}$ mixing resembles the $|\Delta B| = 2$ Hamiltonian of Eq. (7), with the important distinction that now also contributions from internal charm quarks are important:

$$H^{|\Delta S|=2} = [(V_{ts}V_{td}^*)^2 C_{tt} + 2V_{ts}V_{td}^* V_{cs}V_{cd}^* C_{ct} + (V_{cs}V_{cd}^*)^2 C_{cc}]Q + \mathrm{H.c.} \tag{20}$$

with the operator $Q = \bar{d}_L \gamma_\mu s_L \bar{d}_L \gamma^\mu s_L$.[1] As for the case of the B_d and B_s mesons, the contribution from $H^{|\Delta S|=2}$ to M_{12}^K is found from Eq. (6). A new feature is an additive poorly calculable long-distance contribution involving $H^{|\Delta S|=1}$ (see e.g. [37,65]). The Wilson coefficients C_{ij}, i, $j = c, t$, and the operator Q depend on the renormalization scale μ_K at which we evaluate these coefficients and the hadronic matrix element $\langle K|Q|\bar{K}\rangle$. We parametrize the hadronic matrix element as

$$\langle K|Q(\mu_K)|\bar{K}\rangle = \frac{2}{3} m_K^2 f_K^2 \frac{\hat{\mathcal{B}}_K}{b_K(\mu_K)}. \tag{21}$$

Here $f_K \simeq 156$ MeV and m_K are the decay constant and mass of the kaon, respectively, and $\hat{\mathcal{B}}_K$ is the bag parameter, from which a factor $b_K(\mu_K)$ is stripped off. Analogous to the case of B mixing $b_K(\mu_K)$ contains the dependence of $\langle K|Q(\mu_K)|\bar{K}\rangle$ on the renormalization scheme and the renormalization scale μ_K. The standard model values of the Wilson coefficients are

$$\begin{aligned} C_{tt}^{\mathrm{SM}} &= \frac{G_F^2}{4\pi^2} M_W^2 S\left(\frac{\bar{m}_t^2}{M_W^2}\right)\eta_{tt} b_K(\mu_K), \\ C_{ct}^{\mathrm{SM}} &= \frac{G_F^2}{4\pi^2} M_W^2 S\left(\frac{\bar{m}_c^2}{M_W^2}, \frac{\bar{m}_t^2}{M_W^2}\right)\eta_{ct} b_K(\mu_K), \\ C_{cc}^{\mathrm{SM}} &= \frac{G_F^2}{4\pi^2} M_W^2 S\left(\frac{\bar{m}_c^2}{M_W^2}\right)\eta_{cc} b_K(\mu_K), \end{aligned} \tag{22}$$

with the Inami-Lim functions S calculated from the usual box diagrams. By comparing Eqs. (10) and (22) we verify the MFV feature of the standard model $C^{\mathrm{SM}} = C_{tt}^{\mathrm{SM}}$. In C_{cc}^{SM} the Inami-Lim function can be expanded in terms of the tiny quantity $\bar{m}_c^2/M_W^2$ to find $S(x_c) = x_c + O(x_c^2)$. Likewise $S(x_c, x_t) \simeq -x_c \log x_c + x_c F(x_t)$ with $F(\bar{m}_t^2/M_W^2) = 0.56$. From Eqs. (21) and (22), $b_K(\mu_K)$ drops out if $\langle K|H^{|\Delta S|=2}|\bar{K}\rangle$ is expressed in terms of $\hat{\mathcal{B}}_K$. The QCD correction factors η_{cc} [44], η_{ct} [43], and η_{tt} [42] are listed in Table VII. The dominant sources of uncertainty in these quantities are higher-order QCD corrections[2] (η_{cc} also depends on α_s and $\bar{m}_c$ in a sizeable way). The latter dependence is made explicit in Table VII.

In analogy to Eq. (17) we introduce complex parameters for new physics in the three different contributions and write

$$\begin{aligned} M_{12}^K &\equiv \frac{\langle K|H^{|\Delta S|=2}|\bar{K}\rangle}{2M_K} = (V_{ts}V_{td}^*)^2 M_{12}^{tt} + 2V_{ts}V_{td}^* V_{cs}V_{cd}^* M_{12}^{ct} \\ &\quad + (V_{cs}V_{cd}^*)^2 M_{12}^{cc}, \\ M_{12}^{ij} &= M_{12}^{\mathrm{SM},ij}\Delta_K^{ij} \equiv M_{12}^{\mathrm{SM},ij}|\Delta_K^{ij}|e^{i\phi^{\Delta_K^{ij}}}. \end{aligned} \tag{23}$$

The physical quantities associated with K-$\bar{K}$ mixing are the K_L–K_S mass difference $\Delta M_K = M_{K_L} - M_{K_S}$ and the CP-violating quantity ϵ_K. CP violation in $H^{|\Delta S|=1}$ is characterized by ϵ_K'. These quantities are defined as

$$\begin{aligned} \epsilon_K &= \frac{\eta_{00} + 2\eta_{+-}}{3}, \\ \epsilon_K' &= \frac{-\eta_{00} + \eta_{+-}}{3} \quad \text{with} \quad \eta_{ab} \equiv \frac{\mathcal{A}(K_L \to \pi^a\pi^b)}{\mathcal{A}(K_S \to \pi^a\pi^b)}. \end{aligned} \tag{24}$$

Since these two quantities are defined in terms of K_L and K_S, they can be expressed in terms of K-$\bar{K}$ mixing parameters and the isospin decay amplitudes $A(K_0 \to (\pi\pi)_I) = A_I e^{i\delta_I} = a_I e^{i\theta_i} e^{i\delta_I}$, where a_I, δ_I, and θ_I denote the modulus, the "strong" (CP-even) phase and the "weak" (CP-odd) phase of the decay amplitude [37,67,68]. ϵ_K is essentially proportional to the CP phase $\phi_K \equiv \arg(-M_{12}^K/\Gamma_{12}^K)$. In view of the phenomenological "$\Delta I = 1/2$ rule" $a_0/a_2 \approx 22$ (and the fact that all other

[1] We use the same notation for operators in the B and K systems [cf. Eq. (8)], implying the corresponding flavors (b, s, or d) of the quark fields.

[2] Very recently a next-to-next-to-leading order (NNLO) calculation of η_{ct} was performed [66], leading to a value which is 5% larger than the value used here. This result is not yet included in our analysis.

decay modes come with even smaller amplitudes than a_2) one can saturate the inclusive quantity Γ_{12}^K completely by the contribution proportional to a_0^2. Expanding in various small parameters (see Ref. [37] for an elaborate discussion of the approximations involved) one finds:

$$\epsilon_K = \sin\phi_\epsilon e^{i\phi_\epsilon}\left[\frac{\mathrm{Im}M_{12}^K}{\Delta M_K} + \xi\right], \quad \text{with}$$
$$\tan\phi_\epsilon = \frac{2\Delta M_K}{\Delta\Gamma_K} \quad \text{and} \quad \xi = \frac{\mathrm{Im}A_0}{\mathrm{Re}A_0}. \tag{25}$$

The troublesome long-distance contribution to M_{12}^K mentioned after Eq. (20) is eliminated from Eq. (25) by trading $2\,\mathrm{Re}M_{12}^K$ for the experimental value of ΔM_K. Long-distance contributions to $\mathrm{Im}M_{12}^K$ are small [69]. In Eq. (25) ξ comprises the contribution from $\arg(-\Gamma_{12}^K)$ in the limit of A_0 dominance discussed above. The corrections are of order $(a_2/a_0)^2$ and therefore negligible. The usual expression for ϵ_K is obtained from this expression by taking the following further approximations: (i) use $\phi_\epsilon = 45°$ instead of the measured value $\phi_\epsilon = 43.5(7)°$, (ii) neglect ξ, and (iii) compute $\mathrm{Im}M_{12}$ using only the lowest-dimension $d = 6$ operator in the effective Hamiltonian of Eq. (20), which is dominated by top and charm box diagrams. The effect of the three simplifications can be parametrized in terms of the parameter κ_ϵ [9] entering

$$\epsilon_K = \frac{\kappa_\epsilon}{\sqrt{2}} e^{i\phi_\epsilon}\left[\frac{\mathrm{Im}M_{12}^{(6)}}{\Delta M}\right] \tag{26}$$

$$= C_\epsilon \kappa_\epsilon e^{i\phi_\epsilon}\hat{\mathcal{B}}_K\Big[\mathrm{Im}[(V_{cs}V_{cd}^*)^2\Delta_K^{cc}]\eta_{cc}S\left(\frac{\bar{m}_c^2}{M_W^2}\right)$$
$$+ \mathrm{Im}[(V_{ts}V_{td}^*)^2\Delta_K^{tt}]\eta_{tt}S\left(\frac{\bar{m}_t^2}{M_W^2}\right)$$
$$+ 2\,\mathrm{Im}(V_{ts}V_{td}^*V_{cs}V_{cd}^*\Delta_K^{ct})\eta_{ct}S\left(\frac{\bar{m}_c^2}{M_W^2}, \frac{\bar{m}_t^2}{M_W^2}\right)\Big]. \tag{27}$$

The value $\kappa_\epsilon = 1$ corresponds to the approximations (i) through (iii) outlined above. The normalization reads

$$C_\epsilon = \frac{G_F^2 F_K^2 m_K M_W^2}{12\sqrt{2}\pi^2\Delta M_K}. \tag{28}$$

When expressed in terms of Wolfenstein parameters to lowest order in λ, Eq. (26) defines the familiar hyperbola in the $\bar{\rho}$–$\bar{\eta}$ plane.

A series of papers [9,37,69,70] has studied how much the factor κ_ϵ should deviate from 1 in order to account for the terms neglected by the previous approximations. We recall the different elements in Appendix A, separating the uncertainties coming from statistical and systematic sources, and we obtain the estimate

$$\kappa_\epsilon = 0.940 \pm 0.013 \pm 0.023, \tag{29}$$

in good agreement with $\kappa_\epsilon = 0.94 \pm 0.02$ in Ref. [69]. We emphasize that the estimate of κ_ϵ in Eq. (29) relies on the assumption that ϵ_K' is unaffected by new physics (which goes beyond the SM4FC assumption which protects only $I = 2$ final states). From $\epsilon_{K,\mathrm{exp}} = (2.229 \pm 0.010) \times 10^{-3}$ we get the following value for the combination:

$$\epsilon_{K,\mathrm{exp}}^{(0)} = \frac{\epsilon_{K,\mathrm{exp}}}{\kappa_\epsilon} = (2.367 \pm 0.033 \pm 0.049) \times 10^{-3}. \tag{30}$$

In the presence of new physics, the relationship between the measured ϵ_K and the Δ_K^{ij}'s is discussed after Eq. (39).

One can also study the semileptonic CP asymmetry

$$A_L \equiv \frac{\Gamma(K_{\mathrm{long}} \to \ell^+\nu\pi^-) - \Gamma(K_{\mathrm{long}} \to \ell^-\bar{\nu}\pi^+)}{\Gamma(K_{\mathrm{long}} \to \ell^+\nu\pi^-) + \Gamma(K_{\mathrm{long}} \to \ell^-\bar{\nu}\pi^+)}$$
$$= \frac{1 - |q/p|^2}{1 + |q/p|^2},$$

which, however, contains the same information on fundamental parameters as $\mathrm{Re}\epsilon_K$.

C. Master formulas

In this section, we provide the master formulas of the theoretical predictions for the observables relevant to the analysis of new physics contributions in mixing. These formulas reflect the dependences on the most important parameters entering the fit and are obtained from the input values as described in Sec. III. It should be stressed that these numerical equations are shown for illustrative purposes only: the complete formulas are used in the fitting code, which allow one to take into account all the contributions computed so far, together with the correct treatment of the correlations.

Combining Eqs. (3)–(12) with Eq. (17) one finds

$$\Delta M_d = 0.502\ \mathrm{ps}^{-1}\left(\frac{|V_{tb}V_{td}|}{0.0086}\right)^2 \frac{S(\bar{m}_t^2/M_W^2)}{2.35} \times \frac{f_{B_d}^2\mathcal{B}_{B_d}}{(0.17\mathrm{GeV})^2} \cdot |\Delta_d|,$$
$$\Delta M_s = 17.24\ \mathrm{ps}^{-1} \cdot \left(\frac{|V_{tb}V_{ts}^*|}{0.04}\right)^2 \frac{S(\bar{m}_t^2/M_W^2)}{2.35} \times \frac{f_{B_s}^2\mathcal{B}_{B_s}}{(0.21\mathrm{GeV})^2} \cdot |\Delta_s|. \tag{31}$$

The remaining uncertainties in the prefactors of the above formulas are due to the choice of the renormalization scale and the values of α_s and the top quark mass. They are at most 3% and therefore negligible compared to the theoretical error due to the nonperturbative and CKM parameters.

The derivation of the formulas involving Γ_{12}^q is more complicated [12,50,51]. For the B_s system the dependence on the apex $(\bar{\rho}, \bar{\eta})$ of the unitarity triangle is strongly suppressed, in contrast to the B_d system. Furthermore the standard model contribution to a_{fs}^s is tiny and remains

below the present experimental sensitivity, while $a_{\rm fs}^d$ is 1 order of magnitude larger and therefore not completely negligible; see Table IX. Summing up logarithms of the form $m_c^2/m_b^2 \ln m_c^2/m_b^2$ [71] and using the $\overline{\rm MS}$-scheme for the b quark mass one finds from Ref. [12] for the decay rate differences:

$$\Delta\Gamma_d = \left(\frac{f_{B_d}\sqrt{\mathcal{B}_{B_d}}}{0.17\ \text{GeV}}\right)^2\left[0.00241 + 0.00056\frac{\tilde{\mathcal{B}}'_{S,B_d}}{\mathcal{B}_{B_d}} - 0.00047\frac{\mathcal{B}_{R,B_d}}{\mathcal{B}_{B_d}}\right]\cos(\phi_d^{\rm SM} + \phi_d^\Delta), \tag{32}$$

$$\Delta\Gamma_s = \left(\frac{f_{B_s}\sqrt{\mathcal{B}_{B_s}}}{0.21\ \text{GeV}}\right)^2\left[0.0797 + 0.0278\frac{\tilde{\mathcal{B}}'_{S,B_s}}{\mathcal{B}_{B_s}} - 0.0181\frac{\mathcal{B}_{R,B_s}}{\mathcal{B}_{B_s}}\right]\cos(\phi_s^{\rm SM} + \phi_s^\Delta). \tag{33}$$

Now the uncertainties in the coefficients are considerably larger than in the case of the mass differences, but they are still less than about 15%. The dominant theoretical error of the coefficients comes from the renormalization scale μ_1 followed by the CKM factors. One encounters matrix elements of higher-dimensional operators in these expressions, denoted by $\mathcal{B}_R$, which have a power suppression parametrized by $m_b^{\rm pow}$. The general (assuming unitarity of the 3×3 quark mixing matrix) expression for the semileptonic CP asymmetries reads

$$10^4 a_{\rm fs}^q = \left[a_q {\rm Im}\left(\frac{\lambda_u^q}{\lambda_t^q}\right) + b_q {\rm Im}\left(\frac{\lambda_u^q}{\lambda_t^q}\right)^2\right]\frac{\sin(\phi_q^{\rm SM} + \phi_q^\Delta)}{|\Delta_q|}, \tag{34}$$

with $\lambda_x^q = V_{xb}V_{xq}^*$. The coefficients a, b, c read [12,51]

$$\begin{aligned} a_d &= 9.2905 + 0.2973\frac{\tilde{\mathcal{B}}'_{S,B_d}}{\mathcal{B}_{B_d}} + 0.2830\frac{\mathcal{B}_{R,B_d}}{\mathcal{B}_{B_d}},\\ a_s &= 9.4432 + 0.2904\frac{\tilde{\mathcal{B}}'_{S,B_s}}{\mathcal{B}_{B_s}} + 0.2650\frac{\mathcal{B}_{R,B_s}}{\mathcal{B}_{B_s}},\\ b_d &= 0.0720 + 0.0184\frac{\tilde{\mathcal{B}}'_{S,B_d}}{\mathcal{B}_{B_d}} + 0.0408\frac{\mathcal{B}_{R,B_d}}{\mathcal{B}_{B_d}},\\ b_s &= 0.0732 + 0.0180\frac{\tilde{\mathcal{B}}'_{S,B_s}}{\mathcal{B}_{B_s}} + 0.0395\frac{\mathcal{B}_{R,B_s}}{\mathcal{B}_{B_s}},\\ c_d &= -46.8169 - 17.0083\frac{\tilde{\mathcal{B}}'_{S,B_s}}{\mathcal{B}_{B_s}} + 9.2818\frac{\mathcal{B}_{R,B_s}}{\mathcal{B}_{B_s}}, \end{aligned} \tag{35}$$

again with uncertainties in the coefficients of less than 15%. The dominant one comes from the renormalization scale μ_1 followed by the CKM factors. For the semileptonic CP asymmetries in the B_d system we can also write [51]

$$-10^4 a_{\rm fs}^d = \left[c_d + a_d\left(\frac{\cos\beta}{R_t} - 1\right) + b_d\left(\frac{\cos 2\beta}{R_t^2} - 2\frac{\cos\beta}{R_t} + 1\right)\right]\frac{\sin\phi_d^\Delta}{|\Delta_d|} + \left[a_d\frac{\sin\beta}{R_t} + b_d\left(\frac{\sin 2\beta}{R_t^2} - 2\frac{\sin\beta}{R_t}\right)\right]\frac{\cos\phi_d^\Delta}{|\Delta_d|}, \tag{36}$$

where we have written the $(\bar\rho, \bar\eta)$ dependence in terms of the angle β of the unitarity triangle and the side $R_t = \sqrt{(1-\bar\rho)^2 + \bar\eta^2}$.

The mixing-induced CP asymmetries in $B_d \to J/\psi K_S$ and $B_s \to J/\psi\phi$ are very important to constrain ϕ_d and ϕ_s, respectively. For the latter mode an angular analysis is needed to separate the different CP components [72]. The mixing-induced CP asymmetries in the two modes determine

$$\sin(\phi_d^\Delta + 2\beta) \quad \text{and} \quad \phi_s^\Delta - 2\beta_s. \tag{37}$$

Here the angle β_s is defined as positive:

$$\beta_s = -\arg\left(-\frac{V_{ts}^* V_{tb}}{V_{cs}^* V_{cb}}\right) = 0.01818 \pm 0.00085. \tag{38}$$

[This should be compared with $\beta = \arg(-V_{td}^* V_{tb}/V_{cd}^* V_{cb}) \approx 0.38$.][3]

The measured value $|\epsilon_K^{\rm exp}|$ implies the following relation among the CKM elements:

$$1.25\times 10^{-7} = \hat{\mathcal{B}}_K\left[{\rm Im}[(V_{cs}V_{cd}^*)^2\Delta_K^{cc}]\eta_{cc}S\left(\frac{\bar m_c^2}{M_W^2}\right) + {\rm Im}[(V_{ts}V_{td}^*)^2\Delta_K^{tt}]\eta_{tt}S\left(\frac{\bar m_t^2}{M_W^2}\right) + 2\,{\rm Im}(V_{ts}V_{td}^*V_{cs}V_{cd}^*\Delta_K^{ct})\eta_{ct}S\left(\frac{\bar m_c^2}{M_W^2}, \frac{\bar m_t^2}{M_W^2}\right)\right]. \tag{39}$$

Here the number on the LHS originates from

$$1.25\times 10^{-7} = \frac{12\sqrt{2}\pi^2\Delta M_K}{G_{\rm F}^2 f_K^2 m_K M_W^2}\frac{|\epsilon_K^{\rm exp}|}{\kappa_\epsilon}. \tag{40}$$

The peculiar hierarchy of the CKM elements in Eq. (39) enhances the sensitivity to the imaginary part of Δ_K^{cc}. Expanding to lowest nonvanishing order in the Wolfenstein parameter λ shows

[3]It should be emphasized that the Tevatron experiments, which have presented first determinations of $\phi_s^\Delta - 2\beta_s$ from tagged analyses [28,29], also use the notation ϕ_s and β_s, but with a slightly different meaning. Comparing the notation of Refs. [28,29] with our notation one gets

$$\phi_s^{\rm D0} = \phi_s^\Delta - 2\beta_s, \qquad -2\beta_s^{\rm CDF} = \phi_s^\Delta - 2\beta_s.$$

References [28,29] have neglected $2\beta_s$ in the relation between $\Delta\Gamma_s$ and ϕ_s in Eq. (3). This is justified in view of the large experimental errors and the smallness of $2\beta_s$.

$$\begin{aligned}
\mathrm{Im}[(V_{cs}V_{cd}^*)^2\Delta_K^{cc}] &= -2A^2\lambda^6\bar{\eta}\,\mathrm{Re}\Delta_K^{cc} + \lambda^2\,\mathrm{Im}\Delta_K^{cc},\\
\mathrm{Im}[(V_{ts}V_{td}^*)^2\Delta_K^{tt}] &= 2A^4\lambda^{10}(1-\bar{\rho})\bar{\eta}\,\mathrm{Re}\Delta_K^{tt}\\
&\quad + A^4\lambda^{10}[(1-\bar{\rho})^2-\bar{\eta}^2]\,\mathrm{Im}\Delta_K^{tt},\\
2\,\mathrm{Im}(V_{ts}V_{td}^*V_{cs}V_{cd}^*\Delta_K^{ct}) &= 2A^2\lambda^6\bar{\eta}\,\mathrm{Re}\Delta_K^{ct}\\
&\quad + 2A^2\lambda^6(1-\bar{\rho})\,\mathrm{Im}\Delta_K^{ct}. \qquad (41)
\end{aligned}$$

ΔM_K is dominated by physics from low scales. The short-distance contribution is dominated by the charm-charm contribution involving the QCD coefficient η_{cc} [44]. There is an additional long-distance contribution from box diagrams with two internal up quarks, which cannot be calculated reliably. For instance, one could attribute an uncertainty of order 100% to the theory prediction of ΔM_K and try to extract a constraint on $|\Delta_K^{cc}|$ from ΔM_K. While Δ_K^{cc} is very sensitive to any kind of new physics which distinguishes between the first and second quark generations, we will see in Sec. II D that in MFV scenarios all effects on Δ_K^{cc} are totally negligible. In an unspecified non-MFV scenario both ϵ_K and ΔM_K are useless, because Δ_K^{cc}, Δ_K^{ct}, and Δ_K^{tt} are uncorrelated with any other observable entering the global fit of the unitarity triangle, while in MFV scenarios ΔM_K is standard-model-like. Therefore we do not consider ΔM_K any further.

D. Three scenarios

After having introduced our parametrization of new physics in terms of the Δ parameters in Eqs. (17) and (39), we can now discuss the three different physics scenarios which we consider in this article. The common feature of all scenarios is the assumption that all relevant effects of new physics are captured by the Δ parameters. As long as one only considers the quantities entering the global fit of the unitarity triangle in conjunction with the observables of B_s-$\bar{B}_s$ mixing, this property is fulfilled in many realistic extensions of the standard model.[4] However, once a specific model is studied, often other quantities (unrelated to the global fit of the unitarity triangle) constrain the parameter space; prominent examples are branching ratios of rare decays such as $\mathcal{B}(B\to X_s\gamma)$ and $\mathcal{B}(B_s\to\mu^+\mu^-)$. Such effects cannot be included in a model-independent approach like ours. Still, we will see that interesting bounds on the Δ parameters can be found within the broad classes of models defined by our three scenarios. In any specific model covered by our scenarios, the constraints on the Δ parameters can only be stronger, but not weaker than those presented in this paper.

Two scenarios involve the MFV hypothesis. The notion of MFV means that all flavor-violation stems from the Yukawa sector. It is usually implied that all flavor-changing transitions in the quark sector are solely governed by the CKM matrix, while flavor-changing transitions in the lepton sector come with elements of the Pontecorvo-Maki-Nakagawa-Sakata (PMNS) matrix. Strictly speaking, this conclusion is only valid if MFV is invoked at or below the GUT scale. If MFV is built into a GUT model at a higher scale, it is well possible that imprints of the PMNS matrix can be found in FCNC processes of quarks. Indeed, the articles in Ref. [13] discuss supersymmetric GUT models with flavor-blind soft supersymmetry-breaking terms near the Planck scale. The renormalization group evolution involving the large top Yukawa coupling then induces FCNC transitions between right-handed bottom and strange quarks at low energies. In our analysis this situation is a very special case of scenario I discussed below.

1. Scenario I: Non-MFV

In this scenario, we do not assume anything about the flavor structure of the New-Physics interaction. Since here Δ_K^{cc}, Δ_K^{ct}, and Δ_K^{tt} are unrelated to other parameters, we can neither derive any constraints on these parameters nor use ϵ_K in the global fit. While Δ_d and Δ_s are *a priori* independent, the allowed ranges for these parameters are nevertheless correlated through the global fit and the unitarity constraints on the CKM matrix. This can be qualitatively understood as follows. Consider a value for $|\Delta_s|$ which exhausts the range allowed by the hadronic uncertainties in ΔM_s. The good theoretical control over the ratio $\Delta M_d/\Delta M_s$ then fixes $|V_{td}|^2|\Delta_d|$ quite precisely. The global fit of the unitarity triangle further constrains $|V_{td}|\propto\sqrt{(1-\bar{\rho})^2+\bar{\eta}^2}$, so that *a posteriori* the allowed ranges for $|\Delta_d|$ and $|\Delta_s|$ become correlated. Also the flavor-mixed CP-asymmetry a_{fs} measured at the Tevatron experiments correlates the parameters Δ_d and Δ_s.

2. Scenario II: MFV with small bottom Yukawa coupling

We adopt the symmetry-based definition of MFV of Ref. [4] to discuss our two other scenarios. Ignoring the lepton sector here, the starting point is the $[U(3)]^3$ flavor symmetry of the gauge sector of the standard model, which entails the flavor-blindness of this sector. The gauge part of the Lagrangian is invariant under independent unitary rotations of the left-handed quark doublets Q_L^i (where $i=1,2,3$ labels the generation), and the right-handed quark singlets d_R^i and u_R^i in flavor space. In the standard model the $[U(3)]^3$ flavor symmetry is broken by the Yukawa interactions. This symmetry breaking permits discriminating flavor quantum numbers, quark masses and flavor-changing transitions. Within the standard model only the top Yukawa coupling y_t is large, all other Yukawa couplings are small or even tiny. These small parameters pose a challenge to generic extensions of

[4]A notable exception are models with large couplings of a light charged-Higgs boson to down-type fermion. In such models $\mathcal{B}(B\to\tau\nu_\tau)$, which we assume to be standard-model-like, is modified. Another exception are models with a nonunitary 3×3 CKM matrix, e.g with new fermion generations.

the standard model. This challenge is met by the MFV hypothesis which extends the standard model assuming that the only sources of $[U(3)]^3$ flavor symmetry breaking remain the Yukawa couplings. Specifying to the familiar basis of mass eigenstates, we list the following consequences of the MFV hypothesis:

(i) Any flavor-changing transition is governed by the same CKM elements as in the standard model.
(ii) Any chirality flip $q_R \to q_L$ is proportional to the Yukawa coupling y_q (and, by Hermiticity of the Lagrangian, any $q_L \to q_R$ flip is proportional to y_q^*).
(iii) Any flavor-changing transition of a right-handed quark involves a factor of the corresponding Yukawa coupling.
(iv) FCNC transitions have the same pattern of GIM cancellations as in the standard model.

For example, properties (i) and (iii) imply that any $b_R \to s_R$ transition is of the form $V_{ts}V_{tb}^* y_b y_s^* f(|y_t|^2, |y_b|^2, |y_s|^2|)$, where f is some function of $|y_{t,s,b}|^2$. The actual power of Yukawa couplings in the contribution from a given Feynman diagram is determined by the number of chirality flips through property (ii). Property (iv) ensures that any possible contribution proportional to $V_{cs}V_{cb}^*$ is GIM-suppressed, i.e. proportional to $|y_c|^2$, and negligible as in the standard model.

However, we deviate in one important aspect from Ref. [4]. We explicitly allow for CP-violating phases which do not originate from the Yukawa sector, i.e., we proceed as in Ref. [5]. CP violation is an interference phenomenon and involves the differences from otherwise unphysical phases. In order to avoid new CP phases one must align the phases of the Yukawa couplings with those of other parameters which are unrelated to the Yukawa sector. For instance, in the context of the minimal supersymmetric standard model (MSSM) this tuning of phases affects the μ term, the gaugino mass terms, and the trilinear soft SUSY-breaking terms. It is difficult to motivate this alignment from symmetries or through a dynamical mechanism. We therefore explicitly permit extra CP phases outside the Yukawa sector, i.e. we consider effects from flavor-conserving CP phases. Usually such phases are constrained by experimental bounds on electric dipole moments, in particular, for the MSSM, where stringent bounds on flavor-conserving CP phases can only be avoided with quite heavy superparticles. But in our context of generic MFV sizeable flavor-conserving CP phases cannot be excluded *a priori* [73].

References [4,5] consider two possibilities for the dominant flavor-symmetry breaking mechanism. While the large top Yukawa coupling always breaks the flavor symmetries of the gauge sector, one can consider the case that the bottom Yukawa coupling is also large and spoils flavor blindness at an equal level (this occurs in the popular MSSM scenarios with large $\tan\beta$ [74]). Our scenario II corresponds to the case, where only the top Yukawa coupling is large. That is, in scenario II we neglect all effects from down-type Yukawa couplings. The possible $|\Delta B| = 2$ operators are discussed in Refs. [4,5]. Thanks to MFV property (iii), four-quark operators with right-handed b or s fields are accompanied by small (down-type) Yukawa couplings [4,5] and no other operator than Q in Eq. (8) occurs in scenario II. Therefore, the only effect of new physics is to change the coefficient C in Eq. (7).

An important observation is that C will always be real, even in the presence of flavor-conserving CP phases: The MFV hypothesis implies that C is independent of the flavors of the external quarks. If we interchange b_L and q_L, the corresponding four-quark interaction will be governed by the same coefficient C and the effective Hamiltonian will contain the combination

$$(V_{tq}^* V_{tb})^2 C \bar{q}_L \gamma_\mu b_L \bar{q}_L \gamma^\mu b_L + (V_{tb}^* V_{tq})^2 C \bar{B}_L \gamma_\mu q_L \bar{B}_L \gamma^\mu q_L.$$

Now the Hermiticity of the Hamiltonian implies $C = C^*$. (An explicit check is provided by the MSSM, where flavor-conserving CP-violating parameters enter C only through their moduli or real parts). Hence our scenario II corresponds to the case

$$\Delta_s = \Delta_d = \Delta_K^{tt} \quad \text{with} \quad \phi_s^\Delta = \phi_d^\Delta = \phi_K^{ij\Delta} = 0. \tag{42}$$

We next discuss an important extension of the MFV analysis of Ref. [4] in the case of ϵ_K, where we include effects from the charm Yukawa coupling y_c. The potential relevance of these effects becomes clear when one notices that the Inami-Lim functions $S(\bar{m}_c^2/M_W^2, \bar{m}_t^2/M_W^2)$ and $S(\bar{m}_c^2/M_W^2)$ are proportional to $\bar{m}_c^2/M_W^2$. Within the standard model a substantial contribution to the ϵ_K-hyperbola stems from terms which are quadratic in y_c, and we have to extend our analysis of MFV new physics to order y_c^2. Splitting the Wilson coefficients as

$$C = C^{\mathrm{SM}} + C^{\mathrm{NP}}, \qquad C_{ij} = C_{ij}^{\mathrm{SM}} + C_{ij}^{\mathrm{NP}}, \tag{43}$$

MFV constrains the new contributions C^{NP}, C_{ij}^{NP} to obey the following pattern:

$$C_{ij}^{\mathrm{NP}} = V_{is}V_{id}^* V_{js}V_{jd}^* f(|y_i|^2, |y_j|^2), \tag{44}$$

where f is a real-valued function with $f(0, x) = f(x, 0) = 0$ by the GIM mechanism and, of course, $C^{\mathrm{NP}}(\mu) = C_{tt}^{\mathrm{NP}}(\mu)$. We must now distinguish two cases depending on whether the dominant contributions from new physics affect the diagrams with the light charm or up quarks or rather involve particles with a mass similar to or heavier than the top quark.

In the first case, we have to consider new physics contributions C_{ct}^{NP} and C_{cc}^{NP} which involve the charm and up quarks on an internal line. Such contributions occur, for example, in box diagrams in which one or both W bosons are replaced by charged Higgs bosons. These diagrams

with only light internal quark lines lead to negligible effects, if the new particle exchanged between the quark lines is a scalar (like a Higgs boson), because scalars couple left-handed to right-handed fields and come with the penalty of small Yukawa couplings. The extra helicity flip (if an internal quark is right-handed) or the GIM mechanism (on an internal line with only left-handed quarks) brings in extra Yukawa couplings and the contribution to $C_{ct}^{\rm NP}$ and $C_{cc}^{\rm NP}$ is of order $|y_c|^4$ or smaller and negligible compared to standard model contributions, which are proportional to $\bar{m}_c^2 \propto |y_c|^2$. A scaling like in the standard model, with just two powers of $|y_c|$, could occur in principle if the new exchanged particle is a heavy gauge boson mimicking the standard model couplings to the left-handed quark doublets. We are not aware of a realistic theory with such particles and do not consider this possibility further.

The second case corresponds to new physics contributions which involve heavy particles and directly add to the coefficient C in Eq. (10). This class of contributions includes box diagrams with a charged Higgs and one charm and one top quark as internal quark lines. These diagrams indeed give a contribution to $C_{ct}^{\rm NP}$ proportional to $|y_c|^2$. Another prominent example for a contribution of this type are the chargino-squark diagrams in the MSSM and it is worthwhile to discuss this example for illustration, before returning to our generic scenario. The chargino-stop box diagram, which contributes to Δ_K^{tt}, is widely discussed in the literature. However, to our knowledge, nobody has studied the corresponding effect in Δ_K^{ct} or Δ_K^{cc}. The former parameter receives contributions from a box diagram with an scharm on one line and an stop on the other. In the limit $y_c = 0$ there is an exact GIM cancellation between the contributions from the charm and up squarks, which has been invoked to justify the omission of scharm effects. The first nonvanishing contribution is proportional to $|y_c|^2$ (corresponding to $\tilde{c}_L \to \tilde{c}_R$ and $\tilde{c}_R \to \tilde{c}_L$ flips). Since the same flip is needed on the stop line, there is also a factor of $|y_t|^2$ involved. Clearly, we recognize the pattern of Eq. (44) with the same function f as in Δ_K^{tt}. Extending to the generic MFV situation, it is easy to relate Δ_K^{ct} to Δ_K^{tt} for theories in which y_t is small enough that we can expand Δ_K^{ct} and Δ_K^{tt} to the lowest order in y_t (like in the MSSM for moderate values of $\tan\beta$ and not-too-large values of the trilinear breaking term A_t).[5] Then

$$f(|y_i|^2, |y_j|^2) = f_0 |y_i|^2 |y_j|^2 + \mathcal{O}(|y_{i,j}|^6), \qquad (45)$$

and up to small corrections one has $C_{ct}^{\rm NP} = C_{tt}^{\rm NP} |y_c|^2/|y_t|^2$ and $C_{cc}^{\rm NP} = C_{tt}^{\rm NP} |y_c|^4/|y_t|^4$. Since $C_{cc}^{\rm NP}$ is real in scenario II, we can certainly neglect it and set $\Delta_K^{cc} = 1$ in Eq. (39). To account for the situation that y_t is close to 1 we should vary $C_{ct}^{\rm NP}$ around $C_{tt}^{\rm NP} |y_c|^2/|y_t|^2$. A realistic range for $C_{ct}^{\rm NP}$ can be obtained from the standard model situation. In $S(\bar{m}_{c,t}^2/M_W^2)$ the relevant quantity is $\bar{m}_{c,t}/M_W \sim 2y_{c,t}$. However, while $S(\bar{m}_c^2/M_W^2) \simeq \bar{m}_c^2/M_W^2$, $S(\bar{m}_t^2/M_W^2)$ differs from $\bar{m}_t^2/M_W^2$ by a bit less than a factor of 2. We take this as a conservative estimate and choose

$$C_{ct}^{\rm NP} = \lambda_K \frac{\bar{m}_c^2(\mu_{\rm NP})}{\bar{m}_t^2(\mu_{\rm NP})} C_{tt}^{\rm NP} \quad \text{with} \quad 0.5 \le \lambda_K \le 2, \qquad (46)$$

while $C_{cc}^{\rm NP} = 0$. As indicated in Eq. (46), the Yukawa couplings y_c and y_t, which are expressed in terms of $\bar{m}_c$ and $\bar{m}_t$, enter the Wilson coefficients at the scale $\mu_{\rm NP}$ at which the heavy particles of the new physics scenario are integrated out. Since $\bar{m}_c/\bar{m}_t$ is scale-independent, we evaluate this ratio at the scale $\mu = \bar{m}_t$ in the following.

Since no new operators occur in scenario II, our new physics parameters are related to the Wilson coefficient C in a simple way:

$$\Delta_K^{ij} = \frac{C_{ij}}{C_{ij}^{\rm SM}} = 1 + \frac{C_{ij}^{\rm NP}}{C_{ij}^{\rm SM}}. \qquad (47)$$

Equations (46) and (47) imply the relation

$$\begin{aligned}\Delta_K^{ct} &= 1 + \lambda_K \frac{\bar{m}_c^2(\bar{m}_t)}{\bar{m}_t^2(\bar{m}_t)} \frac{C_{tt}^{\rm SM}}{C_{ct}^{\rm SM}} (\Delta_K^{tt} - 1) \\ &= 1 + \lambda_K \frac{\bar{m}_c^2(\bar{m}_t)}{\bar{m}_t^2(\bar{m}_t)} \frac{S(\bar{m}_t^2/M_W^2)\eta_{tt}}{S(\bar{m}_c^2/M_W^2, \bar{m}_t^2/M_W^2)\eta_{ct}} (\Delta_K^{tt} - 1) \qquad (48) \\ &= 1 + 0.017 \lambda_K (\Delta_K^{tt} - 1). \qquad (49)\end{aligned}$$

The numerical value 0.017 is obtained for the central values of Table VII. The smallness of this number roots in the enhancement of $S(\bar{m}_c^2/M_W^2, \bar{m}_t^2/M_W^2)$ by the large leading logarithm $\log(\bar{m}_c^2/M_W^2) = -8.3$, which stems from box diagrams with internal charm and up quarks. This logarithm is absent in the new physics contribution, which is formally of the order of a next-to-leading-order correction. In summary, Eqs. (42) and (48) and $\Delta_K^{cc} = 1$ define our scenario II.

Potential new physics effects governed by y_c have also been studied in [5] in generic $s \to d$ transitions. This reference estimates their size as of order 1% of the contribution governed by y_t and finds them negligible. Our result in Eq. (49), specific to K–$\bar{K}$ mixing, is in agreement with this estimate. In view of the subpercent experimental error of ϵ_K and decreasing theoretical uncertainties, the correction Δ_K^{ct} is not negligible *a priori*.

3. Scenario III: MFV with a large bottom Yukawa coupling

In scenario III we consider a large bottom Yukawa coupling. Then $H_q^{|\Delta B|=2}$ in Eq. (7) is modified to include operators that are not suppressed anymore

[5]The actual expansion parameter is $y_t v/M$, where M is the mass scale of the new particles in the loop and $v = 174$ GeV is the Higgs vacuum expectation value.

$$H_q^{|\Delta B|=2} = (V_{tq}^* V_{tb})^2 [CQ + C_S Q_S + \tilde{C}_S \tilde{Q}_S] + \text{H.c.} \quad (50)$$

Here $Q_S = \bar{q}_L b_R \bar{q}_L b_R$ and $\tilde{Q}_S$ is defined in Eq. (13). MFV does not put any constraint on C_S and $\tilde{C}_S$ which can be complex (an example of an MSSM scenario with a complex C_S can be found in Ref. [75], and an up-to-date renormalization-group analysis of C_S and $\tilde{C}_S$ can be found in the appendix of the fifth article in Ref. [16]). In the following, we will assume that the matrix elements of Q, Q_S, $\tilde{Q}_S$ are affected in the same way by U-spin breaking corrections, so that the presence of new operators in $H_q^{|\Delta B|=2}$ yields a scenario III corresponding to the case $\Delta_s = \Delta_d$ with generally nonzero $\phi_s^\Delta = \phi_d^\Delta$.

C_S and $\tilde{C}_S$ necessarily involve at least two powers of y_b because of MFV property (iii). In the kaon case, the corresponding contribution to analogous coefficients C_S and $\tilde{C}_S$ in $H^{|\Delta S|=2}$ would involve y_s^2 instead. Clearly, such contributions to Δ_K^{tt} and Δ_K^{ct} will have a negligible impact on ϵ_K, but this need not be the case for Δ_K^{cc}, in view of the big lever arm in Eq. (41), meaning that the coefficient of $\text{Im}\Delta_K^{cc}$ is larger than that of $\text{Re}\Delta_K^{cc}$ by 3 orders of magnitude. Contributions to Δ_K^{cc} from box diagrams with new heavy particles involve four powers of $|y_c|$ in addition to the two powers of y_s and are negligible compared to the standard model contribution $\propto |y_c|^2$ even when multiplied by a factor of 1000. New contributions involving internal charm quarks (or some new neutral scalar particle coupling a d_L to an s_R) can be proportional to $|y_c|^2$ as in the standard model, but the two powers of y_s are sufficient to suppress the effect below a level which is relevant for ϵ_K. In addition, in scenario III, C will be a function of $|y_b|^2$, which complicates the relationship to the corresponding coefficient in $H^{|\Delta S|=2}$ and even our proof that C is real does not hold anymore. In summary, our scenario III comes with $\Delta_s = \Delta_d$ and this parameter is complex. The parameters Δ_K^{ij} are as in scenario II (that is, they are real, fulfill Eq. (48), and $\Delta_K^{cc} = 1$), but are now unrelated to $\Delta_{d,s}$.

We disagree with Ref. [5] on one point here, namely, the possibility of $\mathcal{O}(50\%)$ effects in ϵ_K through a sizeable complex contribution to (in our notation) Δ_{tt}. The claimed effect involves two powers of the strange Yukawa coupling y_s. The MFV property links this contribution to a similar one in B-$\bar{B}$ mixing, which involves two powers of y_b instead. A 50% effect in ϵ_K from this source would imply an enhancement of B-$\bar{B}$ mixing by almost 2 orders of magnitude from this term. We do not see how extra contributions with more powers of y_b could possibly reduce this enhancement to a factor below 1.

One ought to mention that scenarios II and III do not exhaust the possibilities offered by MFV. For instance, Refs. [16,74] consider MFV-MSSM scenarios with $M_{\text{SUSY}} \gg M_{A^0} \gtrsim v$, where M_{SUSY} and M_{A^0} denote the masses of the superparticles and the CP-odd Higgs boson, respectively, and $v = 174$ GeV is the electroweak scale. In the MSSM the coefficient C_S is highly suppressed [16],[6] while the operator $\bar{s}_L b_R \bar{s}_R b_L$ occurs with a sizeable coefficient, despite of the suppression with the small strange Yukawa coupling. Its counterpart in the B_d system comes with the even smaller down Yukawa coupling and is negligible. In the scenario of Refs. [16,74] the connection between B_s-$\bar{B}_s$ mixing and B_d-$\bar{B}_d$ mixing is lost. But large effects in B_s-$\bar{B}_s$ mixing are not allowed, due to the experimental bound on $\mathcal{B}(B_s \to \mu\mu)$ [16] (for up-to-date results, see [76]).

4. Testing the standard model

There are various ways to test the standard model. The simplest one is to determine all the relevant parameters from a global fit, and test the fit prediction for a given observable compared with the direct measurement. This kind of test, which can be quantified by computing the relevant pull value, is independent of any underlying new physics scenario.

The second kind of test addresses a definite new physics scenario extending the standard model, and computes the statistical significance that the parameters take their standard model value. In our case it corresponds to testing whether one or several Δ parameters are compatible with $\Delta = 1$.

In the relevant sections below we will perform both kind of tests, and discuss their interpretation.

III. INPUTS

In this section, we discuss all relevant experimental and theoretical inputs entering the fits. The corresponding values and uncertainties are quoted in Tables VI and VII. In general, if there is only one uncertainty quoted, we understand this error as a statistical one. In case of two error contributions, the first one is taken as a statistical error while the second, theoretical, error is treated as an allowed range for the observable or the parameter under consideration. This kind of uncertainty is treated in the Rfit scheme described in Refs. [53,84].

A. Hadronic parameters and method of averaging

Several hadronic inputs are required for the fits presented, and we mostly rely on lattice QCD (LQCD) simulations to estimate these quantities involving strong interactions at low energies. The presence of results from different lattice QCD collaborations with various statistics and systematics make it all the more necessary to combine them in a careful way. The procedure that we have chosen to determine these lattice averages is as follows: We collect

[6]The vanishing of C_S in the MFV-MSSM scenario with $M_{\text{SUSY}} \gg M_{A^0} \gtrsim v$ stems from a softly broken Peccei-Quinn symmetry [4], which we have not built into our scenarios II and III.

the relevant calculations of the quantity that we are interested in and we take only unquenched results with 2 or 2 + 1 dynamical fermions, even those from proceedings without a companion article (flagged with a star). In these results, we separate the error estimates into a Gaussian part and a flat part that is treated *à la* Rfit. The Gaussian part collects the uncertainties from purely statistical origin, but also the systematics that can be controlled and treated in a similar way (e.g., interpolation or fitting in some cases). The remaining systematics constitute the Rfit error. If there are several sources of error in the Rfit category, we add them linearly.[7] The Rfit model is simple but also very strict. It amounts to assuming that the theoretical uncertainty is rigorously constrained by a mathematical bound that is our only piece of information. If Rfit is taken *stricto sensu* and the individual likelihoods are combined in the usual way (by multiplication), the final uncertainty can be underestimated, in particular, in the case of marginally compatible values. We correct this effect by adopting the following averaging recipe. We first combine the Gaussian uncertainties by combining the likelihoods restricted to their Gaussian part. Then we assign to this combination the smallest of the individual Rfit uncertainties. The underlying idea is twofold:

(i) the present state of the art cannot allow us to reach a better theoretical accuracy than the best of all estimates.

(ii) this best estimate should not be penalized by less precise methods (as it would happen be the case if one took the dispersion of the individual central values as a guess of the combined theoretical uncertainty).

It should be stressed that the concept of a theoretical uncertainty is ill-defined, and the combination of them even more. Thus our approach is only one among the alternatives that can be found in the literature [85,86]. In contrast to some of the latter, ours is algorithmic and can be reproduced. Moreover, we differ from the Particle Data Group-like method advocated in Ref. [86] on two points. We separate systematic and statistical errors, which prevents us from assigning a reduced systematics to a combination of several results suffering from the same systematic uncertainty. We do not attempt estimating the (partial) correlations between the results from different collaborations, even though we are aware of their existence (results from the same gauge configuration, using the same procedure to determine the lattice spacing). Whatever the averaging method chosen, one should emphasize that it relies crucially on the quality of the error estimation performed by each collaboration.

[7]Keeping in mind that in many papers this combination is done in quadrature and the splitting between different sources is not published.

The following tables show the inputs used and the average obtained by applying the procedure described above for the following hadronic parameters: the decay constant f_{B_s} for the B_s meson (Table I), the ratio of decay constants f_{B_s}/f_{B_d} (Table II), the scheme-invariant bag parameter $\hat{\mathcal{B}}_{B_s} = 1.523\mathcal{B}_{B_s}(m_b)$ for the B_s meson discussed after Eq. (12) (Table III), the ratio of bag parameters $\mathcal{B}_{B_s}/\mathcal{B}_{B_d}$ (Table IV),[8] and the bag parameter $\mathcal{B}_K(2\ \mathrm{GeV})$ for the neutral kaon (Table V).

We are not aware of lattice estimates for the power-suppressed matrix elements corresponding to $\mathcal{B}_{R_i}$ and $\mathcal{B}_{\tilde{R}_i}$. We will assign them a default value of 1 ± 0.5, taking a flat uncertainty for the two bag parameters contributing the most to $\Delta\Gamma^q$ and a^q_{SL} ($\mathcal{B}_{\tilde{R}_2}$ and $\mathcal{B}_{\tilde{R}_3}$ respectively), whereas the remaining ones are either assigned a Gaussian uncertainty ($\mathcal{B}_{R_0}$, $\mathcal{B}_{R_1}$, $\mathcal{B}_{\tilde{R}_1}$), or determined from the heavy quark effective theory relations Eq. (15) ($\mathcal{B}_{R_2}$, $\mathcal{B}_{R_3}$) for which we allow a 20% power correction modelized as a flat error. All these bag parameters vary independently for B_d and B_s mesons, i.e. we do not assume the exact SU(3) symmetry for them.

B. Observables not affected by new physics in mixing

In this section, we first discuss the observables allowing us to establish an universal preferred region in the $\bar{\rho} - \bar{\eta}$ subspace, independent of any new physics contributions in mixing.

(i) The CKM matrix element $|V_{ud}|$ has been determined from three different methods: superallowed nuclear β-decays, neutron β-decay, and pion β-decay. Currently, the best determination of $|V_{ud}|$ comes from superallowed β-decays where the uncertainty is dominated by the theoretical error; see e.g. Refs. [46,101]. An analysis by Towner and Hardy [77] focusing on an improvement of the isospin-symmetry-breaking terms finds a central value for $|V_{ud}|$ which is larger though still compatible when compared to values quoted in the past, with a slightly reduced uncertainty: $|V_{ud}| = 0.97425 \pm 0.00022$.

(ii) The matrix element $|V_{us}|$ can be determined from $K_{\ell 3}$ decays, from hadronic τ decays, and from semileptonic hyperon decays. We are using the $K_{\ell 3}$ average quoted by Flavianet [78]. The experimental number for $f_+(q^2 = 0) \cdot |V_{us}|$ obtained by averaging results from ISTRA+, KLOE, KTeV, and NA48(/2), as quoted by Flavianet, is

[8]Some of the lattice collaborations [93,94] provide only the parameter $\xi_B = (f_{B_s}/f_{B_d})\sqrt{\mathcal{B}_{B_s}/\mathcal{B}_{B_d}}$ together with the ratio of decay constants, without providing the correlation coefficient between the two values. In such a case, we have extracted the ratio of bag parameters and its uncertainties errors assuming a 100% correlation in the systematic errors between ξ_B and f_{B_s}/f_{B_d}.

TABLE I. Calculations and average used for the decay constant f_{B_s}. N_f stands for the number of dynamical flavors used in the simulation. The first uncertainty quotes the statistical uncertainty, the second the Rfit error.

Collaboration	N_f	$f_{B_s} \pm \sigma_{\text{stat}} \pm \sigma_{R\text{fit}}$	Reference
CP-PACS01	2	$242 \pm 9^{+53}_{-34}$	[87]
MILC02	2	$217 \pm 6^{+58}_{-31}$	[88]
JLQCD03	2	$215 \pm 9^{+19}_{-15}$	[89]
ETMC09	2	$243 \pm 6 \pm 15$	[90]
HPQCD03	2 + 1	$260 \pm 7 \pm 39$	[91]
FNAL-MILC09	2 + 1	$243 \pm 6 \pm 22$	[92]
HPQCD09	2 + 1	$231 \pm 5 \pm 30$	[93]
Our average		$231 \pm 3 \pm 15$	

TABLE II. Calculations and average used for the ratio of decay constants f_{B_s}/f_{B_d}. N_f stands for the number of dynamical flavors used in the simulation. The first uncertainty quotes the statistical uncertainty, the second the Rfit error.

Collaboration	N_f	$f_{B_s}/f_{B_d} \pm \sigma_{\text{stat}} \pm \sigma_{R\text{fit}}$	Reference
CP-PACS01	2	$1.179 \pm 0.018 \pm 0.023$	[87]
MILC02	2	$1.16 \pm 0.01^{+0.08}_{-0.04}$	[88]
JLQCD03	2	$1.13 \pm 0.03^{+0.17}_{-0.02}$	[89]
ETMC09	2	$1.27 \pm 0.03 \pm 0.04$	[90]
FNAL-MILC09	2 + 1	$1.245 \pm 0.028 \pm 0.049$	[92]
HPQCD09	2 + 1	$1.226 \pm 0.020 \pm 0.033$	[93]
RBC/UKQCD10	2 + 1	$1.15 \pm 0.05 \pm 0.20$	[94]
Our average		$1.209 \pm 0.007 \pm 0.023$	

$f_+(q^2 = 0) \cdot |V_{us}| = 0.2163 \pm 0.0005$ leading to $|V_{us}| = 0.2254 \pm 0.0013$ [78,102].

(iii) The matrix element $|V_{cb}|$ is obtained from semileptonic decays $B \to X_c \ell \nu$, where X_c is either a D^* meson (exclusive method) or a sum over all hadronic final states containing charm (inclusive method). For several years the most precise value has been provided by the inclusive method where the theoretical uncertainties have been pushed below the 2% level by determining the relevant nonperturbative heavy quark expansion (HQE) parameters from moment measurements in $B \to X_c \ell \nu$ and $B \to X_s \gamma$ decays. The inclusive $|V_{cb}|$ value used in our analysis is taken from the Heavy Flavour Averaging Group (HFAG) [47], $|V_{cb,\text{incl}}| = (41.85 \pm 0.43 \pm 0.59) \times 10^{-3}$, where the first error contains the experimental and HQE uncertainties and the second reflects the theoretical uncertainty on the total rate prediction for $B \to X_c \ell \nu$. The theoretical uncertainty on the exclusive $|V_{cb}|$ determination in the calculation of the form factor value at zero recoil $F(1)$ has not been competitive so far. A recent calculation provides a significantly smaller error budget: $F(1) = 0.921 \pm 0.013 \pm 0.020$ [103], although the exclusive $|V_{cb}|$ determination still gives a larger uncertainty. Using the average value for the product $F(1)|V_{cb}| = (36.04 \pm 0.52) \times 10^{-3}$ from HFAG [47] and applying a 0.7% QED correction [104], one finds $|V_{cb,\text{excl}}| = (38.85 \pm 0.56_{\text{exp}} \pm 0.55_{\text{theostat}} \pm 0.84_{\text{theosys}}) \times 10^{-3} = (38.85 \pm 0.77 \pm 0.84) \times 10^{-3}$, which has a smaller central value than the inclusive result. We average the two $|V_{cb}|$ values in such a way that the smallest theoretical uncertainty is preserved similarly to our procedure to average lattice inputs and we obtain $|V_{cb}| = (40.89 \pm 0.38 \pm 0.59) \times 10^{-3}$, keeping in mind, however, that the inclusive and exclusive numbers are not in perfect agreement.

TABLE III. Calculations and average used for the bag parameter $\hat{\mathcal{B}}_{B_s}$. N_f stands for the number of dynamical flavors used in the simulation. The first uncertainty quotes the statistical uncertainty, the second the Rfit error.

Collaboration	N_f	$\hat{\mathcal{B}}_{B_s} \pm \sigma_{\text{stat}} \pm \sigma_{R\text{fit}}$	Reference
JLQCD03	2	$1.299 \pm 0.034^{+0.122}_{-0.095}$	[89]
HPQCD06	2 + 1	$1.168 \pm 0.105 \pm 0.140$	[95]
RBC/UKQCD07	2 + 1	$1.21 \pm 0.05 \pm 0.05$	[96]
HPQCD09	2 + 1	$1.326 \pm 0.04 \pm 0.03$	[93]
Our average		$1.28 \pm 0.02 \pm 0.03$	

TABLE IV. Calculations and average used for the bag parameter ratio $\mathcal{B}_{B_s}/\mathcal{B}_{B_d}$. N_f stands for the number of dynamical flavors used in the simulation. The first uncertainty quotes the statistical uncertainty, the second the Rfit error.

Collaboration	N_f	$\mathcal{B}_{B_s}/\mathcal{B}_{B_d} \pm \sigma_{\text{stat}} \pm \sigma_{R\text{fit}}$	Reference
JLQCD03	2	$1.017 \pm 0.016^{+0.076}_{-0.017}$	[89]
HPQCD09	2 + 1	$1.053 \pm 0.020 \pm 0.030$	[93]
RBC/UKQCD10	2 + 1	$0.96 \pm 0.02 \pm 0.03$	[94]
Our average		$1.006 \pm 0.010 \pm 0.030$	

TABLE V. Calculations and average used for the bag parameter $\mathcal{B}_K(2\text{ GeV})$. N_f stands for the number of dynamical flavors used in the simulation. The first uncertainty quotes the statistical uncertainty, the second the Rfit error.

Collaboration	N_f	$\mathcal{B}_K(2\text{ GeV}) \pm \sigma_{\text{stat}} \pm \sigma_{R\text{fit}}$	Reference
JLQCD08	2	$0.537 \pm 0.004 \pm 0.072$	[97]
HPQCD/UKQCD06	2 + 1	$0.618 \pm 0.018 \pm 0.179$	[98]
RBC/UKQCD07	2 + 1	$0.524 \pm 0.010 \pm 0.052$	[99]
ALVdW09	2 + 1	$0.527 \pm 0.006 \pm 0.049$	[100]
Our average		$0.527 \pm 0.0031 \pm 0.049$	

(iv) The two methods to extract $|V_{ub}|$, the inclusive and the exclusive ones (using the theoretically cleanest $B \to \pi \ell \nu$ decays), both suffer from significant theoretical uncertainties. The exclusive measurements prefer values around 3.5×10^{-3} [47]. The numbers quoted are from partial rates measured at large q^2 (> 16 GeV^2) or at small q^2 (< 16 GeV^2), using form factor calculations from lattice QCD [105,106], or light cone sum rules (LCSR) [107], respectively. The fit input is the average of these numbers, following the same procedure as for the lattice QCD parameters: $|V_{ub,\mathrm{excl}}| = (3.51 \pm 0.10 \pm 0.46) \times 10^{-3}$.

The average of inclusive results quoted by HFAG using [47] the shape function (SF) scheme [108] yields $(4.32 \pm 0.16^{+0.22}_{-0.23}) \times 10^{-3}$, where the first uncertainty contains the statistical and experimental systematic uncertainty as well as the modelling errors for $b \to u \ell \nu$ and $b \to c \ell \nu$ transitions. Compared to HFAG, we modify the assignment of the uncertainties as follows. We add the following uncertainties in quadrature: statistical uncertainty, experimental systematics, $b \to c$ and $b \to u$ modeling and the error from the HQE parameters (b-quark mass m_b and μ_π^2). Several theoretical uncertainties can only be guesstimated: the shape function uncertainty, contributions from subleading shape functions, weak annihilations, and the procedure of scale matching. We assign an additional uncertainty on m_b, which reflects higher-order corrections not accounted for in the partial rate predictions for $B \to X_u \ell \nu$ [109]. We choose 50 MeV as the additional uncertainty. All these uncertainties of a second type are added linearly. As a result, we obtain a significantly larger theoretical uncertainty compared to the uncertainty quoted by the HFAG: $(4.32^{+0.21}_{-0.24} \pm 0.45) \times 10^{-3}$. The exclusive and the inclusive inputs are then averaged using the same recipe as for the lattice QCD parameters and we obtain: $|V_{ub}| = (3.92 \pm 0.09 \pm 0.45) \times 10^{-3}$.

(v) A measurement of the branching fraction for $B^+ \to \tau^+ \nu_\tau$ allows one to constrain the product $|V_{ub}| \cdot f_B$ where f_B is the decay constant of the charged B meson. The theoretical prediction for this branching fraction is given by

$$\mathcal{B}(B \to \tau \nu) = \frac{G_F^2 m_{B^+} m_\tau^2}{8\pi} \left(1 - \frac{m_\tau^2}{m_{B^+}^2}\right)^2 |V_{ub}|^2 f_B^2 \tau_{B^+}. \tag{51}$$

We use the experimental value $\tau_{B^+} = 1.639 \times 10^{-12} s$ in our analysis. $\mathcal{B}(B \to \tau \nu)$ combined with the constraint from the oscillation frequency Δm_d (see Sec. III C) removes the dependence on the decay constant f_B (assuming that the decay constant for the charged and neutral B meson is the same, i.e., neglecting isospin-breaking effects of order 1%). First evidence for the decay $B^+ \to \tau^+ \nu_\tau$ has been made by the Belle Collaboration [110] by reconstructing the decay on the recoil of fully reconstructed B-meson decays. Using the same technique the *BABAR* Collaboration found then a 2.2σ excess [111]. By searching for $B^+ \to \tau^+ \nu_\tau$ on the recoil of semileptonic B-meson decays Belle [112] found also evidence for $B^+ \to \tau^+ \nu_\tau$ while *BABAR* found a 2.3σ excess [113]. Recently, the Belle analysis first presented in Ref. [112] has been submitted for publication [114] reporting a slightly shifted central value and the *BABAR* analysis described in Ref. [111] has been updated to the full data set [111] in which evidence has been found for the decay $B^+ \to \tau^+ \nu_\tau$.

The world average for $\mathcal{B}(B^+ \to \tau^+ \nu_\tau)$ that is used in the analysis calculated from the measurements performed by *BABAR* and Belle [110,113–115] is $\mathcal{B}(B^+ \to \tau^+ \nu_\tau) = (1.68 \pm 0.31) \times 10^{-4}$.

(vi) The input for the CKM angle γ ($= \arg[-V_{ud} V_{ub}^* / (V_{cd} V_{cb}^*)]$) is taken from a combined full frequentist analysis of the CKMfitter Group using CP-violating asymmetries in charged B decays to neutral $D^{(*)}$ mesons plus charged $K^{(*)}$ mesons. The data are taken from HFAG using the three different methods proposed by Gronau, London, and Wyler (GLW) [116], and Atwood, Dunietz, and Soni (ADS) [117], and including also the Dalitz plot approach developed by Giri, Grossman, Soffer, and Zupan (GGSZ), and independently by the Belle Collaboration [118]. At the 68.3% confidence level (CL), the result of this analysis is $(71^{+21}_{-25})°$ with a second solution at $\gamma + \pi$. The constraint is shown in Fig. 1.

The above determination of γ raises interesting statistical issues. The angle γ actually appears as

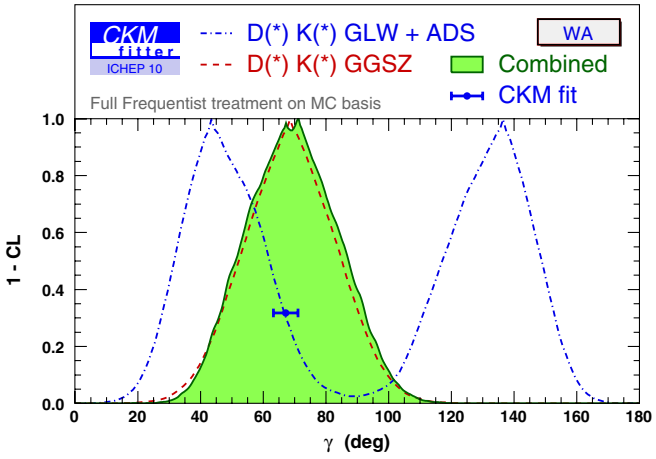

FIG. 1 (color online). Constraint on the angle γ from a combined analysis of $B \to D^{(*)} K^{(*)}$ decays.

the complex phase of a suppressed ratio r_B of decay amplitudes (different r_B's appear for different final states); in other words in the limit $r_B \to 0$ there is no constraint left on the CKM phase, and for finite r_B the error on γ is roughly inversely proportional to r_B itself. It turns out that the current data do not exclude tiny values for the r_B's, one obtains for the DK final state $r_B = 0.103^{+0.015}_{-0.024}$ at 68.3% C.L., the D^*K final state $r_B = 0.116^{+0.025}_{-0.025}$ at 68.3% C.L., and for the final state DK^* final state $r_B = 0.111^{+0.061}_{-0.047}$ at 68.3% C.L. Because the ratio of amplitudes is related to the bare observables nonlinearly, its maximum-likelihood estimate is biased, and it can be shown that this bias overestimates the value of r_B which in turn implies an underestimate of the uncertainty on γ. In the statistical language, this effect yields a significant *undercoverage* of the naïve 68.3% C.L. interval for γ computed from the log-likelihood variation.

A better estimate of the statistical uncertainty on γ can be obtained by inspecting the deviation of the distribution of the log-likelihood among a large number of toy experiments from its asymptotic limit. Problems arise because this distribution is not only nonasymptotic, but also depends on *nuisance parameters*, that is other parameters than γ that are necessary to compute the toy experiments. In such a situation the most conservative approach is called the *supremum* one, since it maximizes the uncertainty over all possible values of the nuisance parameters. To date this method which guarantees the coverage properties by construction is the default one for the treatment of γ in CKMfitter, but it must be kept in mind that it actually leads to overcoverage in general [119].

Another determination of γ which is unaffected by new physics in B–$\bar{B}$ mixing is obtained by combining measurements of α and β: The corresponding quantities are changed into $\alpha - \phi_d^\Delta/2$ and $\beta + \phi_d^\Delta/2$ in the presence of a new physics phase ϕ_d^Δ which therefore drops out of $\gamma = \pi - (\alpha - \phi_d^\Delta/2) - (\beta + \phi_d^\Delta)$. This procedure leads to a significantly more precise determination of γ than $B \to D^{(*)}K^{(*)}$ decays. The individual measurements of $\alpha - \phi_d^\Delta/2$ and $\beta + \phi_d^\Delta/2$ are described in the next section.

C. Observables in the B_d-$\bar{B}_d$ system affected by new physics in mixing

The following observables can be affected by $|\Delta F| = 2$ new physics contributions in the B_d^0-$\bar{B}_d^0$ system:

(i) The oscillation frequency Δm_d in the B_d sector has been measured with O(1%) precision mainly due to the B-factory data [79]. The translation of the measured value for Δm_d into constraints on the CKM parameter combination $|V_{td}V_{tb}^*|^2$ suffers from significant uncertainties in the theoretical calculation of the product $f_{B_d}\sqrt{\mathcal{B}_{B_d}}$ of hadronic parameters. These hadronic parameters can be obtained from lattice QCD computation, computing $f_{B_d}\sqrt{\mathcal{B}_{B_d}}$ from f_{B_s} and $\mathcal{B}_{B_s}$, and the flavor-symmetry breaking ratios f_{B_s}/f_{B_d} and $\mathcal{B}_{B_s}/\mathcal{B}_{B_d}$ as quoted in Sec. III A and summarized in Table VII. The value and uncertainty for the perturbative QCD correction $\hat{\eta}_B$ has been originally estimated in Ref. [49]. With up-to-date values and uncertainties for α_s and the top quark mass one obtains $\hat{\eta}_B = 0.8393 \pm 0.0034$. For the top quark mass we take the average value of the Tevatron Electroweak Working Group [41], $m_t = (172.4 \pm 1.2)$ GeV, combining published and also preliminary results from D0 and CDF. This mass, interpreted as a pole mass, is translated into $\bar{m}_t(\bar{m}_t) = (165.017 \pm 1.156 \pm 0.11)$ GeV in the $\overline{\text{MS}}$-scheme at one-loop order. It should be noted, however, that the identification of the measured mass value to the pole mass is under debate (with potential new systematics coming from this identification); see e.g. [120].

(ii) In the standard model, the predicted decay width difference $\Delta\Gamma_d$ is small: $\Delta\Gamma_d = (38.1^{+7.2}_{-14.1}) \times 10^{-4}$ ps^{-1} [12] (with our inputs). The average between DELPHI and *BABAR* measurements of the ratio $\Delta\Gamma_d/\Gamma_d$ calculated by HFAG [79,121,122] is 0.009 ± 0.037. The experimental uncertainty is much larger than the size of the standard model prediction, $\Delta\Gamma_d/\Gamma_d = (58^{+11}_{-22}) \times 10^{-4}$, and the measured value is in good agreement with the standard model prediction within experimental uncertainties so that stringent constraints on new physics contributions cannot be derived at the present stage of precision. Since a huge amount of statistics will be needed to measure $\Delta\Gamma_d$ at the level predicted by the standard model, this situation will probably not change for quite a long time. Even then if a deviation from the standard model value were observed due to new physics contributions in mixing it would show up beforehand in other observables like a_{SL}^d or $\sin 2\beta$. As a consequence, $\Delta\Gamma_d$ has no visible impact in our discussion and it is not used as an input to the fits presented here.

(iii) CP violation in B_d mixing [i.e., $|q/p| \neq 1$, with q/p defined in Eq. (5)] can be measured from the untagged dilepton rate asymmetry

$$a_{\text{SL}}^d = \frac{N_{\ell^+\ell^+} - N_{\ell^-\ell^-}}{N_{\ell^+\ell^+} + N_{\ell^-\ell^-}} = 2(1 - |q/p|). \quad (52)$$

With a tagged time-dependent decay asymmetry, one measures equivalently

$$A_{\mathrm{SL}}^{q}(t) \equiv \frac{\Gamma(\bar{B}_q^0(t) \to l^+ X) - \Gamma(B_q^0(t) \to l^- X)}{\Gamma(\bar{B}_q^0(t) \to l^+ X) + \Gamma(B_q^0(t) \to l^- X)} \quad (53)$$

$$= \frac{1 - |q/p|^4}{1 + |q/p|^4}$$

$$= 2(1 - |q/p|) + \mathrm{O}((|q/p| - 1)^2), \quad (54)$$

with the time-dependence dropping out. A weighted average of *BABAR*, Belle, and CLEO measurements [123] results in $A_{\mathrm{SL}}^{d} = -(47 \pm 46) \times 10^{-4}$ [79], which is a bit less than 1 standard deviation below the standard model prediction of $a_{\mathrm{SL}}^{d} = (-7.58^{+2.11}_{-0.64}) \times 10^{-4}$ [12,50,51] (with our inputs).

(iv) Within the standard model the measurement of the $S = \sin 2\phi_d^{\psi K}$ coefficient in the time-dependent CP asymmetry $A_{CP}(t) = S \sin(\Delta m_d \cdot t) + C \cos(\Delta m_d \cdot t)$ in decays of neutral B_d mesons to final states $(c\bar{c})K^0$ provides a measurement of the parameter $\sin 2\beta$, where $\beta = \arg[-V_{td}V_{tb}^*/(V_{cd}V_{cb}^*)]$, to a very good approximation. The current uncertainty of 0.023 on $\sin 2\phi_d^{\psi K}$ is still dominated by statistics [79]. The difference between the measured $\sin 2\phi_d^{\psi K}$ coefficient and $\sin 2\beta$ due to penguin contributions has been theoretically estimated in Ref. [124] to be below the 10^{-3} level, while phenomenologically less stringent constraints on this difference are quoted in Refs. [125–128]. When interpreting the measured $\sin 2\phi_d^{\psi K}$ coefficient as $\sin(2\beta + \phi_d^{\Delta})$ the *SM4FC* hypothesis does not rigorously apply. However, the gluonic penguin is *OZI*-suppressed and the Z-penguin is estimated to be small so that new physics in decay is assumed to be negligible with respect to the leading tree amplitude. We neglect the effect from possible new physics in $K - \bar{K}$ mixing on $\sin(2\beta + \phi_d^{\Delta})$, which is justified given the small value of the well-measured CP-violating parameter ϵ_K.

(v) The measurement of $\sin 2\phi_d^{\psi K}$ results in two solutions for $2\beta + \phi_d^{\Delta}$ (in $[0, \pi]$). One of these solutions can be excluded by measuring the sign of $\cos 2\phi_d^{\psi K}$. For a recent review of *BABAR* and Belle measurements, see e.g. Ref. [129]. The current experimental results from *BABAR* and Belle using a time- and angular-dependent analysis of $B^0 \to J/\psi K^{*0}$ decays, a time-dependent Dalitz-plot analysis in $B^0/\bar{B}^0 \to D^{(*)0}/\bar{D}^{(*)0}h^0$ with $B^0/\bar{B}^0 \to D^{(*)0}/\bar{D}^{(*)0}h^0$, and $B^0/\bar{B}^0 \to D^{*+}D^{*-}K_S^0$, disfavor negative $\cos 2\phi_d^{\psi K}$ values but HFAG deems it difficult to average the different measurements or to determine a reliable confidence level as a function of $\cos 2\phi_d^{\psi K}$ [79]. Here, as a simplification, it is only assumed that $\cos 2\phi_d^{\psi K} > 0$.

(vi) The constraint on the CKM angle $\alpha = \pi - \beta - \gamma$ is obtained from time-dependent and time-independent measurements in the decays $B \to \pi\pi$, $B \to \rho\rho$, and $B \to \rho\pi$. The time-dependent CP asymmetries measured in $B \to \pi\pi$ provide information on the effective parameter $\sin(2\alpha_{\mathrm{eff}})$ (which is a function of α and the penguin-to-tree ratio [130]). It is possible to translate this measurement into a constraint on α by exploiting isospin symmetry which allows one to pin down the penguin-to-tree ratio and thus to determine the difference $\alpha - \alpha_{\mathrm{eff}}$ from data [131]. Under the assumption of exact isospin symmetry the amplitudes $A^{+-} \equiv A(B^0 \to \pi^+\pi^-)$, $A^{00} \equiv A(B^0 \to \pi^0\pi^0)$, and $A^{+0} \equiv A(B^+ \to \pi^+\pi^0)$ satisfy a triangular relationship: $\sqrt{2}A^{+0} - \sqrt{2}A^{00} = A^{+-}$. A corresponding relationship holds for the CP conjugated decays: $\sqrt{2}\bar{A}^{+0} - \sqrt{2}\bar{A}^{00} = \bar{A}^{+-}$. These isospin triangles can be reconstructed by measuring the branching fractions and direct CP asymmetries for the final states $B^0 \to \pi^+\pi^-$, $B^0 \to \pi^0\pi^0$, and $B^+ \to \pi^+\pi^0$. Since one measures $\sin(2\alpha_{\mathrm{eff}})$ and since the triangle has a twofold ambiguity for its apex in the complex plane, there is an eightfold ambiguity for α in $[0, \pi]$. The extraction of α from the isospin analysis is independent of any possible new physics contributions in the $\Delta I = 1/2$ decay amplitude except for the singular point $\alpha = 0$ [132]. If there is no new physics contribution in the $\Delta I = 3/2$ decay amplitude (as assumed here), the extraction provides $\alpha = \pi - \gamma - \beta - \phi_d^{\Delta}/2$. As a consequence, α is equivalent to γ if $\beta + \phi_d^{\Delta}$ is measured e.g. from $B \to J/\psi K_S$ as already pointed out above.

Similar in line, an isospin analysis can be performed for the $B \to \rho\rho$ system. In this case the analysis needs to take into account the measured longitudinal polarization of the ρ mesons in the different final states $B^0 \to \rho^+\rho^-$, $B^0 \to \rho^0\rho^0$, and $B^+ \to \rho^+\rho^0$. Finally, the $\rho\pi$ modes provides another crucial input for α, by using a model for the Dalitz decay into three pions in addition to the isospin symmetry [133]. The results of these analyses that are based on the world averages of the various *BABAR* and Belle measurements for the CP asymmetries and branching fractions determined by HFAG [79] are displayed in Fig. 2. The combined analysis results in $\alpha = (89.0^{+4.4}_{-4.2})^\circ$ at 68.3% C.L.

The most stringent constraint on α comes currently from the $B^0 \to \rho\rho$ channel. The uncertainty is driven by the rather large branching fraction

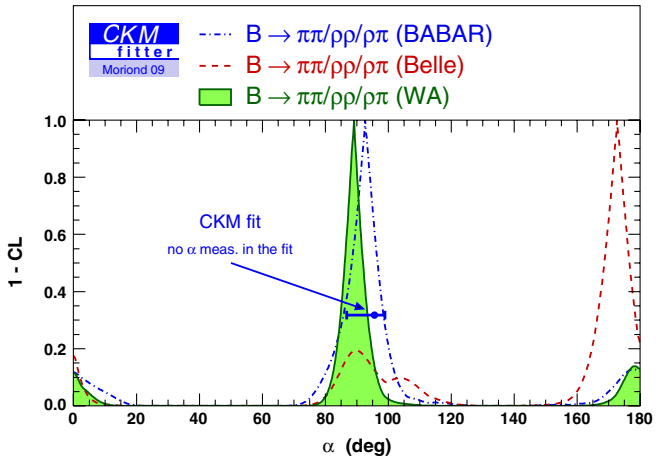

FIG. 2 (color online). Constraint on the angle α from the isospin analyses of $B \to \pi\pi$ and $B \to \rho\rho$ decays and a Dalitz plot analysis of $B \to \rho\pi$ decays. In the presence of new physics in B_d mixing, the quantity shown is $\pi - \gamma - \beta - \phi_d^{\Delta}/2$.

$\mathcal{B}(B^+ \to \rho^+\rho^0)$. The input value for $\mathcal{B}(B^+ \to \rho^+\rho^0)$ has changed recently when the *BABAR* Collaboration presented a new analysis on the final data set [134]. The large branching fraction value leads to an isospin triangle that just closes. The measurement uncertainty is smaller than the expected uncertainty. As a consequence, the current uncertainty quoted for α might be on the optimistic side. It should also be stressed that at this level of precision so-far neglected uncertainties (electroweak penguins, $\pi - \eta^{(\prime)}$ mixing, $\rho - \omega$ mixing, other isospin violations, finite ρ-width, etc.) should be considered in more detail.

TABLE VI. Experimental inputs used in the fits.

Observable	Value and uncertainties	Reference
$\lvert V_{ud}\rvert$	0.97425 ± 0.00022	[77]
$\lvert V_{us}\rvert$	0.2254 ± 0.0013	[78]
m_K	(497.614 ± 0.024) MeV	[46]
G_F	$(1.16637 \pm 0.00001) \times 10^{-5}$ GeV^2	[46]
m_W	(80.398 ± 0.025) GeV	[46]
m_{B_d}	(5.27917 ± 0.00029) GeV	[46]
m_{B^+}	(5.27953 ± 0.00033) GeV	[46]
m_{B_s}	(5.3663 ± 0.0006) GeV	[46]
$\lvert V_{cb}\rvert$	$(40.89 \pm 0.38 \pm 0.59) \times 10^{-3}$	see text
$\lvert V_{ub}\rvert$	$(3.92 \pm 0.09 \pm 0.45) \times 10^{-3}$	see text
$\mathcal{B}(B \to \tau\nu_\tau)$	$(1.68 \pm 0.31) \times 10^{-4}$	see text
γ	$71^{+21}_{-25}{}^\circ$	see text
Δm_d	(0.507 ± 0.005) ps^{-1}	[46]
$a_{\rm SL}^d$	$(-47 \pm 46) \times 10^{-4}$	[79]
$\sin(2\phi_d^{\psi K})$	0.673 ± 0.023	[80]
$\cos(2\phi_d^{\psi K})$	positive	see text
α	$89.0^{+4.4}_{-4.2}{}^\circ$	see text
Δm_s	(17.77 ± 0.12) ps^{-1}	[27]
$A_{\rm SL}$	$(-85 \pm 28) \times 10^{-4}$	see text and [33,81]
$a_{\rm SL}^s$	$(-17 \pm 93) \times 10^{-4}$	[82]
$\phi_s^{\psi\phi}$ vs $\Delta\Gamma_s$	see text	[29,30,83]
$\lvert\epsilon_K\rvert$	$(2.229 \pm 0.010) \times 10^{-3}$	[46]
Δm_K	$(3.483 \pm 0.006) \times 10^{-12}$ MeV	[46]

D. Observables in the B_s-$\bar{B}_s$ system affected by new physics in mixing

We now discuss observables which can be possibly affected by $|\Delta F| = 2$ new physics contributions in the B_s-$\bar{B}_s$ system.

(i) The experimental input for the mass difference Δm_s taken from HFAG is dominated by the measurement of CDF [27]. The dependence of the standard model prediction $\Delta m_s^{\rm SM}$ on $\bar{\rho} - \bar{\eta}$ coordinates appears very weak through the relevant CKM matrix elements term $|V_{ts}^* V_{tb}|^2$, but the value of Δm_s gives a direct constraint in the Δ_s plane, by computing $f_{B_s}\sqrt{\hat{\mathcal{B}}_{B_s}}$ from f_{B_s} and $\mathcal{B}_{B_s}$, given in Table VII. The hadronic matrix element for the B_s system can be related to the B_d one via the flavor-SU(3) breaking correction parameter ξ defined through $f_{B_s}^2 \mathcal{B}_{B_s} = \xi^2 f_{B_d}^2 \mathcal{B}_{B_d}$ Measurements of Δm_s thus reduce the uncertainties on $f_{B_d}^2 \mathcal{B}_{B_d}$ since ξ is better known from lattice QCD than $f_{B_d}^2 \mathcal{B}_{B_d}$. This relation also generates a strong correlation between the new physics parameters $|\Delta_d|$

TABLE VII. Theoretical inputs used in the fits.

Theoretical parameter	Value and uncertainties	Reference
f_{B_s}	$(231 \pm 3 \pm 15)$ MeV	see Sec. III A
$\mathcal{B}_{B_s}(m_b)$	$0.841 \pm 0.013 \pm 0.020$	see Sec. III A
f_{B_s}/f_{B_d}	$1.209 \pm 0.007 \pm 0.023$	see Sec. III A
$\mathcal{B}_{B_s}/\mathcal{B}_{B_d}$	$1.01 \pm 0.01 \pm 0.03$	see Sec. III A
$\hat{\eta}_B$	0.8393 ± 0.0034	see text
$\bar{m}_t(\bar{m}_t)$	$(165.017 \pm 1.156 \pm 0.11)$ GeV	see text and [41]
$\hat{\mathcal{B}}_K$	$(0.724 \pm 0.004 \pm 0.067)$	see Sec. III A
f_K	156.1 MeV	see text
κ_ϵ	$0.940 \pm 0.013 \pm 0.023$	see text
η_{tt}	0.5765 ± 0.0065	[42]
η_{ct}	0.47 ± 0.04	[43]
η_{cc}	$(1.39 \pm 0.35)(\frac{1.29\ \text{GeV}}{\bar{m}_c})^{1.1}$	[44]
λ_K	$(1.25 \pm 0.00 \pm 0.75)$ GeV	see text
$\bar{m}_c(\bar{m}_c)$	$(1.286 \pm 0.013 \pm 0.040)$ GeV	see text
$\tilde{\mathcal{B}}_{S,B_s}/\tilde{\mathcal{B}}_{S,B_d}$	$1.01 \pm 0 \pm 0.03$	[45]
$\tilde{\mathcal{B}}_{S,B_s}(m_b)$	$0.91 \pm 0.03 \pm 0.12$	[45]
$\Lambda_{\overline{\rm MS}}^{(5)}$	(0.222 ± 0.027) GeV	from $\alpha_s(M_Z)$ in [46]
$\bar{m}_s(\bar{m}_b)$	(0.085 ± 0.017) GeV	[12]
$\bar{m}_b(\bar{m}_b)$	(4.248 ± 0.051) GeV	[47]
m_b^{pow}	$(4.7 \pm 0 \pm 0.1)$ GeV	[12]
$\mathcal{B}_{R_0}$	1.0 ± 0.5	[12]
$\mathcal{B}_{\tilde{R}_1}$	1.0 ± 0.5	[12]
$\mathcal{B}_{R_1}$	1.0 ± 0.5	[12]
$\mathcal{B}_{\tilde{R}_2}$	$1.0 \pm 0 \pm 0.5$	[12]
$\mathcal{B}_{\tilde{R}_3}$	$1.0 \pm 0 \pm 0.5$	[12]

and $|\Delta_s|$ when allowing for new physics contributions to mixing.

(ii) The standard model prediction [12] for $a^s_{\rm SL}$ is at least 1 order of magnitude smaller than the one for $a^d_{\rm SL}$; see Table VIII. Compared to the standard model prediction the D0 measurement has a quite large uncertainty, $a^s_{\rm SL} = (-17 \pm 91^{+12}_{-23}) \times 10^{-4}$ [82], and hence does not have a strong impact on the new physics constraints in the B_s sector. It is nevertheless included in our analysis.

(iii) D0 [135] using 1 fb^{-1} and CDF [81] have measured inclusive dimuon CP asymmetries. The D0 result corresponding to the measurement quoted in Ref. [135] presented as $a^d_{\rm SL} + \frac{f_s Z_s}{f_d Z_d} a^s_{\rm SL} = -0.0028 \pm 0.0013 \pm 0.0009$ is provided in [136] whereas CDF [81] quotes the result as

$$A_{\rm SL} = \frac{f_d Z_d a^d_{\rm SL} + f_s Z_s a^s_{\rm SL}}{f_d Z_d + f_s Z_s} = 0.0080 \pm 0.0090 \pm 0.0068, \quad (55)$$

where $f_{d(s)}$ is the fraction of neutral $B_{d(s)}$ mesons in the fragmentation and $Z_{d(s)}$ is given by

$$Z_q = \frac{1}{1 - y_q^2} - \frac{1}{1 + x_q^2}, \quad (56)$$

with $y_q = \Delta\Gamma_q/2\Gamma_q$ and $x_q = \Delta m_q/\Gamma_q$ (see also Ref. [59]). Very recently D0 has presented a new measurement of $A_{\rm SL}$ [33] using 6.1 fb^{-1} integrated luminosity which shows a 3.2σ deviation from the (almost zero) standard model prediction, and is the first direct evidence against the standard model in B meson observables: $A_{\rm SL} = -0.00957 \pm 0.00251 \pm 0.00146$. This result supersedes the former result in Ref. [136]. The average between the new D0 result and the CDF result reads

$$A_{\rm SL} = -0.0085 \pm 0.0028, \quad (57)$$

which is 2.9 standard deviations away from the standard model prediction. For the interpretation of the measured observables we use the following values and uncertainties for $f_{d(s)}$, y_q, and x_q: $f_d = 0.333 \pm 0.030$, $f_s = 0.121 \pm 0.015$ with a correlation coefficient of $+0.439$ are taken from Ref. [47], x_d is calculated from $\Delta m_d = (0.507 \pm 0.005) \times 10^{12} s^{-1}$ [46] and $\tau_{B_d} = (1.525 \pm 0.009) \times 10^{-12} s$ [137], y_d is set to zero since $\Delta\Gamma_d$ is expected to be very small in the standard model and is not affected by new physics in our scenarios, x_s is calculated from $\Delta m_s = (17.77 \pm 0.12) \times 10^{12} s^{-1}$ [46] and y_s from $\tau_{B_s} = (1.515 \pm 0.034) \times 10^{-12} s$ [137], the measurement of $\Delta\Gamma_s$ in $B_s \to J/\psi\phi$ (see below) and the flavor-specific B_s lifetime $\tau^{FS}_{B_s} = (1.417 \pm 0.042) \cdot 10^{-12} s$ [137]. This results in $Z_d = 0.3741 \pm 0.0054$ and $Z_s = 1.0044^{+0.0058}_{-0.0032}$ hence actually the error on $Z_{d,s}$ has negligible impact on our global fits.

(iv) CDF and D0 have presented time-dependent tagged analyses [28,29] of $B_s \to J/\psi\phi$ decays which provide information on Δ_s through $\Delta\Gamma_s$ and $\phi_s^{\psi\phi}$. These analyses supersede the previous untagged studies of Refs. [138,139] (which use the same data sample, but without the tagging information) and we will not use the untagged results in our analysis. These time-dependent tagged analyses have raised a lot of attention recently, in particular, when the UTfit Collaboration claimed an evidence of new physics of at least 3σ based on a global fit where these measurements played a central role [140]. It has been later argued, though, that this conclusion came from an overinterpretation of the data [141].[9] In the framework of the HFAG [79] the CDF and D0 have determined a combined constraint based on the measurements in Refs. [28,29]. In 2009 CDF updated the analysis on a larger dataset using 2.8 fb^{-1} of data [30]. The new average between D0 [29] and CDF [30] was presented in summer 2009 [83]. Using this new average the deviation of the measured value $\phi_s^{\psi\phi}$

TABLE VIII. Fit results of the standard model fit. The notation (!) means that the fit output represents the indirect constraint, i.e. the corresponding direct input has been removed from the analysis.

Quantity	Central	$\pm$C.L. $\equiv 1\sigma$	$\pm$C.L. $\equiv 2\sigma$	$\pm$C.L. $\equiv 3\sigma$
A	$0.815^{+0.011}_{-0.029}$		$0.815^{+0.020}_{-0.038}$	$0.815^{+0.029}_{-0.046}$
λ	$0.22543^{+0.00077}_{-0.00077}$		$0.2254^{+0.0015}_{-0.0015}$	$0.2254^{+0.0023}_{-0.0023}$
$\bar\rho$	$0.144^{+0.029}_{-0.018}$		$0.144^{+0.054}_{-0.028}$	$0.144^{+0.068}_{-0.037}$
$\bar\eta$	$0.342^{+0.016}_{-0.016}$		$0.342^{+0.030}_{-0.028}$	$0.342^{+0.045}_{-0.037}$
$\hat B_K$ (!)	$0.81^{+0.26}_{-0.12}$		$0.81^{+0.34}_{-0.16}$	$0.81^{+0.43}_{-0.19}$
f_{B_s} [MeV] (!)	$234.9^{+9.3}_{-7.9}$		235^{+12}_{-12}	235^{+16}_{-15}
$\hat{\mathcal{B}}_{B_s}$ (!)	$1.115^{+0.090}_{-0.036}$		$1.115^{+0.348}_{-0.071}$	$1.11^{+0.54}_{-0.10}$
f_{B_s}/f_{B_d} (!)	$1.218^{+0.054}_{-0.046}$		$1.22^{+0.11}_{-0.10}$	$1.22^{+0.16}_{-0.15}$
$\mathcal{B}_{B_s}/\mathcal{B}_{B_d}$ (!)	$1.138^{+0.076}_{-0.094}$		$1.14^{+0.16}_{-0.21}$	$1.14^{+0.24}_{-0.30}$
$\tilde{\mathcal{B}}_{S,B_s}(m_b)$ (!)	$-0.6^{+1.4}_{-2.3}$		$-0.6^{+2.8}_{-3.9}$	$-0.6^{+4.3}_{-5.5}$
J [10^{-5}]	$2.98^{+0.16}_{-0.18}$		$2.98^{+0.30}_{-0.23}$	$2.98^{+0.44}_{-0.28}$
α[deg] (!)	$97.6^{+2.4}_{-6.6}$		$97.6^{+3.9}_{-10.7}$	$97.6^{+5.5}_{-12.6}$
β[deg] (!)	$28.09^{+0.70}_{-1.49}$		$28.1^{+1.4}_{-4.1}$	$28.1^{+2.1}_{-7.2}$
γ[deg] (!)	$67.1^{+2.9}_{-4.5}$		$67.1^{+4.4}_{-8.4}$	$67.1^{+5.9}_{-10.4}$
$-2\beta_s$ [deg] (!)	$-2.083^{+0.097}_{-0.097}$		$-2.08^{+0.18}_{-0.19}$	$-2.08^{+0.27}_{-0.28}$
$-2\beta_s$ [deg]	$-2.084^{+0.097}_{-0.097}$		$-2.08^{+0.17}_{-0.19}$	$-2.08^{+0.23}_{-0.28}$

[9] In particular Ref. [140] assumes that the only effect of the SU(3) assumption on the strong phases in the D0 analysis amounts to the suppression of a mirror solution, without any impact on the accuracy and the location of the main solution.

with respect to the standard model value β_s is essentially unchanged and reads 2.3 standard deviations. This average is our default input for the corresponding observables, supplemented by the constraint on the flavor-specific B_s lifetime $\tau_{B_s}^{\rm FS} = (1.417 \pm 0.042) \times 10^{-12}$ [137] which can be viewed as an independent measurement of $\Delta\Gamma_s$. New results for $B_s \to J/\psi\phi$ were presented in summer 2010 by CDF (with 5.2 fb^{-1}) [31] and D0 (with 6.1 fb^{-1}) [29] collaborations, in closer agreement to the standard model expectations, but these measurements have not been combined yet. They have not been included in the present analysis, but are briefly discussed together with the standard model significance tests below.

E. The neutral kaon system

The master formula for ϵ_K has been given in Eq. (39), from the relation between ϵ_K and M_{12}^s. The translation of ϵ_K into a constraint on $\bar{\rho}$ and $\bar{\eta}$ suffers from sizeable uncertainties in the Wolfenstein parameter A (the determination of which being driven by $|V_{cb}|^4$), $\hat{\mathcal{B}}_K$ (see Table VII and Sec. III A), from the long-distance corrections to the relation between M_{12}^K and ϵ_K encoded in κ_ϵ, and, though of less importance, from uncertainties in the QCD corrections coming from η_{cc} [44], from the charm quark mass $\bar{m}_c(\bar{m}_c)$ in the $\overline{\rm MS}$ scheme, from m_t, and the perturbative QCD corrections η_{tt} [44] and η_{ct} [44].

(i) From the experimental point of view, the number on the left-hand side of Eq. (39) has shifted substantially over time. For instance in 1995 the corresponding number was 1.21×10^{-7} [43]. More recently, the numerical value for ϵ_K has shifted by about 2.3% (a 3.7σ effect) between the 2004 and 2006 edition of the Particle Data Group from $(2.284 \pm 0.014) \times 10^{-3}$ [142] down to $(2.232 \pm 0.007) \times 10^{-3}$ [46]. This shift has been mainly driven by improved measurements of the branching fraction $\mathcal{B}(K_L \to \pi^+\pi^-)$ performed by the KTeV, KLOE, and NA48 collaborations leading to a reduction of 5.5% of the semileptonic branching fraction values.

(ii) As discussed in Sec. II B, the relation between ϵ_K and K–$\bar{K}$ mixing is affected by several corrections encoded in κ_ϵ. We have combined them with the experimental result for ϵ_K as indicated in this section.

(iii) The kaon decay constant f_K is taken from the review on pseudoscalar decay constants in Ref. [46] which is calculated from the measured branching fraction $\mathcal{B}(K^+ \to \mu^+\nu_\mu(\gamma))$ and the measured charged kaon decay time using an external input for $|V_{us}|$. In Ref. [46] $|V_{us}| = 0.2255 \pm 0.0019$ from $K_{\ell 3}$ decays is used as external input which leads to $f_K = 155.5 \pm 0.2 \pm 0.8 \pm 0.2$ MeV, where the first error is due to the experimental uncertainties, the second due to the uncertainty from $|V_{us}|$, and the third due to higher-order corrections [46]. With our input of $|V_{us}| = 0.2246 \pm 0.0012$ this translates into $f_K = 156.1 \pm 0.2 \pm 0.6 \pm 0.2$ MeV. In the fit, we do not consider the uncertainties on f_K at this point since they are currently negligible with respect to the other uncertainties. Since the f_K value obtained in this way is anticorrelated with our $|V_{us}|$ input a consistent treatment would require including the leptonic kaon decay in the fit and constrain f_K simultaneously. This would then lead to an even smaller uncertainty on f_K given the improved uncertainty on $|V_{us}|$ imposed by the global fit. Such a fit is technically possible but has not been performed here since the error from f_K on ϵ_K does not play an important role.

(iv) Various determinations of the charm quark mass are available. For instance, the charm quark mass in the kinetic mass scheme can be obtained from fits to data from lepton energy and hadronic mass moments in $B \to X_c\ell\nu$ decays combined with photon energy moments measured in $B \to X_s\gamma$ decays; see e.g. Refs. [79,143]. The most recent value for the kinetic mass quoted by HFAG is $m_c^{\rm kin} = (1.165 \pm 0.050)$ GeV [79], corresponding to a value in the $\overline{\rm MS}$ scheme: $\bar{m}_c(\bar{m}_c) = (1.265 \pm 0.060 \pm 0.050)$ GeV. The first uncertainty on the charm quark mass is correlated with the b-quark mass uncertainty obtained from the same fits quoted in Table VI with a linear correlation coefficient of order 98%. A second uncertainty of 50 MeV has been added following the discussion in Ref. [143], to take into account the low renormalization scale and the size of higher-order perturbative corrections when translating the mass from one scheme to another.

As an alternative, the charm quark mass can also be determined from e^+e^- annihilation data into hadrons created from quark-antiquark pairs. The operator-product expansion (OPE) method consists in writing sum rules for moments of the cross section $\sigma(e^+e^- \to c\bar{c})$, which are dominated by the perturbative term and the contribution proportional to the gluon condensate. An older analysis of Steinhauser and Kühn based on a three-loop calculation finds $\bar{m}_c(\bar{m}_c) = (1.304 \pm 0.027)$ GeV with a small uncertainty [144]. A similar analysis by Jamin and Hoang [145] obtains a consistent result, $\bar{m}_c(\bar{m}_c) = (1.290 \pm 0.070)$ GeV, but quotes a significantly larger uncertainty. This can be ascribed to the choice of the OPE scale separating short- and long-distance physics and it can be viewed as the

impact of (neglected) higher-order terms in perturbation theory on the determination of m_c through such moments. In a more recent calculation at four loops for the perturbative contribution, the uncertainty has been further reduced: $\bar{m}_c(\bar{m}_c) = (1.286 \pm 0.013)$ GeV [146].[10] However, in this reference, there is only a limited discussion of the freedom in the choice of the renormalization scale for the perturbative series and the gluon condensate is varied only in a limited range, even though these two effects were seen as bringing significant systematics in Ref. [145]. In the absence of further studies on the systematics discussed above in the case of the four-loop analysis of Ref. [146], we assign an additional theoretical uncertainty of 0.040 GeV and use as our input value: $\bar{m}_c(\bar{m}_c) = (1.286 \pm 0.013 \pm 0.040)$ GeV which is consistent with the values from the moment fits but has smaller uncertainties.

IV. QUANTITATIVE STUDIES

A. Standard model fit

In this section, we present the current status of the standard model CKM fit.[11] Figure 3 shows the fit results in the $\bar{\rho} - \bar{\eta}$ plane. Table VIII shows the fit results for various parameters. In Tables VIII and IX we also show the result of the fit for observables that have been individually excluded from the fit in order to quantify possible deviations between the individual input values and their fit predictions. The good overall agreement of the combined standard model fit mixes quantities that are in perfect agreement with their fit prediction, with others that are individually at odds. Possible deviations between a selection of measured observables and their standard model predictions are discussed in more detail in the following.

One observes a sizeable discrepancy between the input value of $\mathcal{B}(B \to \tau\nu)$ (see Table VI) and its fit prediction (see Table IX) which is mainly driven by the measured value of $\sin 2\beta$, and was first discussed in Ref. [10]. Removing either $\mathcal{B}(B \to \tau\nu)$ or $\sin 2\beta$ from the list of inputs results in a χ^2 change that corresponds to 2.9 standard deviations. This discrepancy could arise either

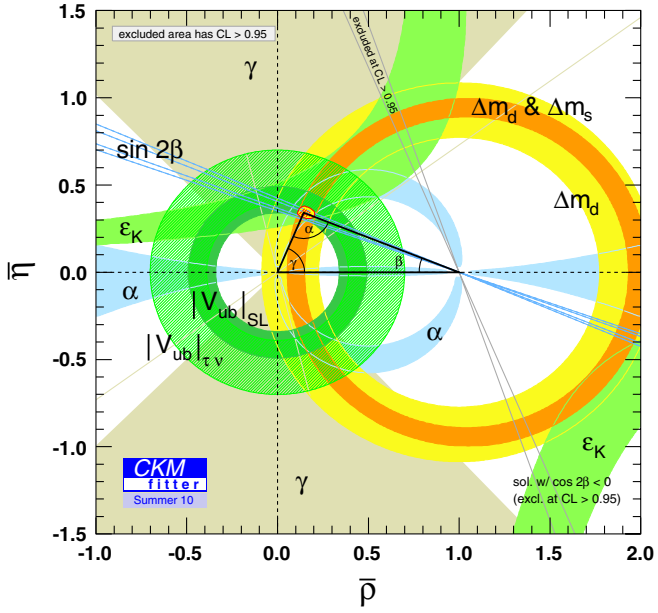

FIG. 3 (color online). Constraint on the CKM $(\bar{\rho}, \bar{\eta})$ coordinates from the global standard model CKM fit. Regions outside the shaded (colored) areas have C.L. $> 95.45\%$. For the combined fit the (yellow) area inscribed by the contour line at the apex of the triangle represents points with C.L. $< 95.45\%$. The shaded area inside this region represents points with C.L. $< 68.3\%$.

from a statistical fluctuation in the measured $\mathcal{B}(B \to \tau\nu)$ value, from too small (large) a value of f_{B_d} ($\hat{\mathcal{B}}_{B_d}$), or from new physics in the $B \to \tau\nu$ and/or $\sin 2\beta$ measurements. There is a specific correlation between $\sin 2\beta$ and $\mathcal{B}(B \to \tau\nu)$ in the global fit that is a bit at odds with the direct experimental determination. This is best viewed in the [$\sin 2\beta$, $\mathcal{B}(B \to \tau\nu)$] plane (see Fig. 4), regarding the prediction from the global fit without using these measurements. The shape of the correlation can be understood more deeply by considering the ratio $\mathcal{B}(B \to \tau\nu)/\Delta m_d$, where the decay constant f_{B_d} cancels, leaving limited theoretical uncertainties restricted to the bag parameter $\hat{\mathcal{B}}_{B_d}$. The formula for the ratio displays explicitly that the correlation between $\mathcal{B}(B \to \tau\nu)$ and the angle $\phi_d^{\psi K}$ is controlled by the values of $\hat{\mathcal{B}}_{B_d}$, and the angles γ and $\alpha = \pi - \beta - \gamma$:

$$\frac{\mathcal{B}(B \to \tau\nu)}{\Delta m_d} = \frac{3\pi}{4} \frac{m_\tau^2}{m_W^2 S(x_t)} \left(1 - \frac{m_\tau^2}{m_{B^+}^2}\right)^2 \tau_{B^+} \times \frac{1}{\hat{\mathcal{B}}_{B_d} \eta_B} \frac{1}{|V_{ud}|^2} \left(\frac{\sin\beta}{\sin\gamma}\right)^2. \quad (58)$$

The comparison of the indirect prediction of $\hat{\mathcal{B}}_{B_d}$ from the above analytical formula [having only $\mathcal{B}(B \to \tau\nu)$, Δm_d, $\sin 2\beta$, α, γ, and $|V_{ud}|$ as inputs, that is an almost completely theory-free determination of $\hat{\mathcal{B}}_{B_d}$] with the current

[10]Using an improved routine for the renormalization-group evolution of the computed value $m_c(3\text{ GeV}) = (0.986 \pm 0.013)$ GeV the same group finds a slightly shifted central value $\bar{m}_c(\bar{m}_c) = 1.268$ GeV [147].

[11]We stress an important difference in our present definition of the standard model CKM fit, with respect to more "traditional" definitions, such as in Ref. [53]: We include here the full input list of Table VI, that is we also take into account $B_s \to J/\psi\phi$ and the semileptonic asymmetries. The latter observables have negligible impact on the determination of the CKM parameters, however, there is some visible effect on the fit predictions for the subleading angles and asymmetries in the B_s system listed in Tables VIII and IX.

TABLE IX. Fit results of the standard model fit. The notation (!) means that the fit output represents the indirect constraint, i.e. the corresponding direct input has been removed from the analysis.

Quantity	Central $\pm$C.L. $\equiv 1\sigma$	$\pm$C.L. $\equiv 2\sigma$	$\pm$C.L. $\equiv 3\sigma$
$\lvert V_{ud}\rvert$ (!)	$0.97426^{+0.00030}_{-0.00030}$	$0.97426^{+0.00060}_{-0.00061}$	$0.97426^{+0.00089}_{-0.00091}$
$\lvert V_{us}\rvert$ (!)	$0.22545^{+0.00095}_{-0.00095}$	$0.2254^{+0.0019}_{-0.0019}$	$0.2254^{+0.0028}_{-0.0029}$
$\lvert V_{ub}\rvert$ (!)	$0.00356^{+0.00015}_{-0.00020}$	$0.00356^{+0.00030}_{-0.00031}$	$0.00356^{+0.00046}_{-0.00042}$
$\lvert V_{cd}\rvert$	$0.22529^{+0.00077}_{-0.00077}$	$0.2253^{+0.0015}_{-0.0015}$	$0.2253^{+0.0023}_{-0.0023}$
$\lvert V_{cs}\rvert$	$0.97341^{+0.00021}_{-0.00018}$	$0.97341^{+0.00039}_{-0.00036}$	$0.97341^{+0.00057}_{-0.00054}$
$\lvert V_{cb}\rvert$ (!)	$0.04508^{+0.00075}_{-0.00528}$	$0.0451^{+0.0014}_{-0.0059}$	$0.0451^{+0.0021}_{-0.0065}$
$\lvert V_{td}\rvert$	$0.00861^{+0.00021}_{-0.00037}$	$0.00861^{+0.00032}_{-0.00054}$	$0.00861^{+0.00044}_{-0.00068}$
$\lvert V_{ts}\rvert$	$0.04068^{+0.00043}_{-0.00138}$	$0.04068^{+0.00081}_{-0.00169}$	$0.0407^{+0.0012}_{-0.0020}$
$\lvert V_{tb}\rvert$	$0.999135^{+0.000057}_{-0.000018}$	$0.999135^{+0.000069}_{-0.000034}$	$0.999135^{+0.000081}_{-0.000051}$
ϕ_d [deg]	$-5.8^{+2.0}_{-3.6}$	$-5.8^{+2.7}_{-4.6}$	$-5.8^{+2.9}_{-5.7}$
ϕ_s [deg]	$0.422^{+0.046}_{-0.181}$	$0.422^{+0.098}_{-0.248}$	$0.42^{+0.16}_{-0.29}$
$\lvert\epsilon_K\rvert$ $[10^{-3}]$ (!)	$2.01^{+0.56}_{-0.65}$	$2.01^{+0.70}_{-0.74}$	$2.01^{+0.84}_{-0.83}$
Δm_d $[\mathrm{ps}^{-1}]$ (!)	$0.555^{+0.073}_{-0.046}$	$0.55^{+0.11}_{-0.10}$	$0.55^{+0.16}_{-0.15}$
Δm_s $[\mathrm{ps}^{-1}]$ (!)	$16.8^{+2.6}_{-1.5}$	$16.8^{+4.1}_{-2.8}$	$16.8^{+5.5}_{-3.4}$
A_{SL} $[10^{-4}]$ (!)	$-3.67^{+1.09}_{-0.40}$	$-3.67^{+1.52}_{-0.85}$	$-3.7^{+1.7}_{-1.3}$
A_{SL} $[10^{-4}]$	$-3.68^{+1.03}_{-0.40}$	$-3.68^{+1.52}_{-0.86}$	$-3.7^{+1.7}_{-1.3}$
$a^s_{\mathrm{SL}} - a^d_{\mathrm{SL}}$ $[10^{-4}]$	$7.93^{+0.66}_{-2.14}$	$7.9^{+1.3}_{-3.0}$	$7.9^{+2.0}_{-3.4}$
a^d_{SL} $[10^{-4}]$ (!)	$-7.58^{+2.11}_{-0.64}$	$-7.6^{+2.9}_{-1.3}$	$-7.6^{+3.3}_{-1.9}$
a^d_{SL} $[10^{-4}]$	$-7.59^{+2.06}_{-0.64}$	$-7.6^{+2.9}_{-1.3}$	$-7.6^{+3.3}_{-1.9}$
a^s_{SL} $[10^{-4}]$ (!)	$0.339^{+0.026}_{-0.090}$	$0.339^{+0.052}_{-0.130}$	$0.339^{+0.079}_{-0.147}$
a^s_{SL} $[10^{-4}]$	$0.339^{+0.026}_{-0.090}$	$0.339^{+0.052}_{-0.130}$	$0.339^{+0.079}_{-0.147}$
$\Delta\Gamma_d$ $[\mathrm{ps}^{-1}]$	$0.00381^{+0.00072}_{-0.00141}$	$0.0038^{+0.0011}_{-0.0016}$	$0.0038^{+0.0013}_{-0.0018}$
$\Delta\Gamma_s$ $[\mathrm{ps}^{-1}]$ (!)	$0.104^{+0.060}_{-0.027}$	$0.104^{+0.066}_{-0.033}$	$0.104^{+0.071}_{-0.039}$
$\Delta\Gamma_s$ $[\mathrm{ps}^{-1}]$	$0.0818^{+0.0274}_{-0.0061}$	$0.082^{+0.057}_{-0.012}$	$0.082^{+0.085}_{-0.018}$
$\mathcal{B}(B\to\tau\nu)$ $[10^{-4}]$ (!)	$0.764^{+0.087}_{-0.072}$	$0.76^{+0.19}_{-0.11}$	$0.76^{+0.29}_{-0.14}$
$\mathcal{B}(B\to\tau\nu)$ $[10^{-4}]$	$0.833^{+0.109}_{-0.089}$	$0.83^{+0.20}_{-0.15}$	$0.83^{+0.28}_{-0.19}$

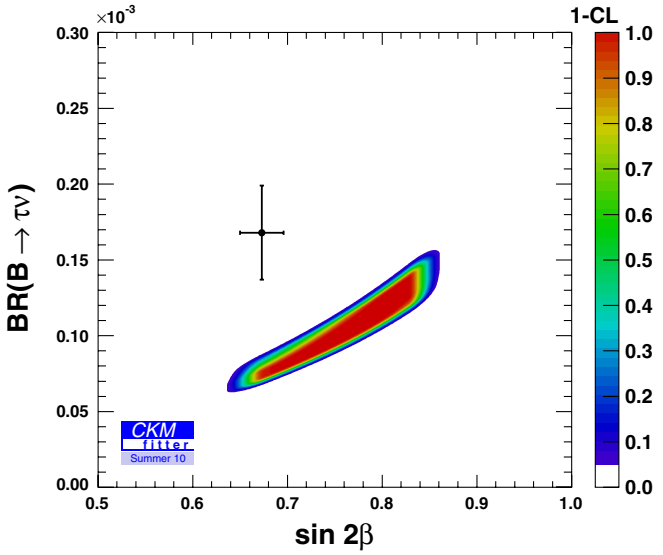

FIG. 4 (color online). Constraint in the [$\sin 2\beta$, $\mathcal{B}(B\to\tau\nu)$] plane. The colored (shaded) constraint represents the prediction for these quantities from the global fit when these inputs are removed while the cross represents the measurements with a 1σ uncertainty.

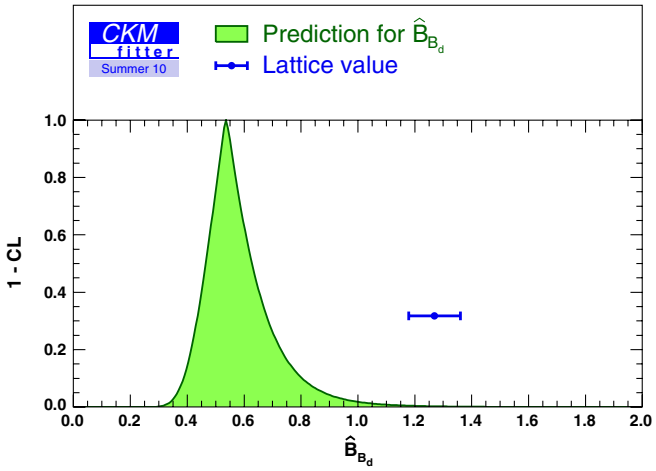

FIG. 5 (color online). Comparison between the $\hat{\mathcal{B}}_{B_d}$ parameter used in the global fit and its prediction. The colored (shaded) constraint represents the prediction of $\hat{\mathcal{B}}_{B_d}$ quantities from the global fit while the blue point represents the input value with the corresponding 1σ uncertainty as used in the global fit.

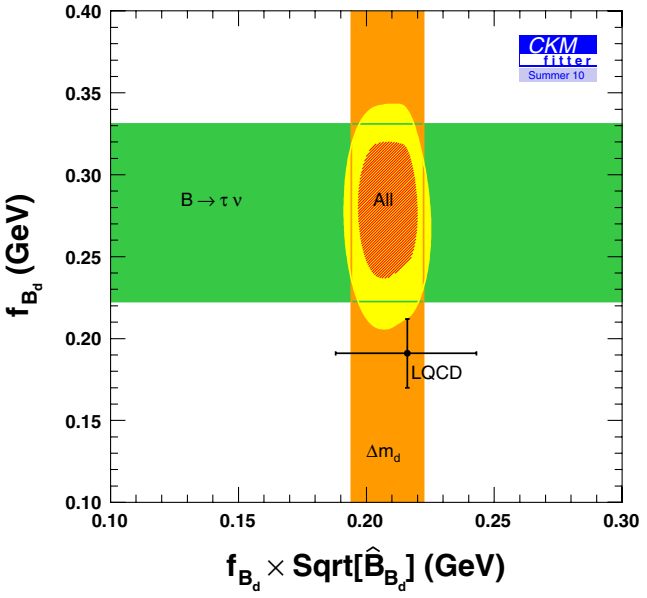

FIG. 6 (color online). Constraint on f_{B_d} and $f_{B_d}\sqrt{\hat{\mathcal{B}}_{B_d}}$. The horizontal (green) band shows the 95.45% C.L. constraint on f_{B_d} when $\mathcal{B}(B \to \tau\nu)$ is included in the fit. The vertical (orange) band represents the 95.45% C.L. constraint on $f_{B_d}\sqrt{\hat{\mathcal{B}}_{B_d}}$ thanks to the Δm_d measurement. The combined 68.3% C.L. and 95.45% C.L. constraint is shown as oval (red and yellow) regions, respectively. The black point shows the 1σ uncertainty on f_{B_d} and $f_{B_d}\sqrt{\hat{\mathcal{B}}_{B_d}}$ as used in the fit.

direct lattice determination $\hat{\mathcal{B}}_{B_d} = 1.269^{+0.092}_{-0.090}$ is given in Fig. 5. For this test the deviation is 2.9σ, dominated first by the experimental error on $\mathcal{B}(B \to \tau\nu)$, α, γ and second by the theoretical uncertainty on $\hat{\mathcal{B}}_{B_d}$. This tests clearly shows that the semileptonic extraction of $|V_{ub}|$ has little to do with the $\mathcal{B}(B \to \tau\nu)$ anomaly. Further insight is provided by Fig. 6 where the constraints on the decay constant f_{B_d} and $f_{B_d}\sqrt{\hat{\mathcal{B}}_{B_d}}$ are shown. We compare the fit inputs f_{B_d} and $f_{B_d}\sqrt{\hat{\mathcal{B}}_{B_d}}$ taken from LQCD calculations with their predictions from the fit. The measured $\mathcal{B}(B \to \tau\nu)$ value leads to the constraint on f_{B_d} represented by the horizontal green band. The vertical orange band represents the constraint on $f_{B_d}\sqrt{\hat{\mathcal{B}}_{B_d}}$ thanks to the Δm_d measurement. The combined prediction for both quantities (red and yellow oval regions) reveals that the predicted value for $f_{B_d}\sqrt{\hat{\mathcal{B}}_{B_d}}$ is in very good agreement with the LQCD input. Therefore, if the discrepancy is driven by too small a f_{B_d} value, the lattice-QCD artifact responsible for this underestimation should not affect the more complicated determination of the $\Delta B = 2$ matrix element proportional to $f_{B_d}\sqrt{\hat{\mathcal{B}}_{B_d}}$. This was already demonstrated in Fig. 5 in order to preserve the good agreement between the predicted and calculated values for $f_{B_d}\sqrt{\hat{\mathcal{B}}_{B_d}}$.

Another potential anomaly related to $|\epsilon_K|$ has been widely discussed in the literature [8,9], but does not show up with our choice of inputs and statistical treatment. More details can be found in the Appendix. Other interesting outcomes of the standard model global fit concern the prediction of the recently measured *CP*-asymmetries by the Tevatron experiments, namely, in $B_s \to J/\psi\phi$ and in dimuonic inclusive decays (see Sec. III). The discrepancy of these measurements with respect to their standard model fit prediction, together with the $\mathcal{B}(B \to \tau\nu)$ anomaly, are summarized in Table X. It is worth noting that the standard model does not correlate these anomalies between each other, because the standard prediction for *CP*-violation ($-2\phi_s^{\psi\phi}$ and $A_{\rm SL}$) in the B_s system is

TABLE X. Pull values for selected parameters and observables in the standard model (SM) and scenario (Sc.) I, II, III global fits, in terms of the number of equivalent standard deviations between the direct measurement (Tables VI and VII) and the full indirect fit predictions (Tables VIII, IX, XI, XII, XIV, XV, XVII, and XVIII). These numbers are computed from the χ^2 difference with and without the input, interpreted with the appropriate number of degrees of freedom. The zero entries are due to the existence of flat likelihoods in the Rfit model for theoretical uncertainties [53,84]. The last three lines show the pulls for specific correlated combinations of the three most anomalous observables.

Quantity	Deviation			
	wrt SM fit	wrt Sc. I	wrt Sc. II	wrt Sc. III
$\hat{B}_K$	0.0σ		0.0σ	
f_{B_s} [MeV]	0.0σ	0.9σ	0.8σ	1.2σ
$\hat{\mathcal{B}}_{B_s}$	1.2σ	0.8σ	0.9σ	0.3σ
f_{B_s}/f_{B_d}	0.0σ	0.9σ	0.0σ	0.0σ
$\mathcal{B}_{B_s}/\mathcal{B}_{B_d}$	1.0σ	0.9σ	1.0σ	0.9σ
$\tilde{\mathcal{B}}_{S,B_s}(m_b)$	1.0σ	0.7σ	1.1σ	0.2σ
α	1.1σ	0.2σ	0.7σ	1.0σ
$\phi_d^\Delta + 2\beta$	2.8σ	0.8σ	2.6σ	1.3σ
γ	0.0σ	0.0σ	0.0σ	0.0σ
$\phi_s^\Delta - 2\beta_s$	2.3σ	0.5σ	2.4σ	1.6σ
$\lvert V_{ud}\rvert$	0.0σ	0.0σ	0.0σ	0.1σ
$\lvert V_{us}\rvert$	0.0σ	0.0σ	0.0σ	0.0σ
$\lvert V_{ub}\rvert$	0.0σ	1.0σ	0.0σ	2.3σ
$\lvert V_{cb}\rvert$	0.0σ	0.0σ	1.6σ	1.8σ
$\lvert\epsilon_K\rvert$	0.0σ		0.0σ	
Δm_d	1.0σ	0.9σ	1.0σ	0.8σ
Δm_s	0.3σ	0.7σ	0.9σ	1.2σ
$A_{\rm SL}$	2.9σ	1.2σ	2.9σ	2.2σ
$a_{\rm SL}^d$	0.9σ	0.2σ	0.8σ	0.3σ
$a_{\rm SL}^s$	0.2σ	0.7σ	0.2σ	0.0σ
$\Delta\Gamma_s$	1.0σ	0.2σ	1.1σ	0.9σ
$\mathcal{B}(B \to \tau\nu)$	2.9σ	0.7σ	2.6σ	1.0σ
$\mathcal{B}(B \to \tau\nu)$ and $A_{\rm SL}$	3.7σ	0.9σ	3.5σ	2.0σ
$\phi_s^\Delta - 2\beta_s$ and $A_{\rm SL}$	3.3σ	0.8σ	3.3σ	2.3σ
$\mathcal{B}(B \to \tau\nu)$, $\phi_s^\Delta - 2\beta_s$ and $A_{\rm SL}$	4.0σ	0.6σ	3.8σ	2.1σ

essentially zero, and hence at leading order has no common parameter with the $\mathcal{B}(B \to \tau\nu)$ anomaly.

B. Scenario I: New physics in B_d-$\bar{B}_d$ mixing and B_s-$\bar{B}_s$ mixing

In this section, we present the CKM fit for scenario I where new physics in mixing is independently allowed in the B_d and B_s systems (i.e. Δ_d and Δ_s are independent). These fits exclude the constraint from ϵ_K since it is not possible to obtain nontrivial constraints for the three new physics parameters in the K sector. The first study of this kind using only B-factory data has been performed in [60] followed by a complete quantitative analysis [53] profiting from the large data sets of *BABAR* and Belle. Analyses taking also into account the B_s system have been performed by the UTfit Collaboration [148,149].

In Fig. 7 we show the $\bar{\rho} - \bar{\eta}$ plane for this fit, allowing us to constrain the parameters of the CKM matrix using observables not affected by new physics according to our hypothesis. There are two allowed solutions in $\bar{\rho} - \bar{\eta}$ which cannot be distinguished when using only $|V_{ud}|$, $|V_{us}|$, $|V_{cb}|$, $|V_{ub}|$ from semileptonic decays and from $B \to \tau\nu$, γ and $\alpha - \phi_d^\Delta/2$ and $\beta + \phi_d^\Delta/2$. Once a_{SL}^d is added, the second solution at negative $\bar{\rho}$ and $\bar{\eta}$ values is clearly

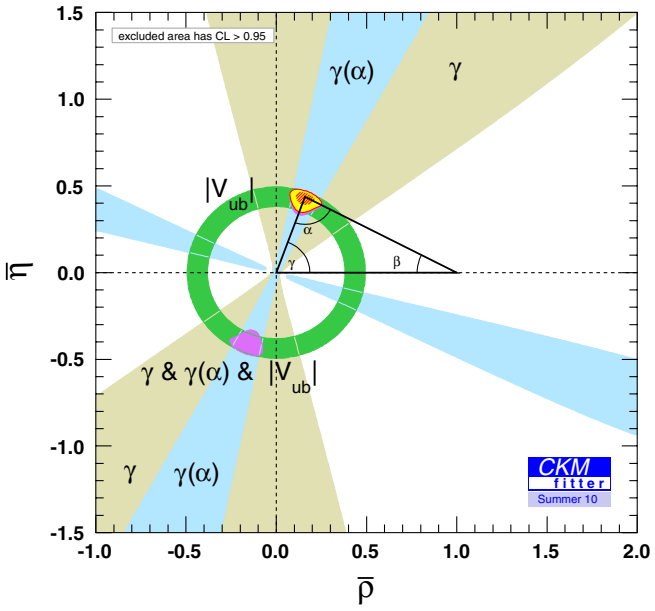

FIG. 7 (color online). Constraint on the CKM $(\bar{\rho}, \bar{\eta})$ coordinates, using only the inputs which are not affected by new physics in mixing: $|V_{ud}|$, $|V_{us}|$, $|V_{cb}|$, $|V_{ub}|$ from semileptonic decays and from $B \to \tau\nu$, γ [directly and from the combination $\gamma(\alpha)$ of $\alpha - \phi_d^\Delta/2$ and $\beta + \phi_d^\Delta/2$]. Regions outside the shaded areas have C.L. $> 95.45\%$. For the combined fit, two solutions are available: the usual solution corresponds to the (yellow) area at the apex of the triangle (points with C.L. $< 95.45\%$, the shaded region corresponding to points with C.L. $< 68.3\%$), and the second solution corresponds to the (purple) dark region for $\bar{\eta} < 0$.

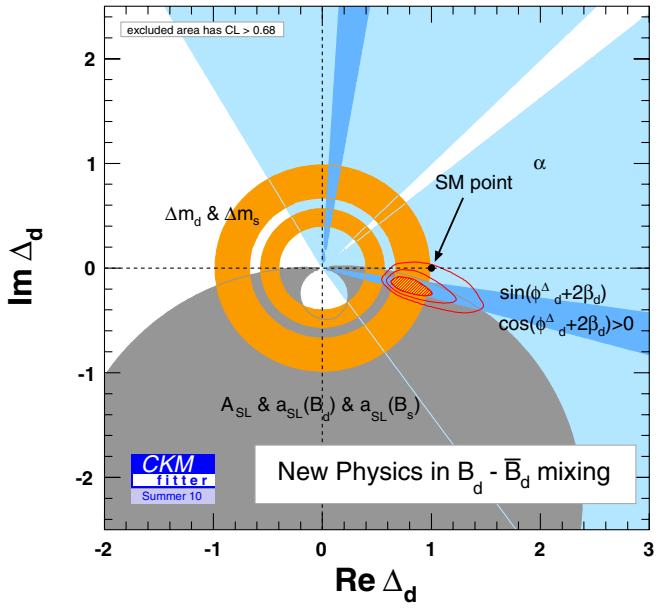

FIG. 8 (color online). Constraint on the complex parameter Δ_d from the fit in scenario I. For the individual constraints the shaded areas represent regions with C.L. $< 68.3\%$. For the combined fit the shaded (red) area shows the region with C.L. $< 68.3\%$ while the two additional contour lines inscribe the regions with C.L. $< 95.45\%$, and C.L. $< 99.73\%$, respectively.

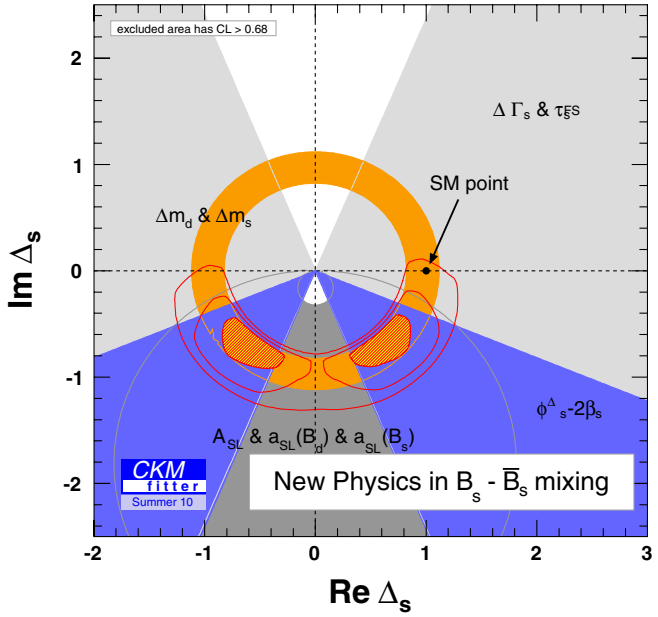

FIG. 9 (color online). Constraint on the complex parameter Δ_s from the fit in scenario . For the individual constraints the shaded areas represent regions with C.L. $< 68.3\%$. For the combined fit the shaded (red) area shows the region with C.L. $< 68.3\%$ while the two additional contour lines inscribe the regions with C.L. $< 95.45\%$, and C.L. $< 99.73\%$, respectively.

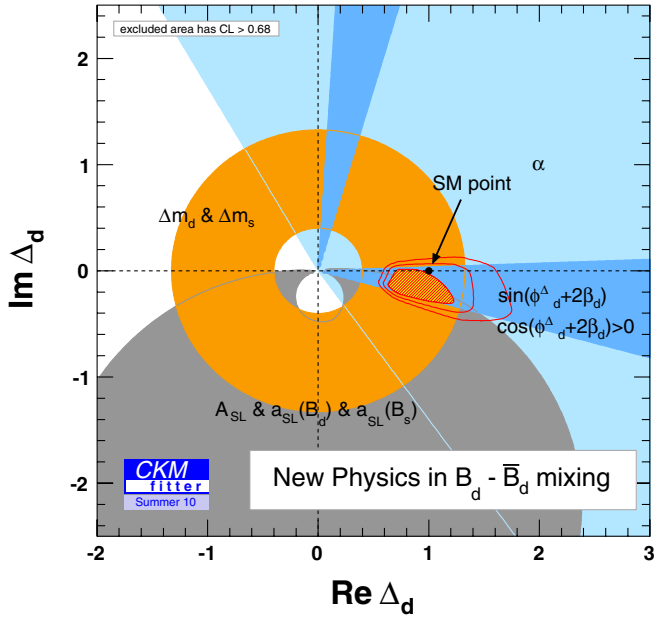

FIG. 10 (color online). Fit result for the complex parameter Δ_s in scenario I when excluding $\mathcal{B}(B \to \tau\nu)$ from the list of inputs. For the combined fit the shaded (red) area shows the region with C.L. $< 68.3\%$ while the two additional contour lines inscribe the regions with C.L. $< 95.45\%$, and C.L. $< 99.73\%$, respectively.

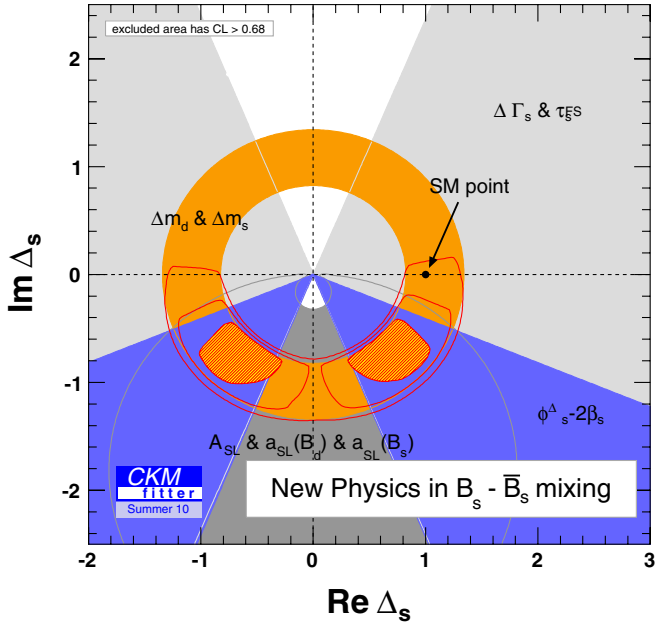

FIG. 11 (color online). Fit result for the complex parameter Δ_d in scenario I when excluding $\mathcal{B}(B \to \tau\nu)$ from the list of inputs. For the combined fit the shaded (red) area shows the region with C.L. $< 68.3\%$ while the two additional contour lines inscribe the regions with C.L. $< 95.45\%$, and C.L. $< 99.73\%$, respectively.

disfavored leaving as the only solution the one with positive $\bar{\rho}$ and $\bar{\eta}$ values. Figures 8 and 9 show the results of the global fit for scenario I in the complex Δ_d and Δ_s planes, respectively. We emphasize that we assume that Δ_d and Δ_s are taken as independent in this scenario, but that some of the constraints correlate them (such that $a_{\rm fs}$ from the inclusive dimuon asymmetry, and the ratio $\Delta m_d/\Delta m_s$). Therefore the figures should be understood as two-dimensional projections of a single multidimensional fit, and not as independent computations. The constraint from Δm_d in the $\mathrm{Re}\Delta_d - \mathrm{Im}\Delta_d$ plane shows two allowed ring-like regions. They correspond to the two allowed solutions in the $\bar{\rho} - \bar{\eta}$ plane when $a^d_{\rm SL}$ is excluded from the list of inputs. Indeed, in this new physics scenario, Δm_d is proportional to the product $|\Delta_d|^2 \cdot |V_{td}V^*_{tb}|^2$, where the second factor is different for the two allowed solutions since it is the side of the unitarity triangle connecting (1, 0) and $(\bar{\rho}, \bar{\eta})$. The impact of $a^d_{\rm SL}$ highlights the power of this measurement to exclude a large region of the possible new physics parameter space even with a measurement precision of $O(5 \times 10^{-3})$. In the combined fit the inner ring (which corresponds to the solution for ϕ^Δ_d in the first quadrant near the $\mathrm{Im}\Delta_d$ axis) in the complex Δ_d plane is disfavored. This leaves us with an allowed region for $|\Delta_d|$ which is in agreement with the standard model value $\Delta_d = 1$, albeit with possible deviations up to 40%. The new physics phase ϕ^Δ_d, mainly driven by the $\mathcal{B}(B \to \tau\nu)$ vs $\sin 2\phi^{\psi K}_d$ correlation, has the best fit value at $-12.9°$. It can be as large as $-21.8°$ ($-27.9°$) at the 2σ (3σ) level and shows currently a deviation from the standard model of 2.7σ. It is interesting to note that the combined individual constraint from $a^d_{\rm SL}$, $a^s_{\rm SL}$, and $A_{\rm SL}$ *also* favors a negative new physics phase ϕ_{Δ_d}, mainly due to the measured negative $a^d_{\rm SL}$ value. When $\mathcal{B}(B \to \tau\nu)$ is excluded from the inputs $\mathrm{Im}\Delta_d$ and hence ϕ_{Δ_d} is in good agreement with the standard model value (see Fig. 10). At the same time

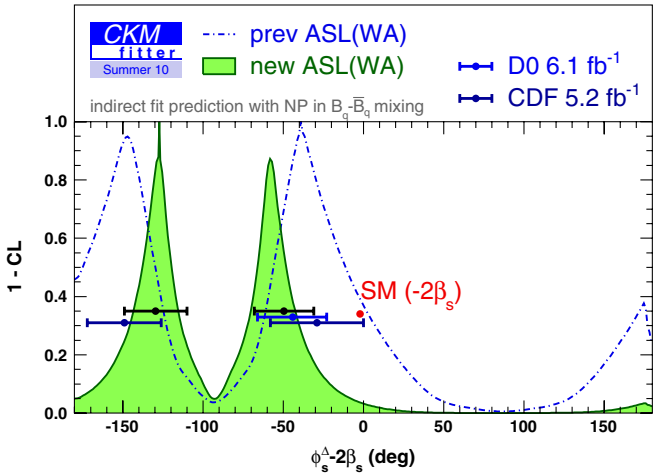

FIG. 12 (color online). New physics scenario I. Indirect constraint on the *CP* phase $\phi^{\psi\phi}_s$, compared with the direct measurement by the Tevatron: previous world average [83] (in black) and the summer 2010 CDF and D0 updates [31,32] (in blue). The dotted line represents the full scenario I fit with the previous world average for $a_{\rm fs}$, while the solid (green) curve is the update after the D0 evidence for a nonzero dimuonic asymmetry.

the allowed range for $|\Delta_d|$ is significantly enlarged since $\mathcal{B}(B \to \tau\nu)$ helps to reduce the uncertainty on Δm_d: The two rings are enlarged and merge into a single one.

The constraint on $|\Delta_s|$ from Δm_s is more stringent than that for $|\Delta_d|$—thanks to the smaller theoretical uncertainty in its prediction compared to Δm_d—and in good agreement with the standard model point. It is interesting to note that also for the B_s system the constraint from $\mathcal{B}(B \to \tau\nu)$ plays a non-negligible role: When removing this measurement from the list of inputs the constraint on $|\Delta_s|$ becomes weaker since this measurement improves the input on the decay constant f_{B_s} through the SU(3)-breaking parameter ξ (compare Fig. 11 with Fig. 9). There is evidence for a nonzero new physics phase ϕ_s^Δ at the 3.1σ level. This discrepancy is driven by the $A_{\rm SL}$ from D0 and by the $\phi_s^{\psi\phi}$ analyses from Tevatron, but is expected to be somewhat relaxed by the updated measurements of $\phi_s^{\psi\phi}$ [31,32].

We also note that there is an interesting difference in the allowed size of the new physics contribution when comparing the B_d and the B_s systems. While in the B_s system the size of the new physics contribution is essentially constrained by the Δm_s measurement alone, this is not the case in the B_d system. Indeed, the theoretical prediction of Δm_d strongly depends on the Wolfenstein parameters $\bar{\rho}$ and $\bar{\eta}$ whereas this dependence is very weak for Δm_s. The constraint on new physics in B_d-mixing relies thus on $|V_{ub}|$ on one hand and γ on the other hand, the latter being currently dominated by the combination of the $\sin 2\phi_d^{\psi K}$ and α measurements which is independent of new physics contributions in B-mixing. The theory prediction for the oscillation frequency Δm_d depends on the quantity $|\Delta_d| \equiv \sqrt{(\mathrm{Re}\Delta_d)^2 + (\mathrm{Im}\Delta_d)^2}$. Without a good constraint on $|\Delta_d|$ from other observables it can only be predicted with a very large uncertainty as observed in Table IX. The only other observables that are sensitive to the modulus of Δ_d are $a_{\rm SL}^d$ and $A_{\rm SL}$ but those are measured with a precision that is significantly above the standard model prediction and thus do not constrain very much the range of Δm_d [even though they proved powerful in eliminating the negative $(\bar{\rho}, \bar{\eta})$ solution] (the same statement holds for Δm_s).

TABLE XI. Fit results in the new physics scenario I. The notation (!) means that the fit output represents the indirect constraint, *i.e.* the corresponding direct input has been removed from the analysis.

Quantity	Central $\pm$C.L. $\equiv 1\sigma$	$\pm$C.L. $\equiv 2\sigma$	$\pm$C.L. $\equiv 3\sigma$
A	$0.801^{+0.024}_{-0.017}$	$0.801^{+0.034}_{-0.026}$	$0.801^{+0.043}_{-0.036}$
λ	$0.22542^{+0.00077}_{-0.00077}$	$0.2254^{+0.0015}_{-0.0015}$	$0.2254^{+0.0023}_{-0.0023}$
$\bar{\rho}$	$0.159^{+0.036}_{-0.035}$	$0.159^{+0.070}_{-0.067}$	$0.16^{+0.14}_{-0.10}$
$\bar{\eta}$	$0.438^{+0.019}_{-0.029}$	$0.438^{+0.033}_{-0.069}$	$0.438^{+0.047}_{-0.113}$
$\mathrm{Re}(\Delta_d)$	$0.735^{+0.182}_{-0.082}$	$0.74^{+0.38}_{-0.13}$	$0.74^{+0.63}_{-0.17}$
$\mathrm{Im}(\Delta_d)$	$-0.168^{+0.055}_{-0.066}$	$-0.17^{+0.12}_{-0.13}$	$-0.17^{+0.20}_{-0.22}$
$\lvert\Delta_d\rvert$	$0.747^{+0.195}_{-0.079}$	$0.75^{+0.40}_{-0.13}$	$0.75^{+0.66}_{-0.17}$
ϕ_d^Δ [deg]	$-12.9^{+3.8}_{-2.7}$	$-12.9^{+8.9}_{-4.9}$	$-12.9^{+14.9}_{-7.0}$
$\mathrm{Re}(\Delta_s)$	$-0.57^{+0.18}_{-0.17}$ *or* $0.56^{+0.19}_{-0.15}$	$-0.57^{+0.39}_{-0.39}$ *or* $0.56^{+0.42}_{-0.36}$	$-0.57^{+1.80}_{-0.64}$
$\mathrm{Im}(\Delta_s)$	$-0.69^{+0.16}_{-0.14}$	$-0.69^{+0.39}_{-0.34}$	$-0.69^{+0.66}_{-0.56}$
$\lvert\Delta_s\rvert$	$0.887^{+0.143}_{-0.064}$	$0.887^{+0.338}_{-0.093}$	$0.89^{+0.46}_{-0.12}$
ϕ_s^Δ [deg]	-130^{+13}_{-12} *or* $-51.6^{+14.2}_{-9.7}$	-130^{+28}_{-28} *or* -52^{+32}_{-25}	-52^{+50}_{-123}
f_{B_s} [MeV] (!)	278^{+83}_{-34}	278^{+125}_{-58}	278^{+155}_{-82}
f_{B_s}/f_{B_d} (!)	$1.09^{+0.11}_{-0.23}$	$1.09^{+0.27}_{-0.41}$	$1.09^{+0.50}_{-0.47}$
$\hat{\mathcal{B}}_{B_s}$ (!)	$2.21^{+0.70}_{-1.06}$	$2.2^{+1.7}_{-1.6}$	$2.2^{+2.9}_{-2.1}$
$\mathcal{B}_{B_s}/\mathcal{B}_{B_d}$ (!)	$0.48^{+0.69}_{-0.24}$	>0.12	>0.01
$\tilde{\mathcal{B}}_{S,B_s}(m_b)$ (!)	$3.4^{+2.2}_{-3.0}$	$3.4^{+5.2}_{-4.5}$	$3.4^{+8.7}_{-7.7}$
J $[10^{-5}]$	$3.69^{+0.19}_{-0.22}$	$3.69^{+0.31}_{-0.55}$	$3.69^{+0.43}_{-0.93}$
α [deg] (!)	79^{+22}_{-15}	79^{+37}_{-24}	79^{+50}_{-31}
β [deg] (!)	$27.2^{+1.1}_{-3.1}$	$27.2^{+2.0}_{-6.0}$	$27.2^{+2.8}_{-9.1}$
γ [deg] (!)	$70.0^{+4.3}_{-4.5}$	$70.0^{+8.5}_{-9.2}$	70^{+13}_{-20}
$\phi_d^\Delta + 2\beta$ [deg] (!)	28^{+17}_{-32}	28^{+38}_{-55}	28^{+74}_{-79}
ϕ_d [deg]	$-17.9^{+4.9}_{-5.8}$	$-17.9^{+10.2}_{-9.5}$	-18^{+17}_{-12}
$\phi_s^\Delta - 2\beta_s$ [deg] (!)	-127^{+13}_{-17} *or* -58^{+17}_{-13}	< -94 *or* -58^{+52}_{-34}	$<40 >135$
$\phi_s^\Delta - 2\beta_s$ [deg]	-132^{+13}_{-12} *or* $-54.6^{+14.5}_{-9.3}$	-132^{+28}_{-28} *or* -55^{+32}_{-25}	-55^{+51}_{-122}
ϕ_s [deg]	-129^{+13}_{-11} *or* -51^{+14}_{-10}	-129^{+28}_{-27} *or* -51^{+32}_{-25}	-51^{+50}_{-123}

TABLE XII. Fit results in the new physics scenario I. The notation (!) means that the fit output represents the indirect constraint, i.e. the corresponding direct input has been removed from the analysis.

Quantity	Central $\pm$C.L. $\equiv 1\sigma$	$\pm$C.L. $\equiv 2\sigma$	$\pm$C.L. $\equiv 3\sigma$
$\lvert V_{ud}\rvert$ (!)	$0.97426^{+0.00030}_{-0.00030}$	$0.97426^{+0.00060}_{-0.00061}$	$0.97426^{+0.00089}_{-0.00091}$
$\lvert V_{us}\rvert$ (!)	$0.22542^{+0.00095}_{-0.00095}$	$0.2254^{+0.0019}_{-0.0019}$	$0.2254^{+0.0028}_{-0.0029}$
$\lvert V_{ub}\rvert$ (!)	$0.00501^{+0.00104}_{-0.00064}$	$0.0050^{+0.0015}_{-0.0011}$	$0.0050^{+0.0020}_{-0.0016}$
$\lvert V_{cd}\rvert$	$0.22529^{+0.00077}_{-0.00077}$	$0.2253^{+0.0015}_{-0.0015}$	$0.2253^{+0.0023}_{-0.0023}$
$\lvert V_{cs}\rvert$	$0.97344^{+0.00019}_{-0.00021}$	$0.97344^{+0.00037}_{-0.00039}$	$0.97344^{+0.00055}_{-0.00057}$
$\lvert V_{cb}\rvert$ (!)	$0.0407^{+0.0121}_{-0.0075}$	$0.041^{+0.032}_{-0.018}$	$0.041^{+0.047}_{-0.032}$
$\lvert V_{td}\rvert$	$0.00871^{+0.00047}_{-0.00042}$	$0.00871^{+0.00079}_{-0.00078}$	$0.0087^{+0.0011}_{-0.0015}$
$\lvert V_{ts}\rvert$	$0.04001^{+0.00112}_{-0.00078}$	$0.0400^{+0.0015}_{-0.0012}$	$0.0400^{+0.0019}_{-0.0015}$
$\lvert V_{tb}\rvert$	$0.999161^{+0.000032}_{-0.000047}$	$0.999161^{+0.000047}_{-0.000063}$	$0.999161^{+0.000062}_{-0.000079}$
Δm_d [ps^{-1}] (!)	$0.25^{+0.34}_{-0.16}$	>0.04	
Δm_s [ps^{-1}] (!)	$8.6^{+14.7}_{-5.2}$	>0.6	
$A_{\rm SL}$ [10^{-4}] (!)	-42^{+20}_{-19}	-42^{+29}_{-27}	-42^{+40}_{-33}
$A_{\rm SL}$ [10^{-4}]	$-55.7^{+14.9}_{-8.7}$	-56^{+31}_{-16}	-56^{+42}_{-21}
$a^s_{\rm SL} - a^d_{\rm SL}$ [10^{-4}]	-39^{+31}_{-24}	-39^{+58}_{-39}	-39^{+75}_{-54}
$a^d_{\rm SL}$ [10^{-4}] (!)	$-36.2^{+13.9}_{-5.9}$	-36^{+23}_{-11}	-36^{+35}_{-16}
$a^d_{\rm SL}$ [10^{-4}]	$-36.7^{+13.4}_{-5.5}$	-37^{+23}_{-11}	-37^{+34}_{-16}
$a^s_{\rm SL}$ [10^{-4}] (!)	$-84.9^{+33.4}_{-9.8}$	-85^{+64}_{-20}	-85^{+83}_{-27}
$a^s_{\rm SL}$ [10^{-4}]	-75^{+30}_{-18}	-75^{+56}_{-29}	-75^{+74}_{-36}
$\Delta\Gamma_d$ [ps^{-1}] (!)	$0.00577^{+0.00095}_{-0.00257}$	$0.0058^{+0.0015}_{-0.0035}$	$0.0058^{+0.0022}_{-0.0040}$
$\Delta\Gamma_s$ [ps^{-1}] (!)	$-0.118^{+0.068}_{-0.034}$ *or* $0.128^{+0.029}_{-0.062}$	$0.128^{+0.053}_{-0.305}$	$0.128^{+0.068}_{-0.324}$
$\Delta\Gamma_s$ [ps^{-1}]	$-0.109^{+0.029}_{-0.025}$ *or* $0.106^{+0.035}_{-0.020}$	$-0.109^{+0.074}_{-0.049}$ $0.106^{+0.057}_{-0.065}$	$0.106^{+0.076}_{-0.284}$
$\mathcal{B}(B\to\tau\nu)$ [10^{-4}] (!)	$1.457^{+0.073}_{-0.405}$	$1.46^{+0.15}_{-0.84}$	$1.46^{+0.23}_{-0.89}$
$\mathcal{B}(B\to\tau\nu)$ [10^{-4}]	$1.468^{+0.072}_{-0.143}$	$1.47^{+0.15}_{-0.38}$	$1.47^{+0.22}_{-0.64}$

Tables XI and XII show the fit results for various parameters and observables. We also show the result of the fit for quantities that have been individually excluded from the fit in order to quantify possible deviations between the individual input values and their fit predictions. The corresponding pull values are listed in Table X. Among other things it is interesting to note that the indirect fit prediction for the dimuonic asymmetry $A_{\rm SL} = (-42^{+20}_{-19}) \times 10^{-4}$ is consistent at 1.2 standard deviations with the D0/CDF average $(-85 \pm 28) \times 10^{-4}$ used here, and remains more precise in spite of the uncertainties on the theoretical and new physics parameters. Hence future improvements of this measurement are expected to give crucial information on the underlying physics.

Another important output of our global analysis is the prediction of the difference $a^s_{\rm SL} - a^d_{\rm SL}$, that will be measured by the LHCb experiment in the near future [150]. It reads $a^s_{\rm SL} - a^d_{\rm SL} = (-39^{+31}_{-24}) \times 10^{-4}$ ($-93 \times 10^{-4} < a^s_{\rm SL} - a^d_{\rm SL} < 36 \times 10^{-4}$ at the 3σ level), to be compared to the standard model result $a^s_{\rm SL} - a^d_{\rm SL} = (7.93^{+0.66}_{-2.14}) \times 10^{-4}$ ($4.5 \times 10^{-4} < a^s_{\rm SL} - a^d_{\rm SL} < 9.9 \times 10^{-4}$ at 3σ).

In contrast to the standard model fit, our scenario I relates the B_d and B_s anomalies through the correlated determination of the Δ parameters. Hence it is particularly interesting to compute the p-values associated with the hypothesis that some specific combination of the Δ parameters take their standard model value. This is shown in Table XIII. We have listed several hypotheses because the ''standard model'' null hypothesis is *composite*, i.e. it does not allow one to compute the expected distribution of measurements in a given set of experiments, because the standard model does not predict the value of its fundamental parameters. Hence one is *a priori* free to choose among the numerical hypotheses tested in Table XIII the one that models the standard model hypothesis. This choice introduces some arbitrariness, and thus slightly different

TABLE XIII. p-values for various standard model hypotheses in the framework of new physics scenario I, in terms of the number of equivalent standard deviations. These numbers are computed from the χ^2 difference with and without the hypothesis constraint, interpreted with the appropriate number of degrees of freedom.

Hypothesis	p-value
$\mathrm{Im}(\Delta_d) = 0$ (1D)	2.7σ
$\mathrm{Im}(\Delta_s) = 0$ (1D)	3.1σ
$\Delta_d = 1$ (2D)	2.7σ
$\Delta_s = 1$ (2D)	2.7σ
$\mathrm{Im}(\Delta_d) = \mathrm{Im}(\Delta_s) = 0$ (2D)	3.8σ
$\Delta_d = \Delta_s$ (2D)	2.1σ
$\Delta_d = \Delta_s = 1$ (4D)	3.6σ

answers to the same underlying question. In the present context, one may view the hypothesis $\Delta_d = \Delta_s = 1$ as the most natural choice to represent the standard model: This hypothesis is excluded at 3.6σ by our global analysis.

However, one should be aware that this hypothesis somewhat dilutes the most anomalous pieces of information that are related to CP-violation, by including in the test CP-conserving components (corresponding to the real part of Δ_d and Δ_s). Let us imagine that we consider a more general class of models allowing for CP-violation in several different processes that are compatible with the standard model. We would have introduced a different Δ parameter for each process. The test corresponding to all Δ parameters being equal to 1 would then receive a small contribution from the three anomalies that we have discussed, but this would be hidden by the other measurements in agreement with the standard model expectations. This illustates why it is sometimes worth testing reduced hypotheses, such as $\mathrm{Im}(\Delta_d) = \mathrm{Im}(\Delta_s) = 0$, in order to single out specific deviations from the standard model. The latter CP hypothesis is excluded at 3.8σ by our global analysis.

We also learn from this table that scenario III, to be discussed below, is slightly disfavored by the data when one considers it as a subcase of scenario I ($\Delta_d = \Delta_s$), in agreement with the third paper of Ref. [34]. Finally as already stressed above, the various evidences against the standard model shown in Table XIII will be relaxed when the new Tevatron average of the $B_s \to J/\psi\phi$ tagged analysis is available [31,32]. However, a very rough estimate allows us to predict that at least the $\mathrm{Im}(\Delta_d) = \mathrm{Im}(\Delta_s) = 0$ hypothesis (i.e. no CP-violating phase in either B_d or B_s mixing amplitudes) will remain disfavored by more than 3 standard deviations. Indeed although the mixing CP-phase is expected to come back closer to the standard model value [31,32], it remains compatible with the indirect constraint from the dimuonic asymmetry, as shown by Fig. 12. In particular, the best value for $\phi_s^{\Delta} - 2\beta_s$ is only about 1 standard deviation below the most recent CDF and D0 updates for $B_s \to J/\psi\phi$ [31,32], not included in the present analysis. Again it would be interesting to know the precise form of the combined CDF and D0 likelihoods in order to quantify by how much the difference of the indirect global fit prediction of A_{SL} with its direct measurement is increased with respect to our estimate of 1.2σ in Table X.

C. Scenario II: MFV with small bottom Yukawa coupling

In this section, we discuss the MFV scenario which allows one to connect the B and kaon sectors. This kind of numerical analysis was first presented in [151]. In this scenario, there is only one additional real new physics parameter Δ; see Eq. (42). As a consequence, this scenario has difficulties to describe a situation where the data prefer a nonzero new physics phase in B-mixing. Indeed the scenario II hypothesis embedded in scenario I, that is $\Delta_d = \Delta_s = \Delta$ with $\mathrm{Im}(\Delta) = 0$, is disfavored by 3.7 standard deviations. The quality of the fit does not change when ϵ_K is removed from the list of inputs.

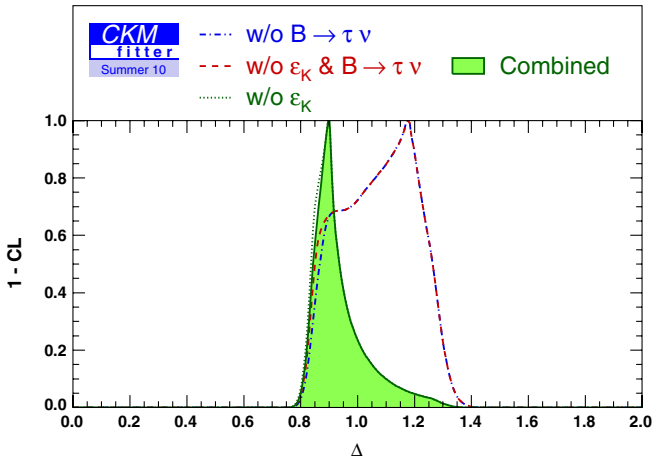

FIG. 13 (color online). Constraint on the real parameter Δ from the fit in scenario II. The red dashed line represents the constraint if only B_d and B_s observables are used excluding $\mathcal{B}(B \to \tau\nu)$ and ϵ_K. When adding ϵ_K the constraint is essentially unchanged (blue dotted-dashed line). A significantly stronger constraint is obtained when adding $\mathcal{B}(B \to \tau\nu)$ (dotted green). The full constraint when adding both, $\mathcal{B}(B \to \tau\nu)$ and ϵ_K, is shown as a solid (green) curve.

Figure 13 shows the impact of the various constraints on the parameter Δ. The constraint is only slightly changed when adding to the B-meson observables—where $\mathcal{B}(B \to \tau\nu)$ has been excluded—the ϵ_K constraint. On the other hand, when adding $\mathcal{B}(B \to \tau\nu)$, the constraint gets significantly stronger at the 1σ level while at 2σ the reduction in the allowed parameter space is modest. In Tables XIV and XV we further provide the constraints on individual parameters obtained from the combined fit in scenario II as well as predictions for the parameters not used as fit inputs. The compatibility of the parameter Δ with 1 is good, meaning that this new physics scenario does not describe the data better than the standard model, as expected, since all discussed anomalies seem to require new CP phases.

D. Scenario III: Generic MFV

In Fig. 14 we present the result from the combined fit to B_d and B_s observables in the complex plane $\Delta = \Delta_s = \Delta_d$ for the MFV hypothesis allowing for a large bottom Yukawa coupling y_b (scenario III). In scenario III, Δ can have a sizeable complex component proportional to y_b^2. One expects that the constraint $\Delta_s = \Delta_d$ reduces the size of the allowed new physics contributions significantly with respect to the general case studied in scenario I. However,

TABLE XIV. Fit results in the new physics scenario II. The notation (!) means that the fit output represents the indirect constraint, i.e. the corresponding direct input has been removed from the analysis.

Quantity	Central $\pm$C.L. $\equiv 1\sigma$	$\pm$C.L. $\equiv 2\sigma$	$\pm$C.L. $\equiv 3\sigma$
A	$0.8172^{+0.0093}_{-0.0199}$	$0.817^{+0.019}_{-0.037}$	$0.817^{+0.028}_{-0.047}$
λ	$0.22543^{+0.00077}_{-0.00077}$	$0.2254^{+0.0015}_{-0.0015}$	$0.2254^{+0.0023}_{-0.0023}$
$\bar{\rho}$	$0.145^{+0.026}_{-0.019}$	$0.145^{+0.048}_{-0.028}$	$0.145^{+0.066}_{-0.037}$
$\bar{\eta}$	$0.342^{+0.016}_{-0.011}$	$0.342^{+0.030}_{-0.024}$	$0.342^{+0.045}_{-0.038}$
Δ	$0.899^{+0.072}_{-0.069}$	$0.90^{+0.31}_{-0.10}$	$0.90^{+0.45}_{-0.13}$
B_K (!)	$0.88^{+0.23}_{-0.15}$	$0.88^{+0.34}_{-0.26}$	$0.88^{+0.44}_{-0.31}$
f_{B_s} [MeV] (!)	$254.5^{+8.4}_{-11.9}$	254^{+17}_{-37}	254^{+26}_{-72}
$\hat{\mathcal{B}}_{B_s}$ (!)	$0.763^{+0.545}_{-0.075}$	$0.76^{+0.80}_{-0.14}$	$0.76^{+1.12}_{-0.19}$
f_{B_s}/f_{B_d} (!)	$1.217^{+0.053}_{-0.035}$	$1.217^{+0.113}_{-0.076}$	$1.22^{+0.16}_{-0.18}$
$\mathcal{B}_{B_s}/\mathcal{B}_{B_d}$ (!)	$1.136^{+0.076}_{-0.095}$	$1.14^{+0.16}_{-0.19}$	$1.14^{+0.24}_{-0.28}$
$\tilde{\mathcal{B}}_{S,B_s}(m_b)$ (!)	$-0.9^{+1.3}_{-2.2}$	$-0.9^{+2.6}_{-3.7}$	$-0.9^{+4.0}_{-5.1}$
J $[10^{-5}]$	$2.99^{+0.15}_{-0.12}$	$2.99^{+0.29}_{-0.29}$	$2.99^{+0.44}_{-0.42}$
α [deg] (!)	$93.3^{+5.7}_{-4.5}$	$93.3^{+8.5}_{-6.7}$	$93.3^{+10.6}_{-8.6}$
β [deg] (!)	$28.05^{+0.70}_{-2.27}$	$28.1^{+1.4}_{-4.8}$	$28.1^{+2.1}_{-7.4}$
γ [deg] (!)	$67.1^{+2.9}_{-3.8}$	$67.1^{+4.5}_{-7.2}$	$67.1^{+6.0}_{-10.0}$
ϕ_d [deg]	$-5.7^{+1.5}_{-3.3}$	$-5.7^{+2.5}_{-4.2}$	$-5.7^{+2.8}_{-5.2}$
$-2\beta_s$ [deg] (!)	$-2.085^{+0.071}_{-0.095}$	$-2.08^{+0.15}_{-0.18}$	$-2.08^{+0.23}_{-0.27}$
$-2\beta_s$ [deg]	$-2.083^{+0.070}_{-0.097}$	$-2.08^{+0.15}_{-0.19}$	$-2.08^{+0.24}_{-0.28}$
ϕ_s [deg]	$0.401^{+0.042}_{-0.124}$	$0.401^{+0.090}_{-0.211}$	$0.40^{+0.14}_{-0.26}$

our fit result in Fig. 14 still allows for a new physics contribution of order -20% to $+40\%$. The new physics phase in this scenario shows evidence for a deviation from the standard model because both $a_{\rm fs}$ and the ϕ_s^Δ measurement on the one hand and the discrepancy between $\sin 2\phi_d^{\psi K}$ and $\mathcal{B}(B \to \tau\nu)$, on the other hand, prefer a negative new physics phase in $B_{d,s}$ mixing.

Compared to scenario II this model is in much better agreement with the data regardless of whether one takes into account $\mathcal{B}(B \to \tau\nu)$ as an input or not. While the B_d sector constraints do not allow too large a new physics phase, the B_s sector prefers a large new physics phase, though with large errors. As a consequence and as already discussed above, the quality of the fit in scenario III is manifestly worse (2.1σ) than in scenario I.

In this scenario, the B_d and B_s systems decouple from the kaon system and hence the constraint on $\mathrm{Re}\Delta$ and $\mathrm{Im}\Delta$ cannot be improved by adding ϵ_K as this introduces the additional new physics parameter Δ_K^{tt} in the theoretical prediction for ϵ_K. However, when including ϵ_K in the fit one is able to constrain Δ_K^{tt} from the fitted values of the CKM parameters. The parameter is in agreement with the standard model expectation but could differ by more than 40% from $\Delta_K^{tt} = 1$. Similarly to the previous scenarios, one-dimensional results from the fit in scenario III are shown in Tables XVII and XVIII. Again one sees that, in

TABLE XV. Fit results in the new physics scenario II. The notation (!) means that the fit output represents the indirect constraint, i.e. the corresponding direct input has been removed from the analysis.

Quantity	Central $\pm$C.L. $\equiv 1\sigma$	$\pm$C.L. $\equiv 2\sigma$	$\pm$C.L. $\equiv 3\sigma$
$\lvert V_{ud}\rvert$(!)	$0.97426^{+0.00030}_{-0.00030}$	$0.97426^{+0.00060}_{-0.00061}$	$0.97426^{+0.00089}_{-0.00091}$
$\lvert V_{us}\rvert$(!)	$0.22545^{+0.00095}_{-0.00095}$	$0.2254^{+0.0019}_{-0.0019}$	$0.2254^{+0.0028}_{-0.0029}$
$\lvert V_{ub}\rvert$(!)	$0.00357^{+0.00015}_{-0.00014}$	$0.00357^{+0.00030}_{-0.00029}$	$0.00357^{+0.00046}_{-0.00044}$
$\lvert V_{cd}\rvert$	$0.22529^{+0.00077}_{-0.00077}$	$0.2253^{+0.0015}_{-0.0015}$	$0.2253^{+0.0023}_{-0.0023}$
$\lvert V_{cs}\rvert$	$0.97341^{+0.00018}_{-0.00018}$	$0.97341^{+0.00036}_{-0.00036}$	$0.97341^{+0.00054}_{-0.00054}$
$\lvert V_{cb}\rvert$(!)	$0.0493^{+0.0028}_{-0.0061}$	$0.0493^{+0.0048}_{-0.0094}$	$0.0493^{+0.0066}_{-0.0116}$
$\lvert V_{td}\rvert$	$0.00863^{+0.00020}_{-0.00023}$	$0.00863^{+0.00032}_{-0.00055}$	$0.00863^{+0.00043}_{-0.00082}$
$\lvert V_{ts}\rvert$	$0.04078^{+0.00038}_{-0.00097}$	$0.04078^{+0.00076}_{-0.00171}$	$0.0408^{+0.0011}_{-0.0021}$
$\lvert V_{tb}\rvert$	$0.999131^{+0.000040}_{-0.000016}$	$0.999131^{+0.000071}_{-0.000032}$	$0.999131^{+0.000088}_{-0.000048}$
ϵ_K $[10^{-3}]$ (!)	$1.87^{+0.54}_{-0.55}$	$1.87^{+0.95}_{-0.67}$	$1.87^{+1.21}_{-0.77}$
Δm_d $[\mathrm{ps}^{-1}]$ (!)	$0.554^{+0.073}_{-0.047}$	$0.554^{+0.114}_{-0.095}$	$0.55^{+0.16}_{-0.14}$
Δm_s $[\mathrm{ps}^{-1}]$ (!)	$16.2^{+1.7}_{-1.4}$	$16.2^{+3.7}_{-2.6}$	$16.2^{+8.5}_{-3.6}$
$A_{\rm SL}$ $[10^{-4}]$ (!)	$-4.04^{+1.01}_{-0.53}$	$-4.0^{+1.9}_{-1.1}$	$-4.0^{+2.4}_{-1.6}$
$A_{\rm SL}$ $[10^{-4}]$	$-4.06^{+0.96}_{-0.55}$	$-4.1^{+1.9}_{-1.1}$	$-4.1^{+2.4}_{-1.7}$
$a^s_{\rm SL} - a^d_{\rm SL}$ $[10^{-4}]$	$8.74^{+0.99}_{-1.97}$	$8.7^{+1.9}_{-4.0}$	$8.7^{+2.8}_{-4.9}$
$a^d_{\rm SL}$ $[10^{-4}]$ (!)	$-8.36^{+1.93}_{-0.94}$	$-8.4^{+3.9}_{-1.8}$	$-8.4^{+4.7}_{-2.7}$
$a^d_{\rm SL}$ $[10^{-4}]$	$-8.37^{+1.90}_{-0.95}$	$-8.4^{+3.8}_{-1.8}$	$-8.4^{+4.7}_{-2.7}$
$a^s_{\rm SL}$ $[10^{-4}]$ (!)	$0.373^{+0.045}_{-0.083}$	$0.373^{+0.078}_{-0.168}$	$0.37^{+0.11}_{-0.21}$
$a^s_{\rm SL}$ $[10^{-4}]$	$0.373^{+0.045}_{-0.083}$	$0.373^{+0.078}_{-0.168}$	$0.37^{+0.11}_{-0.21}$
$\Delta\Gamma_d$ $[\mathrm{ps}^{-1}]$ (!)	$0.00426^{+0.00056}_{-0.00154}$	$0.0043^{+0.0011}_{-0.0021}$	$0.0043^{+0.0016}_{-0.0024}$
$\Delta\Gamma_s$ $[\mathrm{ps}^{-1}]$ (!)	$0.110^{+0.079}_{-0.022}$	$0.110^{+0.089}_{-0.037}$	$0.110^{+0.097}_{-0.051}$
$\Delta\Gamma_s$ $[\mathrm{ps}^{-1}]$	$0.0946^{+0.0174}_{-0.0082}$	$0.095^{+0.047}_{-0.025}$	$0.095^{+0.088}_{-0.037}$
$\mathcal{B}(B \to \tau\nu)$ $[10^{-4}]$ (!)	$0.653^{+0.277}_{-0.040}$	$0.653^{+0.404}_{-0.077}$	$0.65^{+0.52}_{-0.11}$
$\mathcal{B}(B \to \tau\nu)$ $[10^{-4}]$	$0.92^{+0.12}_{-0.10}$	$0.92^{+0.23}_{-0.26}$	$0.92^{+0.33}_{-0.34}$

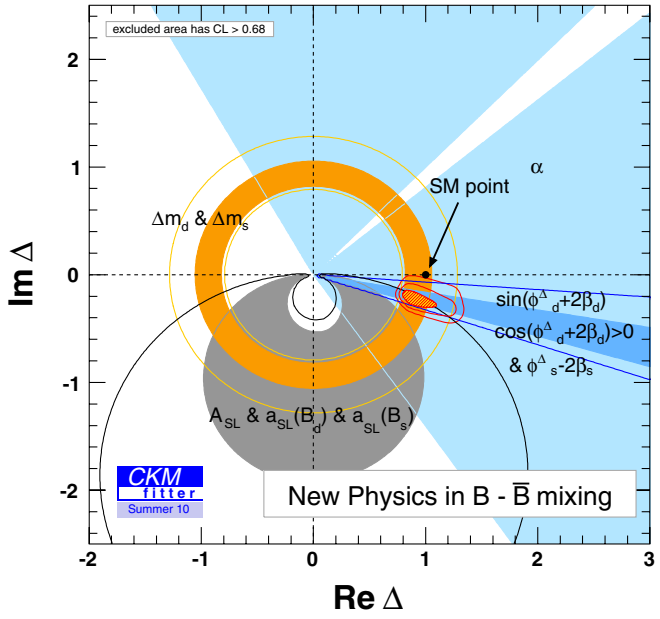

FIG. 14 (color online). Constraint on the complex parameter $\Delta \equiv \Delta_d = \Delta_s$ from the fit in scenario III. For the individual constraints the colored areas represent regions with CL $<$ 68.3%. In addition, a C.L. $<$ 95.45% contour is shown for the individual constraints obtained from Δm_d and Δm_s, from A_{SL}, a^d_{SL}, and a^s_{SL}, and from $\phi^{\psi K}_d$ and $\phi^{\psi\phi}_s$. For the combined fit the shaded (red) area shows the region with C.L. $<$ 68.3% while the two additional contour lines inscribe the regions with CL $<$ 95.45% and CL $<$ 99.73%, respectively.

particular, the semileptonic asymmetries $a^d_{\rm SL}$ and $A_{\rm SL}$ are more precisely predicted than the measurements, so that improvements of the data will be extremely instructive. The asymmetry difference is now predicted to be $a^s_{\rm SL} - a^d_{\rm SL} = (18.6^{+2.0}_{-10.2}) \times 10^{-4}$ $(-1 \times 10^{-4} < a^s_{\rm SL} - a^d_{\rm SL} < 25 \times 10^{-4}$ at 3σ), hence a moderate positive value is preferred with respect to scenario I that predicts a larger negative value.

Finally, two tests of the standard model are interesting to study within scenario III, and are shown in Table XVI. As in scenario I, they show evidence for new physics, and that scenario III describes the data significantly better than either the standard model or scenario II, assuming as before that the improved data on $B_s \to J/\psi\phi$ do not change the overall picture dramatically.

TABLE XVI. p-values for various standard model hypotheses in the framework of new physics scenario III, in terms of the number of equivalent standard deviations. These numbers are computed from the χ^2 difference with and without the hypothesis constraint, interpreted with the appropriate number of degrees of freedom.

Hypothesis	p-value
$\mathrm{Im}(\Delta) = 0$ (1D)	3.5σ
$\Delta = 1$ (2D)	3.3σ

V. CONCLUSIONS

In this paper, we have studied three different scenarios of new physics in $|\Delta F| = 2$ transitions. The complex parameters quantifying the new physics contributions to $B_q - \bar{B}_q$ mixing are $\Delta_q \equiv |\Delta_q| \cdot e^{i\phi^\Delta_q} \equiv M^q_{12}/M^{\mathrm{SM},q}_{12}$. In $K - \bar{K}$ mixing three parameters Δ^{tt}_K, Δ^{ct}_K, and Δ^{cc}_K are needed.

We have first recalled the result of the standard model fit using the current available data sets. In the B system an interesting effect is observed: The inclusion of $\mathcal{B}(B \to \tau\nu)$ obtained from a combination of *BABAR* and Belle measurements deviates from its prediction in the standard model fit by 2.9σ which either points to a large statistical fluctuation in the experimental numbers, to a problem in the calculation of both the decay constant f_{B_d} and the bag parameter $\mathcal{B}_{B_d}$ on the lattice, or to new physics contributions in $\sin 2\beta$ and/or in $B \to \tau\nu$. If there were new physics contributions to B_d mixing this discrepancy would point to a negative nonvanishing new physics phase ϕ^Δ_d. A second hint for a deviation is observed in the B_s-$\bar{B}_s$ mixing phase $\phi^\Delta_s - 2\beta_s$ measured in $B_s \to J/\psi\phi$ though the significance is here only around 2.3σ. The largest discrepancy actually comes from the recent improved measurement of the dimuonic asymmetry by the D0 Collaboration, which is at odds at the 3.2σ level with respect to the indirect fit

TABLE XVII. Fit results in the new physics scenario III. The notation (!) means that the fit output represents the indirect constraint, i.e. the corresponding direct input has been removed from the analysis.

Quantity	Central	$\pm$C.L. $\equiv 1\sigma$	$\pm$C.L. $\equiv 2\sigma$	$\pm$C.L. $\equiv 3\sigma$
A	$0.7928^{+0.0288}_{-0.0092}$		$0.793^{+0.040}_{-0.018}$	$0.793^{+0.050}_{-0.027}$
λ	$0.22536^{+0.00077}_{-0.00077}$		$0.2254^{+0.0015}_{-0.0015}$	$0.2254^{+0.0023}_{-0.0023}$
$\bar{\rho}$	$0.177^{+0.032}_{-0.012}$		$0.177^{+0.059}_{-0.026}$	$0.177^{+0.072}_{-0.042}$
$\bar{\eta}$	$0.439^{+0.011}_{-0.022}$		$0.439^{+0.021}_{-0.050}$	$0.439^{+0.031}_{-0.086}$
$\mathrm{Re}(\Delta)$	$0.876^{+0.126}_{-0.061}$		$0.876^{+0.346}_{-0.097}$	$0.88^{+0.43}_{-0.13}$
$\mathrm{Im}(\Delta)$	$-0.226^{+0.057}_{-0.048}$		$-0.23^{+0.11}_{-0.12}$	$-0.23^{+0.18}_{-0.19}$
$\lvert\Delta\rvert$	$0.907^{+0.128}_{-0.070}$		$0.91^{+0.35}_{-0.11}$	$0.91^{+0.45}_{-0.14}$
ϕ^Δ [deg]	$-14.4^{+2.9}_{-2.1}$		$-14.4^{+6.5}_{-4.2}$	$-14.4^{+11.4}_{-6.3}$
Δ^{tt}_K	$1.01^{+0.40}_{-0.38}$		$1.01^{+0.53}_{-0.43}$	$1.01^{+0.69}_{-0.47}$
f_{B_s} [MeV] (!)	274^{+20}_{-24}		274^{+46}_{-51}	274^{+77}_{-83}
$\hat{\mathcal{B}}_{B_s}$ (!)	$1.44^{+0.33}_{-0.61}$		$1.44^{+0.99}_{-1.37}$	$1.4^{+1.6}_{-1.5}$
f_{B_s}/f_{B_d} (!)	$1.230^{+0.066}_{-0.048}$		$1.23^{+0.13}_{-0.10}$	$1.23^{+0.18}_{-0.21}$
$\mathcal{B}_{B_s}/\mathcal{B}_{B_d}$ (!)	$1.155^{+0.090}_{-0.138}$		$1.16^{+0.18}_{-0.24}$	$1.16^{+0.28}_{-0.40}$
$\tilde{\mathcal{B}}_{S,B_s}(m_b)$ (!)	$1.14^{+0.98}_{-1.91}$		$1.1^{+2.8}_{-4.0}$	$1.1^{+4.6}_{-5.4}$
J $[10^{-5}]$	$3.61^{+0.16}_{-0.14}$		$3.61^{+0.27}_{-0.37}$	$3.61^{+0.36}_{-0.67}$
α [deg] (!)	$88.0^{+4.4}_{-4.9}$		$88.0^{+6.9}_{-6.6}$	$88.0^{+10.4}_{-8.0}$
β [deg] (!)	$28.01^{+0.66}_{-1.47}$		$28.0^{+1.3}_{-3.4}$	$28.0^{+2.0}_{-8.5}$
γ [deg] (!)	$68.1^{+1.3}_{-4.3}$		$68.1^{+2.6}_{-8.0}$	$68.1^{+3.9}_{-9.8}$
$\phi^\Delta + 2\beta$ [deg] (!)	$32.7^{+7.4}_{-8.1}$		33^{+16}_{-29}	33^{+27}_{-45}
ϕ_d [deg]	$-20.9^{+3.8}_{-4.5}$		$-20.9^{+7.8}_{-7.9}$	-21^{+13}_{-11}
$\phi^\Delta - 2\beta_s$ [deg] (!)	$-16.6^{+3.7}_{-2.2}$		$-16.6^{+8.1}_{-4.3}$	$-16.6^{+13.9}_{-6.5}$
$\phi^\Delta - 2\beta_s$ [deg]	$-17.1^{+3.0}_{-2.1}$		$-17.1^{+6.8}_{-4.3}$	$-17.1^{+11.8}_{-6.4}$
ϕ_s [deg]	$-13.9^{+2.9}_{-2.1}$		$-13.9^{+6.6}_{-4.3}$	$-13.9^{+11.4}_{-6.4}$

TABLE XVIII. Fit results in the new physics scenario III. The notation (!) means that the fit output represents the indirect constraint, i.e. the corresponding direct input has been removed from the analysis.

Quantity	Central $\pm$C.L. $\equiv 1\sigma$	$\pm$C.L. $\equiv 2\sigma$	$\pm$C.L. $\equiv 3\sigma$
$\lvert V_{ud}\rvert$(!)	$0.97430^{+0.00030}_{-0.00030}$	$0.97430^{+0.00060}_{-0.00060}$	$0.97430^{+0.00089}_{-0.00090}$
$\lvert V_{us}\rvert$(!)	$0.22534^{+0.00095}_{-0.00095}$	$0.2253^{+0.0019}_{-0.0019}$	$0.2253^{+0.0028}_{-0.0029}$
$\lvert V_{ub}\rvert$(!)	$0.00577^{+0.00045}_{-0.00068}$	$0.00577^{+0.00086}_{-0.00124}$	$0.0058^{+0.0012}_{-0.0017}$
$\lvert V_{cd}\rvert$	$0.22524^{+0.00077}_{-0.00077}$	$0.2252^{+0.0015}_{-0.0015}$	$0.2252^{+0.0023}_{-0.0023}$
$\lvert V_{cs}\rvert$	$0.97347^{+0.00018}_{-0.00018}$	$0.97347^{+0.00036}_{-0.00037}$	$0.97347^{+0.00053}_{-0.00056}$
$\lvert V_{cb}\rvert$(!)	$0.0323^{+0.0036}_{-0.0035}$	$0.0323^{+0.0096}_{-0.0076}$	$0.032^{+0.017}_{-0.011}$
$\lvert V_{td}\rvert$	$0.00847^{+0.00032}_{-0.00032}$	$0.00847^{+0.00046}_{-0.00061}$	$0.00847^{+0.00058}_{-0.00076}$
$\lvert V_{ts}\rvert$	$0.03961^{+0.00137}_{-0.00037}$	$0.03961^{+0.00184}_{-0.00074}$	$0.0396^{+0.0022}_{-0.0011}$
$\lvert V_{tb}\rvert$	$0.999179^{+0.000016}_{-0.000057}$	$0.999179^{+0.000031}_{-0.000077}$	$0.999179^{+0.000046}_{-0.000094}$
Δm_d [ps^{-1}] (!)	$0.562^{+0.081}_{-0.068}$	$0.56^{+0.13}_{-0.12}$	$0.56^{+0.18}_{-0.20}$
Δm_s [ps^{-1}] (!)	$14.9^{+2.3}_{-1.1}$	$14.9^{+4.8}_{-2.0}$	$14.9^{+7.9}_{-2.9}$
$A_{\rm SL}$ [10^{-4}] (!)	$-22.6^{+7.9}_{-3.4}$	$-22.6^{+12.9}_{-7.9}$	-23^{+19}_{-14}
$A_{\rm SL}$ [10^{-4}]	$-23.4^{+5.5}_{-3.6}$	$-23.4^{+11.0}_{-9.0}$	-23^{+17}_{-14}
$a^s_{\rm SL} - a^d_{\rm SL}$ [10^{-4}]	$18.6^{+2.0}_{-10.2}$	$18.6^{+4.1}_{-17.2}$	$18.6^{+6.3}_{-19.4}$
$a^d_{\rm SL}$ [10^{-4}] (!)	$-32.4^{+11.2}_{-3.8}$	$-32.4^{+15.9}_{-7.7}$	-32^{+22}_{-12}
$a^d_{\rm SL}$ [10^{-4}]	$-32.5^{+10.2}_{-3.8}$	$-32.5^{+15.5}_{-7.7}$	-33^{+22}_{-12}
$a^s_{\rm SL}$ [10^{-4}](!)	$-13.9^{+3.4}_{-4.2}$	$-13.9^{+7.5}_{-13.2}$	-14^{+12}_{-19}
$a^s_{\rm SL}$ [10^{-4}]	$-13.9^{+3.4}_{-4.2}$	$-13.9^{+7.5}_{-13.2}$	-14^{+12}_{-19}
$\Delta\Gamma_d$ [ps^{-1}] (!)	$0.00432^{+0.00053}_{-0.00180}$	$0.0043^{+0.0012}_{-0.0023}$	$0.0043^{+0.0015}_{-0.0027}$
$\Delta\Gamma_s$ [ps^{-1}] (!)	$0.164^{+0.021}_{-0.074}$	$0.164^{+0.031}_{-0.097}$	$0.164^{+0.040}_{-0.109}$
$\Delta\Gamma_s$ [ps^{-1}]	$0.100^{+0.023}_{-0.019}$	$0.100^{+0.072}_{-0.034}$	$0.100^{+0.090}_{-0.046}$
$\mathcal{B}(B\to\tau\nu)$ [10^{-4}] (!)	$1.36^{+0.10}_{-0.35}$	$1.36^{+0.23}_{-0.59}$	$1.36^{+0.31}_{-0.77}$
$\mathcal{B}(B\to\tau\nu)$ [10^{-4}]	$1.38^{+0.13}_{-0.12}$	$1.38^{+0.23}_{-0.34}$	$1.38^{+0.31}_{-0.52}$

prediction (2.9σ when the average with the CDF measurement of the same quantity is made). Furthermore, the correction factor κ_ϵ [9] in the theoretical prediction of ϵ_K decreases the quality of the standard model fit. However, with our inputs (especially the range for $\hat{\mathcal{B}}_K$ in Table VII) and with the conservative Rfit error treatment of theoretical uncertainties used in our fit we do not observe a significant deviation between the measured ϵ_K value and its prediction from a standard model fit excluding the ϵ_K measurement.

In our new physics scenario I, we have considered uncorrelated new physics contributions to B_d, B_s and K mixing. That is, the complex parameters Δ_d and Δ_s are allowed to vary independently and the kaon sector is omitted, since the new physics parameters Δ^{tt}_K, Δ^{ct}_K, and Δ^{cc}_K are unrelated to all other observables entering the fit. The experimental data are well described in this scenario which can accommodate negative new physics phases preferred by (a) the discrepancy between $\mathcal{B}(B\to\tau\nu)$ and $\sin 2\beta$ both measured at the B-factories *BABAR* and Belle, (b) the $2\beta_s$ measurements in $B_s\to J/\psi\phi$ at the Tevatron, and (c) the dimuon asymmetry $a_{\rm fs}$ measured by D0. The size of the new physics contribution both in B_s-mixing and B_d-mixing can be as large as 40% and the hypothesis of zero new CP phases, $\phi_d = \phi_s = 0$, is disfavored by as much as 3.8 standard deviations in this scenario (see Table XIII). The large parameter region emphasizes that, despite of the success of the B-factories and the Tevatron, there is still considerable room for new physics in B_d as well as in B_s mixing.

In addition, we have considered two minimal flavor violation scenarios. The first MFV scenario, scenario II, corresponds to small bottom Yukawa couplings, leading to $\Delta_d = \Delta_s = \Delta^{tt}_K = \Delta$ with all new physics phases identical to zero, $\phi^\Delta_s = \phi^\Delta_d = \phi^{ij\Delta}_K = 0$. This scenario $\Delta_d = \Delta_s = \Delta^{tt}_K = \Delta$ with vanishing new physics phases has been widely studied in the literature. In this scenario, the new physics parameter Δ^{cc}_K is equal to 1 to a very good approximation and Δ^{ct}_K only deviates by a few percent from 1 where the deviation can be estimated in terms of Δ^{tt}_K. Since in this scenario no new physics phases are allowed, the deviations seen in the standard model fit are still present. As a consequence, this MFV scenario is currently disfavored by 3.7 standard deviations, but not totally excluded yet. The new physics parameter Δ can deviate from 1 by about $+40\%$ at 95% C.L. The constraint gets only slightly relaxed when removing either $\mathcal{B}(B\to\tau\nu)$ or ϵ_K from the inputs to the fit.

Our scenario III is a generic MFV scenario with large bottom Yukawa coupling and arbitrary new flavor-blind CP phases. In this scenario, the kaon sector is unrelated to the B-sector. As in scenario II, one has $\Delta_d = \Delta_s = \Delta$,

however, this time with a complex parameter Δ. The new physics parameters in ϵ_K are unrelated to Δ and ϵ_K can be removed from the input list. However, when including ϵ_K one is able to constrain the new physics parameter Δ_K^{tt} which is found to be consistent with the standard model value of 1, but can deviate from unity by about $\pm 40\%$. The fit describes the data significantly better than the standard model fit and better than the fit in scenario II because the data prefer a negative new physics phase in B_d and in B_s mixings. The hypothesis of a zero new CP phase, $\mathrm{Im}\Delta = 0$, is disfavored by 3.5 standard deviations (see Table XVI). As in the other new physics scenarios, the allowed size of the new physics contribution in B_d and in B_s mixing can be as large as $+40\%$.

The several scenarios discussed here show that we have indeed sensitivity to new physics in the $|\Delta F| = 2$ sector. While the overall picture of current data reveals strong hints for new physics, the current experimental uncertainties prevent us from excluding the standard model, as highlighted by the p-values of each hypothesis. It has to be seen how this picture evolves with the improvement of both experimental and theoretical results. When we completed this study, new results from the Tevatron experiments were given for the measurement of $\phi_s^{\psi\phi}$, in better agreement with the standard model, which will be included in our analysis once the CDF and D0 Collaborations have agreed on a combination of their results. Importantly, more precise measurement of the CP asymmetries in flavor-specific decays, a_{SL}^q, from either the Tevatron or the LHC experiments, may become crucial in the future. For the time being the theory-and-data driven fit predictions for a_{SL}^q are more precise than the direct measurements, as can be verified by comparing e.g. Tables VI and XII. Hence more precise future data on a_{SL}^q could help to discriminate between the standard model and different scenarios of new physics. Meanwhile, our predictions of a_{SL}^d in Tables XII, XIV, and XVII are an important side result of our analyses: They permit a fast extraction of a_{SL}^s from future measurements of a_{fs} (or $a_{\mathrm{SL}}^s - a_{\mathrm{SL}}^d$ considered by LHCb), which is more accurate than what is obtained using the experimental value of a_{fs}^d listed in Table VI.

As an illustration of this statement, we show the indirect fit prediction for the difference $a_{\mathrm{SL}}^s - a_{\mathrm{SL}}^d$ as a function of $\phi_s^\Delta - 2\beta_s$, in the standard model and the new physics scenarios I and III in Fig. 15. The prediction in scenario and III differs by about 2 standard deviations, hence a precise direct measurement of either observable could not only exclude the standard model, but also could select one of the new physics scenarios. Thanks to the specific two-dimensional correlation it could also invalidate all scenarios, which would then imply that there are other sources of new physics than just contributions to the mixing amplitudes. The LHCb experiment is expected to measure both CP asymmetries, with an accuracy of about

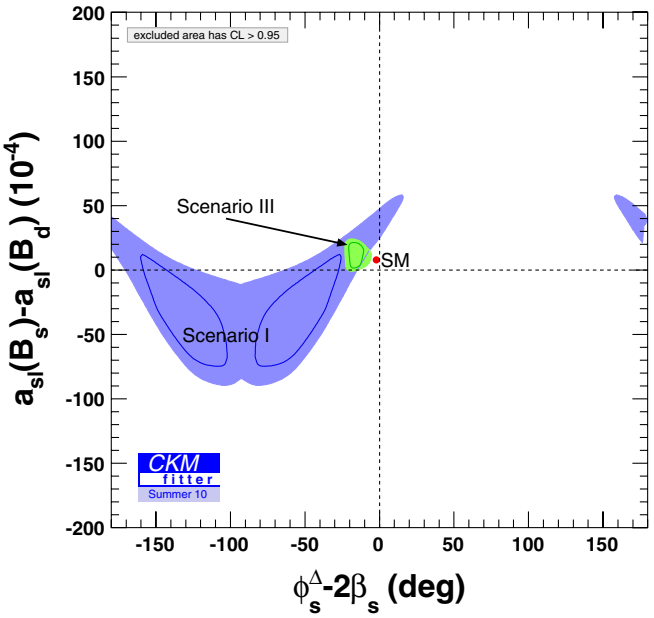

FIG. 15 (color online). Indirect fit prediction for the difference $a_{sl}^s - a_{sl}^d$ as a function of $\phi_s^\Delta - 2\beta_s$, in the standard model and the new physics scenarios I and III. The allowed regions correspond to C.L. $< 95.45\%$. The prediction from scenario II is not shown since it is very close to the SM. Note that for this plot, the direct measurement of $\phi_s^\Delta - 2\beta_s$ in $B_s \to J/\psi\phi$ is removed from the inputs.

$\sigma(\phi_s^\Delta - 2\beta_s) = 4^\circ$ and $\sigma(a_{\mathrm{SL}}^s - a_{\mathrm{SL}}^d) = 20 \times 10^{-4}$ for 1 fb^{-1} of integrated luminosity [150].

On the other hand, significant improvements on the measurement of $\mathcal{B}(B \to \tau\nu)$ can only be expected from a Super-B-like electron-positron machine since the *BABAR* and Belle results do already rely on most of the available statistics collected at the B-factories PEP-II and KEKb. Since the theoretical translation of the ratio $\mathcal{B}(B \to \tau\nu)/\Delta M_d$ into a constraint on CKM and new physics parameters relies on the calculation of the decay constant f_{B_d} and the bag parameter $\mathcal{B}_{B_d}$, future progress in lattice QCD calculations is also very important. The same remark applies to the hadronic matrix elements entering M_{12}^s and Γ_{12}^s. We hope that the current exciting experimental situation will stimulate novel activities in lattice gauge theory in this direction.

APPENDIX A: RELATIONSHIP BETWEEN ϵ_K AND K-$\bar{K}$ MIXING

1. Corrections to the usual ϵ_K formula

In Sec. II B, we have discussed the connection between ϵ_K and K-$\bar{K}$ mixing. The resulting equation, Eq. (26), has been obtained thanks to several approximations (concerning the phase ϕ_ϵ, neglect of ξ, computation of M_{12} from lowest-dimension operators of the effective Hamiltonian). The corrections to these approximations are encoded in the deviation of the factor κ_ϵ from 1. A series of papers

[9,37,69,70] has assessed more precisely the value of this factor in order to account for the terms neglected by the previous approximations.

$\xi \neq 0$ and $\phi_\epsilon \neq 45°$ imply $\kappa_\epsilon \neq 1$ and Ref. [9] finds $\kappa_\epsilon = 0.92 \pm 0.02$. In Ref. [86] a lattice QCD calculation of $\mathrm{Im}A_2$ is combined with the experimental value of ϵ'_K/ϵ_K to compute ξ and finds agreement with Ref. [9] while quoting an even smaller uncertainty: $\kappa_\epsilon = 0.92 \pm 0.01$. Finally, correcting for $\mathrm{Im}M_{12}^K \neq \mathrm{Im}M_{12}^{(6)}$ by including higher-order terms of the operator product expansion leads to $\kappa_\epsilon = 0.94 \pm 0.02$. Actually, in the correction factor κ_ϵ, the three approximations have to be treated in different ways, since they mix uncertainties from experimental and theoretical origins. The correction from ϕ_ϵ is of experimental nature and can be treated easily.

The correction involving ξ could be computed by combining the experimental value of $\mathrm{Re}A_0$ and the theoretical computation of $\mathrm{Im}A_0$ using the effective Hamiltonian $H^{|\Delta S|=1}$. However, the latter is dominated by the matrix element of the QCD penguin in the $I = 0$ channel $\langle(\pi\pi)_0|Q_6|K\rangle$, which is poorly known. Here we follow the method of Refs. [9,70,86] which uses ϵ'_K to correlate $\langle(\pi\pi)_0|Q_6|K\rangle$ with A_2. The latter amplitude involves the matrix element of the electroweak penguin Q_8 in the $I = 2$ channel, $\langle(\pi\pi)_2|Q_8|K\rangle$, which has been computed using lattice simulations and sum rules. Indeed, one finds [9]

$$\frac{\epsilon'_K}{\epsilon_K} = -\omega\frac{\xi}{\sqrt{2}|\epsilon_K|}(1-\Omega), \quad \text{with} \quad \omega = \frac{\mathrm{Re}A_2}{\mathrm{Re}A_0}, \qquad \Omega = \frac{1}{\omega}\frac{\mathrm{Im}A_2}{\mathrm{Im}A_0}. \tag{A1}$$

$\omega = 0.0450$ is obtained from experiment, whereas Ω describes the weight of the (imaginary part of the) $I = 2$ contribution with respect to the $I = 0$ one.

In practice, a numerical estimate of the contributions from other (subleading) operators than Q_6 and Q_8 in $H^{|\Delta S|=1}$ has been obtained [68,152,153] under the assumptions that $\mathrm{Im}A_0$ and $\mathrm{Im}A_2$ can be computed accurately combining the effective Hamiltonian approach and experimental values for $\mathrm{Re}A_0$ and $\mathrm{Re}A_2$:

$$\frac{\epsilon'_K}{\epsilon_K} = N_0 + N_1 \cdot R_6 + N_2 \cdot R_8, \qquad R_6 = R_6[(\epsilon'/\epsilon)_{\mathrm{exp}}, R_8], \tag{A2}$$

where N_0, N_1, N_2 are numbers, coming mainly from λ_t, the experimental values for the real parts of A_0 and A_2, and R_6 and R_8 are rescaled bag parameters. Following the review of Ref. [154], the authors of Ref. [152] proposed the following conservative range $R_8 = 1.0 \pm 0.2$ which we will follow. Using $\epsilon'_K/\epsilon_K = (1.65 \pm 0.26) \times 10^{-3}$, one can use Eq. (A2) to determine Ω, which corresponds to the ratio between the $I = 2$ and $I = 0$ contributions to ϵ'_K/ϵ_K. In principle, this would require to split N_0 into two pieces coming, respectively, from $I = 0$ and $I = 2$, and to assess the size of these contributions following Ref. [68]. A quicker way to obtain a similar estimate consists in computing [153]:

$$\Omega_1 = \frac{N_2 \cdot R_8}{N_0 + N_1 \cdot R_6} \qquad \Omega_2 = \frac{N_0 + N_2 \cdot R_8}{N_1 \cdot R_6} \tag{A3}$$

where Ω_1 and Ω_2 correspond to the (extreme) hypothesis that N_0 is saturated either by $I = 0$ or $I = 2$ contributions. Equation (A1) can be then used to compute ξ in either hypotheses, and we will take the spread of the obtained values as a (conservative) systematic uncertainty in the determination of ξ. A more detailed analysis of the contributions to N_0 would allow us to decrease this systematic uncertainty.

The last correction comes from higher-dimension contributions to $\mathrm{Im}M_{12}$. As shown in Ref. [69], there are two different corrections at $d = 8$, corresponding to the $\Delta S = 2$ $d = 8$ operators and the double insertion of $\Delta S = 1$ operators connected by a u, c loop. The first is expected to be very suppressed compared to the $d = 6$ contributions, whereas the second one is essentially dominated by long-distance pion exchanges estimated in chiral perturbation theory for weak processes, leading to

$$\epsilon_K = \sin\phi_\epsilon e^{i\phi_\epsilon}\left[\frac{\mathrm{Im}M_{12}^{(6)}}{\Delta M} + \rho\xi\right], \qquad \rho = 0.6 \pm 0.3. \tag{A4}$$

For our purposes, it will be simpler to combine these corrections with the experimental input for ϵ_K:

$$\epsilon_K^{(0)} = \epsilon_K\left(\frac{1}{\sqrt{2}\sin\phi_\epsilon} + \rho\frac{\epsilon'_K}{\epsilon_K}\frac{1}{\omega(1-\Omega)}\right) \equiv \frac{\epsilon_{K,\mathrm{exp}}}{\kappa_\epsilon}, \tag{A5}$$

where $\epsilon_K^{(0)}$ denote the approximate value of ϵ_K in Eq. (26) with $\kappa_\epsilon = 1$. Depending on the choice of Ω (i.e. the respective part of $I = 0$ and $I = 2$ contributions in the formula for ϵ'/ϵ), we get

$$\kappa_\epsilon^{(1)} = 0.943 \pm 0.003(\epsilon'/\epsilon) \pm 0.012(\phi_\epsilon) \pm 0.004(R_8) \pm 0.015(\rho), \tag{A6}$$

$$\kappa_\epsilon^{(2)} = 0.940 \pm 0.003(\epsilon'/\epsilon) \pm 0.012(\phi_\epsilon) \pm 0.004(R_8) \pm 0.018(\rho). \tag{A7}$$

Combining the first two errors in quadrature for the Gaussian part and the last two errors linearly and taking the spread of the values into the Rfit part, we obtain the estimate

$$\kappa_\epsilon = 0.940 \pm 0.013 \pm 0.023, \tag{A8}$$

in good agreement with $\kappa_\epsilon = 0.94 \pm 0.02$ in Ref. [69]. This determination relies on the assumption that ϵ'_K is not affected by new physics.

2. Error budget for ϵ_K

Recently, it has been claimed that there is a discrepancy between the ϵ_K constraint and its prediction [8,9]. With the

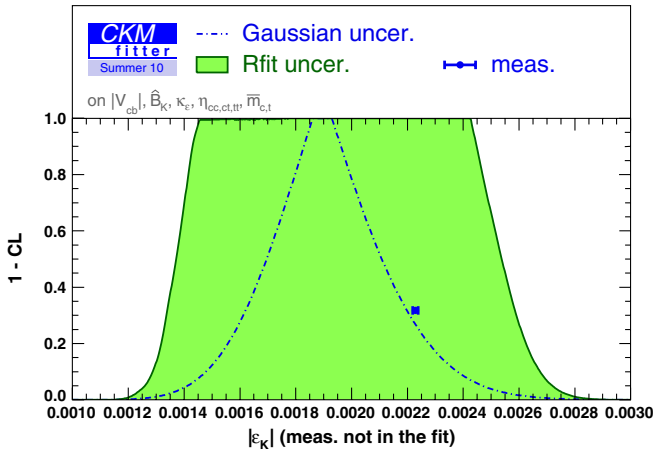

FIG. 16 (color online). Constraint on $|\epsilon_K|$ predicted from the global fit, compared to the experimental value. The green (shaded) curve is obtained with our Rfit treatment of the uncertainties for the parameters entering Eq. (26). The dashed curve is obtained by treating all the errors as Gaussian.

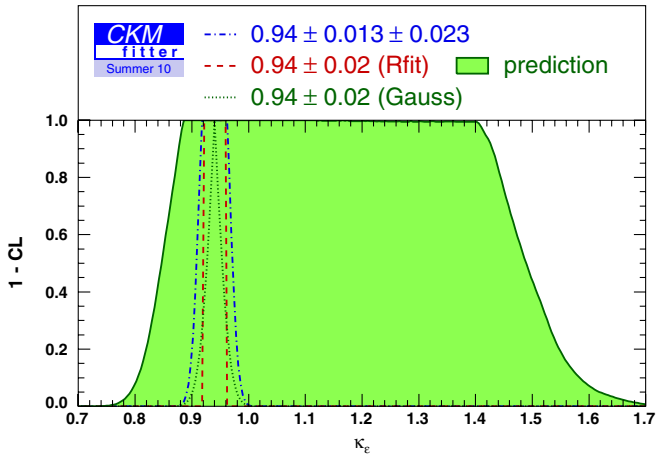

FIG. 17 (color online). Constraint on κ_ϵ predicted from the global fit using Eq. (26), compared to three different theoretical inputs $\kappa_\epsilon = 0.94 \pm 0.02$ with either a Rfit or a Gaussian treatment of the error, or $\kappa_\epsilon = 0.94 \pm 0.013 \pm 0.023$ corresponding to our own treatment of the uncertainties involved in its evaluation.

input values used in our fit and with the Rfit treatment of theoretical uncertainties we do not observe any sizeable discrepancy when comparing the prediction for ϵ_K (Table VIII) with its measured value (Table VI). This can also be seen in Fig. 3 where the combined fit prefers a region in $\bar{\rho}$ and $\bar{\eta}$ that is close to the edge of, though still inside, the 95% C.L. region of the ϵ_K constraint.

As illustrated in Fig. 16 one can obtain a minor discrepancy at 1.2σ if one treats as Gaussian all the parameters involved in Eq. (26) (i.e., $|V_{cb}|$, $\mathcal{B}_K$, κ_ϵ, the QCD correction terms $\eta_{cc,ct,tt}$, and the masses $\bar{m}_{c,t}$), but such a treatment of the systematics remains questionable. Another way of seeing the absence of discrepancy is to compare the prediction for κ_ϵ and estimates of these quantity. One can see clearly from Fig. 17 that the global fit can cope easily with a value of κ_ϵ down to 0.9, and that the prediction from the global fit agrees well with the recent estimates of this quantity.

In order to make the comparison of our $|\epsilon_K|$ analysis with the one of Ref. [86] easier we treat all the errors as Gaussian and calculate the error budget for the fit prediction of $|\epsilon_K|$. With our inputs we find

$$\begin{aligned} 10^3|\epsilon_K| &= 1.893 \pm 0.020|_A \pm 0.020|_\lambda \pm 0.063|_{(\bar{\rho},\bar{\eta})} \\ &\quad \pm 0.180|_{\mathcal{B}_K} \pm 0.019|_{\text{top}} \pm 0.084|_{\text{charm}} \pm 0.054|_{\kappa_\epsilon} \\ &= 1.89^{+0.26}_{-0.23}, \end{aligned} \tag{A9}$$

which is 1.2σ away from the experimental measurement, while with the inputs of the last reference in [86] we find

$$\begin{aligned} 10^3|\epsilon_K| &= 1.769 \pm 0.019|_A \pm 0.019|_\lambda \pm 0.061|_{(\bar{\rho},\bar{\eta})} \\ &\quad \pm 0.062|_{\mathcal{B}_K} \pm 0.018|_{\text{top}} \pm 0.067|_{\text{charm}} \pm 0.033|_{\kappa_\epsilon} \\ &= 1.77^{+0.18}_{-0.16}, \end{aligned} \tag{A10}$$

which is 2.4σ away from the experimental measurement, in agreement with [86]. Hence we see that the difference between our analysis and Ref. [86] mainly comes from our input for $\mathcal{B}_K$ that has a larger theoretical error, and from our central value for $|\epsilon_K|$ that is larger because of the different analysis of the CKM parameters. We thus conclude that the potential anomaly in $|\epsilon_K|$ cannot yet be precisely quantified independently of the theoretical inputs and therefore deserves further investigations.

[1] N. Cabibbo, Phys. Rev. Lett. **10**, 531 (1963); M. Kobayashi and T. Maskawa, Prog. Theor. Phys. **49**, 652 (1973).
[2] L. Wolfenstein, Phys. Rev. Lett. **51**, 1945 (1983).
[3] A. J. Buras, M. E. Lautenbacher, and G. Ostermaier, Phys. Rev. D **50**, 3433 (1994).
[4] R. S. Chivukula and H. Georgi, Phys. Lett. B **188**, 99 (1987); L. J. Hall and L. Randall, Phys. Rev. Lett. **65**, 2939 (1990); E. Gabrielli and G. F. Giudice, Nucl. Phys. **B433**, 3 (1995); **B507**, 549(E) (1997); A. Ali and D. London, Eur. Phys. J. C **9**, 687 (1999); A. J. Buras, P. Gambino, M. Gorbahn, S. Jager, and L. Silvestrini, Phys. Lett. B **500**, 161 (2001); G. D'Ambrosio, G. F. Giudice, G. Isidori, and A. Strumia, Nucl. Phys. **B645**, 155 (2002).
[5] A. L. Kagan, G. Perez, T. Volansky, and J. Zupan, Phys. Rev. D **80**, 076002 (2009).

[6] S. Bertolini, F. Borzumati, A. Masiero, and G. Ridolfi, Nucl. Phys. **B353**, 591 (1991).

[7] M. Dine and A. E. Nelson, Phys. Rev. D **48**, 1277 (1993); M. Dine, A. E. Nelson, and Y. Shirman, Phys. Rev. D **51**, 1362 (1995); M. Dine, A. E. Nelson, Y. Nir, and Y. Shirman, Phys. Rev. D **53**, 2658 (1996).

[8] E. Lunghi and A. Soni, Phys. Lett. B **666**, 162 (2008).

[9] A. J. Buras and D. Guadagnoli, Phys. Rev. D **78**, 033005 (2008); **79**, 053010 (2009).

[10] O. Deschamps (CKMfitter Group), in *Proceedings of the International Conference for High Energy Physics, Philadelphia, 2008*, eConf C080730 (2008).

[11] M. Beneke, Phys. Lett. B **620**, 143 (2005); H. n. Li and S. Mishima, J. High Energy Phys. 03 (2007) 009; arXiv:hep-ph/0610120; H. n. Li, S. Mishima, and A. I. Sanda, Phys. Rev. D **72**, 114005 (2005); A. R. Williamson and J. Zupan, Phys. Rev. D **74**, 014003 (2006); **74**, 039901(E) (2006); J. Zupan, in *Proceedings of 5th International Conference on Flavor Physics and CP Violation (FPCP 2007), Bled, Slovenia, 2007*, eConf C070512 (2007); T. Hurth, in *Proceedings of the 34th International Conference in High Energy Physics (ICHEP08), Philadelphia, 2008*, eConf C080730 (2008).

[12] A. Lenz and U. Nierste, J. High Energy Phys. 06 (2007) 072.

[13] T. Moroi, Phys. Lett. B **493**, 366 (2000); D. Chang, A. Masiero, and H. Murayama, Phys. Rev. D **67**, 075013 (2003); R. Harnik, D. T. Larson, H. Murayama, and A. Pierce, Phys. Rev. D **69**, 094024 (2004); S. Jäger and U. Nierste, Eur. Phys. J. C **33**, s256 (2004); in *Proceedings of the 12th International Conference on Supersymmetry and Unification Of Fundamental Interactions (SUSY 04), Tsukuba, Japan, 2004*, edited by K. Hagiwara, J. Kanzaki, and N. Okada (KEK, Tsukuba, 2004), p. 67.

[14] M. Albrecht, W. Altmannshofer, A. J. Buras, D. Guadagnoli, and D. M. Straub, J. High Energy Phys. 10 (2007) 055; J. K. Parry and H. h. Zhang, Nucl. Phys. **B802**, 63 (2008); J. h. Park and M. Yamaguchi, Phys. Lett. B **670**, 356 (2009); P. Ko, J. h. Park, and M. Yamaguchi, J. High Energy Phys. 11 (2008) 051; S. Trine, S. Westhoff, and S. Wiesenfeldt, J. High Energy Phys. 08 (2009) 002; F. Borzumati and T. Yamashita, Prog. Theor. Phys. **124**, 761 (2010); B. Dutta, Y. Mimura, and Y. Santoso, Phys. Rev. D **82**, 055017 (2010); C. Biggio and L. Calibbi, J. High Energy Phys. 10 (2010) 037.

[15] L. Randall and S. f. Su, Nucl. Phys. **B540**, 37 (1999); P. Ball, S. Khalil, and E. Kou, Phys. Rev. D **69**, 115011 (2004); M. Ciuchini and L. Silvestrini, Phys. Rev. Lett. **97**, 021803 (2006); M. Endo and S. Mishima, Phys. Lett. B **640**, 205 (2006); J. Foster, K.-i. Okumura, and L. Roszkowski, Phys. Lett. B **641**, 452 (2006); S. Khalil, Phys. Rev. D **74**, 035005 (2006); S. Baek, J. High Energy Phys. 09 (2006) 077; R. Arnowitt, B. Dutta, B. Hu, and S. Oh, Phys. Lett. B **641**, 305 (2006); R.-M. Wang *et al.*, High Energy Phys. Nucl. Phys. **31**, 332 (2007); W. Altmannshofer, A. J. Buras, and D. Guadagnoli, J. High Energy Phys. 11 (2007) 065; S.-L. Chen *et al.*, J. High Energy Phys. 09 (2007) 044; T. Goto, Y. Okada, T. Shindou, and M. Tanaka, Phys. Rev. D **77**, 095010 (2008); N. Kifune, J. Kubo, and A. Lenz, Phys. Rev. D **77**, 076010 (2008); P. Ko and J.-h. Park, and M. Yamaguchi, Phys. Rev. D **80**, 035019 (2009); K. Kawashima, J. Kubo, and A. Lenz, Phys. Lett. B **681**, 60 (2009); L. L. Everett, J. Jiang, P. G. Langacker, and T. Liu, Phys. Rev. D **82**, 094024 (2010); J. K. Parry, Phys. Lett. B **694**, 363 (2011); P. Ko and J. h. Park, Phys. Rev. D **82**, 117701 (2010); S. F. King, J. High Energy Phys. 09 (2010) 114; J. Kubo and A. Lenz, Phys. Rev. D **82**, 075001 (2010); R. M. Wang, Y. G. Xu, M. L. Liu, and B. Z. Li, J. High Energy Phys. 12 (2010) 034.

[16] A. J. Buras, P. H. Chankowski, J. Rosiek, and L. Slawianowska, Phys. Lett. B **546**, 96 (2002); Nucl. Phys. **B659**, 3 (2003); M. S. Carena, A. Menon, R. Noriega-Papaqui, A. Szynkman, and C. E. M. Wagner, Phys. Rev. D **74**, 015009 (2006); S. Trine, arXiv:0710.4955; M. Gorbahn, S. Jager, U. Nierste, and S. Trine, arXiv:0901.2065; A. Crivellin and U. Nierste, Phys. Rev. D **81**, 095007 (2010); W. Altmannshofer, A. J. Buras, S. Gori, P. Paradisi, and D. M. Straub, Nucl. Phys. **B830**, 17 (2010).

[17] R. Mohanta and A. K. Giri, Phys. Rev. D **76**, 075015 (2007); A. Lenz, Phys. Rev. D **76**, 065006 (2007); S.-L. Chen *et al.*, Eur. Phys. J. C **59**, 899 (2009); C.-H. Chen, C. S. Kim, and Y. W. Yoon, Phys. Lett. B **671**, 250 (2009); J. K. Parry, Phys. Rev. D **78**, 114023 (2008); Mod. Phys. Lett. A **24**, 1835 (2009).

[18] L. x. Lu and Z. j. Xiao, Commun. Theor. Phys. **47**, 1099 (2007); S. L. Chen, N. G. Deshpande, X. G. He, J. Jiang, and L. H. Tsai, Eur. Phys. J. C **53**, 607 (2008); A. S. Joshipura and B. P. Kodrani, Phys. Lett. B **670**, 369 (2009); E. Lunghi and A. Soni, J. High Energy Phys. 09 (2007) 053; A. S. Joshipura and B. P. Kodrani, Phys. Rev. D **77**, 96003 (2008); **81**, 035013 (2010); B. A. Dobrescu, P. J. Fox, and A. Martin, Phys. Rev. Lett. **105**, 041801 (2010); M. Jung, A. Pich, and P. Tuzon, J. High Energy Phys. 11 (2010) 003; A. J. Buras, M. V. Carlucci, S. Gori, and G. Isidori, J. High Energy Phys. 10 (2010) 009.

[19] V. Barger, C. W. Chiang, J. Jiang, and P. Langacker, Phys. Lett. B **596**, 229 (2004); X. G. He and G. Valencia, Phys. Rev. D **74**, 013011 (2006); S. Baek, J. H. Jeon, and C. S. Kim, Phys. Lett. B **641**, 183 (2006); J. M. Cabarcas, D. Gomez Dumm, and R. Martinez, Phys. Rev. D **77**, 036002 (2008); S. Baek, J. H. Jeon, and C. S. Kim, Phys. Lett. B **664**, 84 (2008); C. H. Chen, C. Q. Geng, and L. Li, Phys. Lett. B **670**, 374 (2009); V. Barger, L. L. Everett, J. Jiang, P. Langacker, T. Liu, and C. E. M. Wagner, J. High Energy Phys. 12 (2009) 048; Q. Chang, X. Q. Li, and Y. D. Yang, J. High Energy Phys. 02 (2010) 082; C. H. Chen, Phys. Lett. B **683**, 160 (2010).

[20] S. Chang, C. S. Kim, and J. Song, J. High Energy Phys. 02 (2007) 087; M. Blanke, A. J. Buras, B. Duling, S. Gori, and A. Weiler, J. High Energy Phys. 03 (2009) 001; M. Bauer, S. Casagrande, U. Haisch, and M. Neubert, J. High Energy Phys. 09 (2010) 017; C. Delaunay, O. Gedalia, S. J. Lee, and G. Perez, arXiv:1007.0243.

[21] A. J. Buras, K. Gemmler, and G. Isidori, Nucl. Phys. **B843**, 107 (2011).

[22] J. P. Lee and K. Y. Lee, arXiv:0809.0751.

[23] A. Arhrib and W. S. Hou, Eur. Phys. J. C **27**, 555 (2003); W. S. Hou, M. Nagashima, and A. Soddu, Phys. Rev. D **76**, 016004 (2007); A. Soni, A. K. Alok, A. Giri, R. Mohanta, and S. Nandi, Phys. Lett. B **683**, 302 (2010); M. Bobrowski, A. Lenz, J. Riedl, and J. Rohrwild, Phys.

Rev. D **79**, 113006 (2009); A. Soni, A. K. Alok, A. Giri, R. Mohanta, and S. Nandi, Phys. Rev. D **82**, 033009 (2010); A. J. Buras, B. Duling, T. Feldmann, T. Heidsieck, C. Promberger, and S. Recksiegel, J. High Energy Phys. 09 (2010) 106; W. S. Hou and C. Y. Ma, Phys. Rev. D **82**, 036002 (2010); O. Eberhardt, A. Lenz, and J. Rohrwild, Phys. Rev. D **82**, 095006 (2010); D. Choudhury and D. K. Ghosh, arXiv:1006.2171.

[24] J. A. Aguilar-Saavedra, Phys. Rev. D **67**, 035003 (2003); **69**, 099901(E) (2004); J. A. Aguilar-Saavedra, F. J. Botella, G. C. Branco, and M. Nebot, Nucl. Phys. **B706**, 204 (2005); F. J. Botella, G. C. Branco, and M. Nebot, Phys. Rev. D **79**, 096009 (2009); R. Mohanta and A. K. Giri, Phys. Rev. D **78**, 116002 (2008).

[25] M. Blanke, A. J. Buras, D. Guadagnoli, and C. Tarantino, J. High Energy Phys. 10 (2006) 003; M. Blanke, A. J. Buras, A. Poschenrieder, C. Tarantino, S. Uhlig, and A. Weiler, J. High Energy Phys. 12 (2006) 003; M. Blanke *et al.*, arXiv:0805.4393; M. Blanke, A. J. Buras, B. Duling, S. Recksiegel, and C. Tarantino, Acta Phys. Pol. B **41**, 657 (2010).

[26] V. M. Abazov *et al.* (D0 Collaboration), Phys. Rev. Lett. **97**, 021802 (2006); A. Abulencia *et al.* (CDF Collaboration), Phys. Rev. Lett. **97**, 062003 (2006); V. M. Abazov *et al.* (D0 Collaboration), D0 Note 5618, http://www-d0.fnal.gov/Run2Physics/WWW/results/prelim/B/B54/B54.pdf.

[27] A. Abulencia *et al.* (CDF Collaboration), Phys. Rev. Lett. **97**, 242003 (2006).

[28] T. Aaltonen *et al.* (CDF Collaboration), Phys. Rev. Lett. **100**, 161802 (2008).

[29] V. M. Abazov *et al.* (D0 Collaboration), Phys. Rev. Lett. **101**, 241801 (2008).

[30] T. Aaltonen *et al.* (CDF Collaboration), CDF Report No. 9458.

[31] T. Aaltonen *et al.* (CDF Collaboration), CDF Report No. 10206.

[32] V. M. Abazov *et al.* (D0 Collaboration), D0 Conference Report No. 6098.

[33] V. M. Abazov *et al.* (D0 Collaboration), Phys. Rev. D **82**, 032001 (2010); Phys. Rev. Lett. **105**, 081801 (2010).

[34] A. Dighe, A. Kundu, and S. Nandi, Phys. Rev. D **82**, 031502 (2010); C. H. Chen and G. Faisel, arXiv:1005.4582; Z. Ligeti, M. Papucci, G. Perez, and J. Zupan, Phys. Rev. Lett. **105**, 131601 (2010); C. W. Bauer and N. D. Dunn, arXiv:1006.1629; N. G. Deshpande, X. G. He, and G. Valencia, Phys. Rev. D **82**, 056013 (2010); B. Batell and M. Pospelov, Phys. Rev. D **82**, 054033 (2010); C. H. Chen, C. Q. Geng, and W. Wang, J. High Energy Phys. 11 (2010) 089; Y. Bai and A. E. Nelson, Phys. Rev. D **82**, 114027 (2010); K. Blum, Y. Hochberg, and Y. Nir, J. High Energy Phys. 09 (2010) 035; A. J. Buras, G. Isidori, and P. Paradisi, arXiv:1007.5291.

[35] C. Tarantino, arXiv:hep-ph/0702235; A. J. Lenz, AIP Conf. Proc. **1026**, 36 (2008).

[36] A. Lenz, U. Nierste, and G. Ostermaier, Phys. Rev. D **56**, 7228 (1997); A. Lenz, arXiv:hep-ph/0011258.

[37] K. Anikeev *et al.*, Chaps. 1.3 and 8.3, arXiv:hep-ph/0201071.

[38] U. Nierste, in *Proceedings of the XXXIXth Rencontres de Moriond, Electroweak Interactions and Unified Theories, La Thuile, Aosta Valley, Italy, 2004*, edited by J. Tran Thanh Van, arXiv:hep-ph/0406300; R. N. Cahn and M. P. Worah, Phys. Rev. D **60**, 076006 (1999).

[39] J. S. Hagelin and M. B. Wise, Nucl. Phys. **B189**, 87 (1981); J. S. Hagelin, Nucl. Phys. **B193**, 123 (1981); A. J. Buras, W. Slominski, and H. Steger, Nucl. Phys. **B245**, 369 (1984); E. H. Thorndike, Annu. Rev. Nucl. Part. Sci. **35**, 195 (1985).

[40] T. Inami and C. S. Lim, Prog. Theor. Phys. **65**, 297 (1981); **65**, 1772(E) (1981).

[41] Tevatron Electroweak Working Group, 2008, http://tevewwg.fnal.gov.

[42] A. J. Buras, M. Jamin, and P. H. Weisz, Nucl. Phys. **B347**, 491 (1990).

[43] S. Herrlich and U. Nierste, Phys. Rev. D **52**, 6505 (1995); Nucl. Phys. **B476**, 27 (1996), numerical update in [155].

[44] S. Herrlich and U. Nierste, Nucl. Phys. **B419**, 292 (1994), numerical update in [155].

[45] D. Becirevic, V. Gimenez, G. Martinelli, M. Papinutto, and J. Reyes, J. High Energy Phys. 04 (2002) 025.

[46] C. Amsler *et al.* (Particle Data Group), Phys. Lett. B **667**, 1 (2008), and 2009 partial update for the 2010 edition. Cutoff date for this update was January 15, 2009.

[47] E. Barberio *et al.* (Heavy Flavour Averaging Group), arXiv:1010.1589.

[48] Reference [42], with a numerical update according to [12].

[49] G. Buchalla, A. J. Buras, and M. E. Lautenbacher, Rev. Mod. Phys. **68**, 1125 (1996).

[50] M. Beneke, G. Buchalla, and I. Dunietz, Phys. Rev. D **54**, 4419 (1996); M. Beneke, G. Buchalla, C. Greub, A. Lenz, and U. Nierste, Phys. Lett. B **459**, 631 (1999); M. Ciuchini, E. Franco, V. Lubicz, F. Mescia, and C. Tarantino, J. High Energy Phys. 08 (2003) 031.

[51] M. Beneke, G. Buchalla, A. Lenz, and U. Nierste, Phys. Lett. B **576**, 173 (2003).

[52] T. Goto, N. Kitazawa, Y. Okada, and M. Tanaka, Phys. Rev. D **53**, 6662 (1996); Y. Grossman, Y. Nir, and M. P. Worah, Phys. Lett. B **407**, 307 (1997); G. Barenboim, G. Eyal, and Y. Nir, Phys. Rev. Lett. **83**, 4486 (1999).

[53] J. Charles *et al.* (CKMfitter Group), Eur. Phys. J. C **41**, 1 (2005); updated at http://ckmfitter.in2p3.fr/.

[54] O. Deschamps, S. Descotes-Genon, S. Monteil, V. Niess, S. T'Jampens, and V. Tisserand, Phys. Rev. D **82**, 073012 (2010).

[55] M. Blanke, A. J. Buras, D. Guadagnoli, and C. Tarantino, J. High Energy Phys. 10 (2006) 003.

[56] A. J. Buras, P. Gambino, M. Gorbahn, S. Jäger, and L. Silvestrini, Phys. Lett. B **500**, 161 (2001).

[57] H. Lacker and A. Menzel, J. High Energy Phys. 07 (2010) 006.

[58] J. M. Soares and L. Wolfenstein, Phys. Rev. D **47**, 1021 (1993); N. G. Deshpande, B. Dutta, and S. Oh, Phys. Rev. Lett. **77**, 4499 (1996); J. P. Silva and L. Wolfenstein, Phys. Rev. D **55**, 5331 (1997); A. G. Cohen *et al.*, Phys. Rev. Lett. **78**, 2300 (1997); Y. Grossman, Y. Nir, and M. Worah, Phys. Lett. B **407**, 307 (1997).

[59] Y. Grossman, Y. Nir, and G. Raz, Phys. Rev. Lett. **97**, 151801 (2006).

[60] S. Laplace, Z. Ligeti, Y. Nir, and G. Perez, Phys. Rev. D **65**, 094040 (2002).

[61] K. Agashe *et al.*, arXiv:hep-ph/0509117.

[62] Z. Ligeti, M. Papucci, and G. Perez, Phys. Rev. Lett. **97**, 101801 (2006).
[63] P. Ball and R. Fleischer, Eur. Phys. J. C **48**, 413 (2006).
[64] M. Bobrowski, A. Lenz, J. Riedl, and J. Rohrwild, arXiv:0904.3971; J. High Energy Phys. 03 (2010) 009.
[65] U. Nierste, arXiv:0904.1869.
[66] J. Brod and M. Gorbahn, Phys. Rev. D **82**, 094026 (2010).
[67] L. L. Chau, Phys. Rep. **95**, 1 (1983).
[68] A. J. Buras, arXiv:hep-ph/0505175.
[69] A. J. Buras, D. Guadagnoli, and G. Isidori, Phys. Lett. B **688**, 309 (2010).
[70] E. A. Andriyash, G. G. Ovanesyan, and M. I. Vysotsky, Phys. Lett. B **599**, 253 (2004).
[71] M. Beneke, G. Buchalla, C. Greub, A. Lenz, and U. Nierste, Nucl. Phys. **B639**, 389 (2002).
[72] I. Dunietz, R. Fleischer, and U. Nierste, Phys. Rev. D **63**, 114015 (2001).
[73] L. Mercolli and C. Smith, Nucl. Phys. **B817**, 1 (2009).
[74] L. J. Hall, R. Rattazzi, and U. Sarid, Phys. Rev. D **50**, 7048 (1994); R. Hempfling, Phys. Rev. D **49**, 6168 (1994); M. Carena, M. Olechowski, S. Pokorski, and C. E. M. Wagner, Nucl. Phys. **B426**, 269 (1994); T. Blazek, S. Raby, and S. Pokorski, Phys. Rev. D **52**, 4151 (1995); C. Hamzaoui, M. Pospelov, and M. Toharia, Phys. Rev. D **59**, 095005 (1999); K. S. Babu and C. F. Kolda, Phys. Rev. Lett. **84**, 228 (2000); M. Carena, D. Garcia, U. Nierste, and C. E. M. Wagner, Nucl. Phys. **B577**, 88 (2000); M. S. Carena, D. Garcia, U. Nierste, and C. E. M. Wagner, Phys. Lett. B **499**, 141 (2001); G. Degrassi, P. Gambino, and G. F. Giudice, J. High Energy Phys. 12 (2000) 009; G. Isidori and A. Retico, J. High Energy Phys. 11 (2001) 001; 09 (2002) 063; F. Borzumati, C. Greub, and Y. Yamada, Phys. Rev. D **69**, 055005 (2004); L. Hofer, U. Nierste, and D. Scherer, J. High Energy Phys. 10 (2009) 081.
[75] S. Baek and P. Ko, Phys. Rev. Lett. **83**, 488 (1999).
[76] V. M. Abazov *et al.* (D0 Collaboration), Conference Note 5906, http://www-d0.fnal.gov/Run2Physics/WWW/results/prelim/B/B56/B56.pdf; T. Aaltonen *et al.* (CDF Collaboration), Phys. Rev. Lett. **100**, 101802 (2008); Public Note 9892, http://www-cdf.fnal.gov/physics/new/bottom/090813.blessed-Bsd2mumu//bsmumupub3.7fb_v01.pdf.
[77] J. C. Hardy and I. S. Towner, Phys. Rev. C **79**, 055502 (2009).
[78] M. Antonelli *et al.*, Eur. Phys. J. C **69**, 399 (2010).
[79] E. Barberio *et al.* (Heavy Flavor Averaging Group), arXiv:0808.1297, and online update at http://www.slac.stanford.edu/xorg/hfag, updated summer 2008.
[80] E. Barberio *et al.* (Heavy Flavor Averaging Group), arXiv:0808.1297, and online update at http://www.slac.stanford.edu/xorg/hfag, updated FPCP09 2009, respectively, summer 2009.
[81] CDF Collaboration, Public Note 9015, 2007.
[82] V. Abazov *et al.* (D0 Collaboration), Phys. Rev. D **82**, 012003 (2010).
[83] G. Punzi, Proc. Sci., EPS-HEP2009 (2009) 022 [arXiv:1001.4886]. See also the combination page at http://tevbwg.fnal.gov/results/Summer2009_betas/.
[84] A. Höcker *et al.* (CKMfitter Group), Eur. Phys. J. C **21**, 225 (2001).
[85] V. Lubicz and C. Tarantino, Nuovo Cimento Soc. Ital. Fis. B **123**, 674 (2008).
[86] J. Laiho, E. Lunghi, and R. S. Van de Water, Phys. Rev. D **81**, 034503 (2010); J. Laiho, "Lattice Input to CKM Measurements," in Proceedings of the Flavor Physics and CP Violation Conference, Torino, Italy, 2010 (unpublished); E. Lunghi, "Lessons for New Physics from CKM Studies," in Proceedings of the Flavor Physics and CP Violation Conference, Torino, Italy, 2010 (unpublished).
[87] A. Ali Khan *et al.* (CP-PACS Collaboration), Phys. Rev. D **64**, 054504 (2001).
[88] C. Bernard *et al.* (MILC Collaboration), Phys. Rev. D **66**, 094501 (2002).
[89] S. Aoki *et al.* (JLQCD Collaboration), Phys. Rev. Lett. **91**, 212001 (2003).
[90] B. Blossier *et al.* (ETM Collaboration), Proc. Sci., LAT2009 (2009) 151 [arXiv:0911.3757].
[91] M. Wingate, C. T. H. Davies, A. Gray, G. P. Lepage, and J. Shigemitsu, Phys. Rev. Lett. **92**, 162001 (2004).
[92] C. Bernard *et al.* (Fermilab Lattice, MILC, and HPQCD Collaborations), Proc. Sci., LAT2008 (2008) 278 [arxiv:0904.1895].
[93] E. Gamiz, C. T. H. Davies, G. P. Lepage, J. Shigemitsu, and M. Wingate (HPQCD Collaboration), Phys. Rev. D **80**, 014503 (2009).
[94] C. Albertus *et al.*, Phys. Rev. D **82**, 014505 (2010).
[95] E. Dalgic *et al.*, Phys. Rev. D **76**, 011501 (2007).
[96] C. Albertus *et al.* (RBC and UKQCD Collaborations), Proc. Sci., LAT2007 (2007) 376.
[97] S. Aoki *et al.* (JLQCD Collaboration), Phys. Rev. D **77**, 094503 (2008).
[98] E. Gamiz, S. Collins, C. T. H. Davies, G. P. Lepage, J. Shigemitsu, and M. Wingate (HPQCD Collaboration and UKQCD Collaboration), Phys. Rev. D **73**, 114502 (2006).
[99] D. J. Antonio *et al.* (RBC Collaboration and UKQCD Collaboration), Phys. Rev. Lett. **100**, 032001 (2008).
[100] C. Aubin, J. Laiho, and R. S. Van de Water, Phys. Rev. D **81**, 014507 (2010).
[101] E. Blucher *et al.*, in *Proceedings of the CKM 2005 Workshop (WG1), UC San Diego, 2005*, arXiv:hep-ph/0512039.
[102] P. A. Boyle *et al.*, arXiv:1004.0886.
[103] C. Bernard *et al.*, Phys. Rev. D **78**, 094505 (2008); **79**, 014506 (2009).
[104] A. Sirlin, Nucl. Phys. **B196**, 83 (1982).
[105] M. Okamoto *et al.*, Nucl. Phys. B, Proc. Suppl. **140**, 461 (2005); arXiv:hep-lat/0409116.
[106] E. Gulez *et al.* (HPQCD Collaboration), Phys. Rev. D **73**, 074502 (2006); **75**, 119906(E) (2007).
[107] P. Ball and R. Zwicky, Phys. Rev. D **71**, 014015 (2005).
[108] B. O. Lange, M. Neubert, and G. Paz, Phys. Rev. D **72**, 073006 (2005).
[109] M. Neubert (private communication).
[110] K. Ikado *et al.* (Belle Collaboration), Phys. Rev. Lett. **97**, 251802 (2006).
[111] B. Aubert *et al.* (*BABAR* Collaboration), Phys. Rev. D **77**, 011107 (2008).
[112] I. Adachi *et al.* (Belle Collaboration), arXiv:0809.3834.
[113] B. Aubert *et al.* (*BABAR* Collaboration), Phys. Rev. D **81**, 051101 (2010).

[114] K. Hara *et al.* (Belle Collaboration), Phys. Rev. D **82**, 071101 (2010).
[115] P. d. A. Sanchez *et al.* (*BABAR* Collaboration), arXiv:1008.0104.
[116] M. Gronau and D. London, Phys. Lett. B **253**, 483 (1991); M. Gronau and D. Wyler, Phys. Lett. B **265**, 172 (1991).
[117] D. Atwood, I. Dunietz, and A. Soni, Phys. Rev. Lett. **78**, 3257 (1997).
[118] A. Giri, Y. Grossman, A. Soffer, and J. Zupan, Phys. Rev. D **68**, 054018 (2003).
[119] K. Trabelsi, ''Measurement(s) of $\gamma/\phi 3$,'' in Proceedings of the CKM08 Workshop, Rome, Italy, 2008 (unpublished).
[120] U. Langenfeld, S. O. Moch, and P. Uwer, Phys. Rev. D **80**, 054009 (2009).
[121] J. Abdallah *et al.* (DELPHI Collaboration), Eur. Phys. J. C **28**, 155 (2003); B. Aubert *et al.* (*BABAR* Collaboration), Phys. Rev. D **70**, 012007 (2004).
[122] B. Aubert *et al.* (*BABAR* Collaboration), Phys. Rev. Lett. **92**, 181801 (2004).
[123] J. Bartelt *et al.* (CLEO Collaboration), Phys. Rev. Lett. **71**, 1680 (1993); G. Bonvicini *et al.* (CLEO Collaboration), Phys. Lett. B **490**, 36 (2000); D. E. Jaffe *et al.* (CLEO Collaboration), Phys. Rev. Lett. **86**, 5000 (2001); B. Aubert *et al.* (*BABAR* Collaboration), Phys. Rev. Lett. **96**, 251802 (2006); *Proceedings of the 33rd International Conference on High Energy Physics (ICHEP 06), Moscow, Russia, 2006* (World Scientific, Singapore, 2006); E. Nakano *et al.* (Belle Collaboration), Phys. Rev. D **73**, 112002 (2006).
[124] H. Boos, T. Mannel, and J. Reuter, Phys. Rev. D **70**, 036006 (2004).
[125] Y. Grossman, A. Kagan, and Z. Ligeti, Phys. Lett. B **538**, 327 (2002).
[126] H.-n. Li and S. Mishima, J. High Energy Phys. 03 (2007) 009.
[127] M. Ciuchini, M. Pierini, and L. Silvestrini, Phys. Rev. Lett. **95**, 221804 (2005).
[128] S. Faller, M. Jung, R. Fleischer, and T. Mannel, Phys. Rev. D **79**, 014030 (2009).
[129] H. Lacker (*BABAR* Collaboration and Belle Collaboration), Nucl. Phys. B, Proc. Suppl. **170**, 14 (2007).
[130] J. Charles, Phys. Rev. D **59**, 054007 (1999).
[131] M. Gronau and D. London, Phys. Rev. Lett. **65**, 3381 (1990).
[132] J. Charles *et al.*, arXiv:hep-ph/0607246.
[133] A. E. Snyder and H. R. Quinn, Phys. Rev. D **48**, 2139 (1993).
[134] B. Aubert *et al.* (*BABAR* Collaboration), Phys. Rev. Lett. **102**, 141802 (2009).
[135] V. M. Abazov *et al.* (D0 Collaboration), Phys. Rev. D **74**, 092001 (2006).
[136] V. M. Abazov *et al.* (D0 Collaboration), Phys. Rev. D **76**, 057101 (2007).
[137] E. Barberio *et al.* (Heavy Flavour Averaging Group), arXiv:0808.1297 and online update at http://www.slac.stanford.edu/xorg/hfag, updated PDG 2009.
[138] V. M. Abazov *et al.* (D0 Collaboration), Phys. Rev. Lett. **98**, 121801 (2007).
[139] T. Aaltonen *et al.* (CDF Collaboration), Phys. Rev. Lett. **100**, 121803 (2008).
[140] M. Bona *et al.* (UTfit Collaboration), PMC Phys. A **3**, 6 (2009).
[141] J. Charles (CKMfitter Group), Nucl. Phys. B, Proc. Suppl. **185**, 17 (2008).
[142] S. Eidelman *et al.* (Particle Data Group), Phys. Lett. B **592**, 1 (2004).
[143] O. Buchmüller and H. Flächer, Phys. Rev. D **73**, 073008 (2006); Lepton Photon 2007 update at http://www.slac.stanford.edu/xorg/hfag/semi/LP07/gbl$_$fits/kinetic/lp07-update.pdf.
[144] J. H. Kühn and M. Steinhauser, Nucl. Phys. **B619**, 588 (2001); **B640**, 415(E) (2002).
[145] A. H. Hoang and M. Jamin, Phys. Lett. B **594**, 127 (2004).
[146] J. H. Kuhn, M. Steinhauser, and C. Sturm, Nucl. Phys. **B778**, 192 (2007); arXiv:hep-ph/0702103.
[147] M. Steinhauser, arXiv:0809.1925.
[148] M. Bona *et al.* (UTfit Collaboration), Phys. Rev. Lett. **97**, 151803 (2006).
[149] M. Bona *et al.* (UTfit Collaboration), J. High Energy Phys. 03 (2008) 049.
[150] G. Raven, ''Prospects for CP Violation in $B_s^0 \to J/\psi\phi$ from First LHCb Data,'' in Proceedings of the ICHEP 2010 Conference, Paris, France, 2010 (unpublished).
[151] M. Bona *et al.* (UTfit Collaboration), J. High Energy Phys. 03 (2006) 080.
[152] A. J. Buras and M. Jamin, J. High Energy Phys. 01 (2004) 048.
[153] D. Guadagnoli (private communication).
[154] V. Cirigliano, J. F. Donoghue, E. Golowich, and K. Maltman, Phys. Lett. B **555**, 71 (2003).
[155] M. Battaglia *et al.*, CERN Yellow Report CERN-2003-002, 2002 (unpublished).